Universitetet i Stavanger

FACULTY OF SCIENCE AND TECHNOLOGY

MASTER'S THESIS

Study programme/specialisation: Petroleum Engineering/Drilling	Spring semester, 2018 Open
Author: Kristian Tande Klepaker	…… (signature of author)
Programme coordinator: Bernt Sigve Aadnøy Supervisor(s): Tron Golder Kristiansen	
Title of master's thesis: An Evaluation of the Liner Deformations in the Valhall Field	
Credits: 30 Studiepoeng	
Keywords: Chalk Compaction Failure Liner Deformation	Number of pages: 111 Stavanger, 15th of June 2018

Evaluation of Liner Deformations in the Valhall Field

Stavanger, 15th of June 2018

Page left intentionally blank

Acknowledgements

This Thesis was made in cooperation with Aker BP during the spring of 2018. The Engineering Geology Manager, Tron Golder Kristiansen, came up with the subject to interest of Aker BP which was the basis for the Thesis.

He has been my advisor throughout the last 6 months supporting me in the work with the Thesis. He is a excellent consultant, and I would like to thank him a lot for his patience, understanding and help during this time. His ideas and advice has been very valuable.

I would also like to thank Terje Moen and Lasse Hermansson, both with Ridge AS, for helpful discussions and setting me in contact with other people that could assist.

In addition, I would express my gratitude to the people at the Ridge offices for hosting me and letting me be a part of their engineering environment.

At last, I want to thank my professional adviser at the Department of Petroleum Engineering at the University of Stavanger; Bernt Sigve Aadnøy. Who has been very enthusiastic about the Thesis from the start and provided me with a lot of good ideas.

Abstract

Valhall is one of the giant, high porosity chalk reservoir in the southern part of the Norwegian Continental Shelf. The field has been in production since 1982 with pressure depletion and reservoir compaction as main drive mechanisms. Already since pre-production well testing and throughout the its lifetime, challenges involving well failure both in the overburden and reservoir has been encountered. This has led to several re-developed well designs.

The main purpose of this Thesis is to give an extensive evaluation of the liner deformation problems located in the reservoir area. Casing and liner collapse has been a well-known problem on the Valhall field for a long time. The shear failure problems in the overburden has been assessed, and this Thesis only focuses on deformation of production liners in the reservoir section.

To obtain the data presented in this study, more than 2 000 pages of well history for both abandoned and producing wells on Valhall has been explored. All the wells showing clear indication of deformation encounter an obstruction, restriction or an unpassable point downhole, have been recorded. From these wells a collection of reservoir, liner and wellbore data have been conducted. The data has been analysed by cross plotting to investigate any correlations. In addition, presentation of the vast amount of data has been shown in Tables.

Examination shows that high angle wells in high porosity zones have failed with link to chalk influx. Due to pressure depletion and subsequently substantial compaction, stress re-distributions in the weak high porosity chalk formation has led to severe problems solids production and fault re-activation. Excessive chalk influx resulting in large cavities around the wellbore induces a non-uniform load on the liner due to loss of lateral restrain. This effect has ultimately led to liner buckling in low angle wells and collapse in high angle wells.

The implementation of heavy wall liners in 1994, was a great success. However, this study shows that more than 21% of these have clear indications of collapse. This suggest a dynamic load not anticipated. The compacting overburden collapse and hits the liner and the impact of the forces is released in a matter of seconds. Caliper logs should be conducted to either confirm or deny the theory of deformation in the heavy wall liners.

Abbreviations

1D	1 Dimension
4D	4 Dimension
AICD	Autonomous Inflow Control Device
API	American Petroleum Institute
ASA	Allmennaksjeselskap
BP	British Petroleum
CT	Coiled Tubing
DCS	Danish Continental Shelf
DDH	Drilling Data Handbook
DL	Dogleg Severity
Do	Outside Diameter
DP	Drilling Platform
GLV	Gas Lift Valve
GOR	Gas to Oil Ratio
HCl	Hydrochloric
HW	Heavy Wall
ID	Inner Diameter
IP	Injection Platform
lbs	Pounds
m	Meter
ICD	Inflow Control Device
MC	Mohr Coulomb
MD	Measured Depth
mD	Millidarcy
MD	Measured Depth
NCS	Norwegian Continental Shelf
NOCO	Norwegian Oil Consortium AS & Co
OD	Outer Diameter
P&A.	Plug & Abandonment

PCP	Production and Compression Platform
PDO	Plan for Development and Operation
PH	Accommodation and Processing Platform
PLT	Production Logging Tool
PPF	Pounds per Foot
PTA	Pressure Transient Analysis
QP	Quarters Platform
RKB	Rotary Kelly Bushing
SD	Shut-down
SPF	Shots per Foot
SR	Slenderness Ratio
TD	Total Depth
TVD	True Vertical Depth
UiS	Universitetet i Stavanger
UK	United Kingdom
WC	Water Cut
WHP	Well Head Platform
WL	Wire line
WP	Wellhead Platform

Nomenclature

ΔP_{dd}	Drawdown pressure
P_{res}	Reservoir pressure
P_{wf}	Flowing well pressure
P_{cc}	Chalk pore collapse pressure
S_w	Water saturation
κ	Pore collaspse pressure parameter
$\emptyset_{ini}$	Initial porosity
P_b	Yielding burst pressure
σ_y	Yield stress
D	Outside diameter
P_{yc}	Yield strength collapse pressure
t	Wall thickness
P_{pc}	Plastic collapse pressure
P_{tc}	Transitional collapse pressure
P_{ec}	Elastic collapse pressure
F_y	Axial yield force
σ_{VME}	Von-mises stress
σ_z	Axial stress
σ_θ	Tangential stress
σ_r	Radial stress
P_i	Internal pressure
P_o	External pressure
r_i	Inner wall radius
r_o	Outer wall radius
r	Radius at where stress occurs
σ_a	Axial stress
F_a	Actual axial force
ΔT	Change in temperature

F_e	Effective axial force
A_i	Inner area of pipe
A_o	Outer area of pipe
T	torque
ΔP	Pressure difference
d_o	Outer diameter
d_i	Inner diameter
β	Beta
x	Dimensionless parameter
y	Dimensionless parameter
σ_b	Bending stress
M	Bending moment
y	Vertical distance from neutral axis
I	Area moment of inertia
π	Phi
σ_{DL}	Bending caused by dogleg
E	Elastic modulus
R	Radius of curvature
DL	Dogleg severity
F_c	Critical buckling force
L	Length
k	Constant
w_c	Effective weigth per unit length
r_c	Radial distance clearence
α	Well inclination from vertical direction
S	Effective stress
σ	Total stress
$\propto$	Biot's constant
K_{fr}	Bulk modulus of framework
K_s	Bulk modulus of solids

$\Delta\varepsilon_v$	Change in volumetric strain
ΔS	Change in effective stress
M_r	Rock deformation modulus
M_e	Elastic deformation
$M_{e\text{-}p}$	Transition between elastic and plastic deformation
M_p	Plastic deformation
ε_v	Volumetric strain
ε_{ve}	Instantaneous elastic volumetric strain
ε_{vp}	Instantaneous plastic volumetric strain
$\varepsilon_{vp(t)}$	Time dependent plastic volumetric strain
C	Material constant
D_m	Material constant
v	Poisson's ratio
α_T	Thermal expansion coefficient
τ_{max}	Maximum shear stress
σ_n	Normal stress
φ	Frictional coefficient
ε_z	Vertical strain
Δh	Change in reservoir thickness
h	Initial res. thickness
C_m	Uniaxial compaction coefficient
C_b	Drained bulk compressibility
Δh_s	Surface subsidence
R_T	Transfer ratio
$\sigma_1, \sigma_2\ and\ \sigma_3$	Principal stresses
σ_H	Maximum horizontal stress
σ_h	Minimum horizontal stress

Table of Contents

1. Introduction 17

2. Valhall 18

2.1 Valhall in short 18

2.1 Field development 20

2.2 Reservoir description 22

2.3 Well design 25

3. Theory 26

3.1 Rock mechanics in chalk formations 26

3.1.1 Solids production 26

3.1.1.1 Valhall challenges 26

3.1.1.2 Parameters affecting chalk production 28

3.1.1.3 Chalk liquefication 29

3.1.1.4 Chalk influx 29

3.1.2 Water impact on chalk stability 31

3.2 Tubular deformation modes 32

3.2.1 Burst 32

3.2.2 Collapse 32

3.2.2.1 Yield strength collapse 33

3.2.2.2 Plastic collapse 33

3.2.2.3 Transitional collapse 34

3.2.2.4 Elastic collapse 34

3.2.3 Axial strength 34

3.2.3.1 Tension and compression 34

3.2.4 Combined stress effects 34

3.2.5 Bending 39

3.2.6 Buckling 40
3.2.1 Perforated pipes structural strength 41
3.3 Tubular failure due to rock deformation 42
3.4 Compaction of the formation 44
3.5 Wellbore instability mechanisms 46
3.5.1 Naturally fractures and faulted formations 47
3.5.2 Tectonic and high in-situ stress 48
3.5.3 Well trajectory (inclination and azimuth) 48
3.5.4 Transient reservoir pressures 49
3.5.5 Mobile formations and unconsolidated rock 49
3.5.6 Physical/chemical rock-fluid interaction 50
4. Liner and casing deformation scenarios 51
4.1 Shear failures 52
4.1.1 Formation-induced shear 52
4.1.2 Fault shear 54
4.1.3 Injection shear 56
4.1.4 Production shear 57
4.1.5 Compaction shear (under fault shear?) 57
4.2 Collapse failures 58
4.2.1 Compaction-induced collapse 58
4.2.2 Non-uniform load 59
4.2.2.1 Uni-directional load, uniform along diameter 61
4.2.2.2 Concentrated opposed line loads 63
4.2.2.3 Opposed line loads, complete restrain in perpendicular direction 64
4.3 Liner deformation challenges on Valhall 65
4.3.1 Compaction-induced deformation 66
4.3.2 Overburden 66

4.3.3 Non-uniform load case on Valhall 68
4.3.4 Remedial action 68
4.3.4.1 Concentric cemented liners 68
4.3.4.2 Heavy wall liners 69
4.3.4.3 Well management 70
4.3.5 Valhall vs. Ekofisk 70
5. Valhall failures - well data analysis 72
5.1 Data collection 72
5.2 Heavy wall liner vs. conventional liners 72
5.3 Analysis of dependencies of well deformation parameters 73
5.3.1 Distance to perforations 73
5.3.2 Inclination at collapse depth 74
5.3.3 Porosity at collapsed depth 75
5.3.3.1 Porosity vs. acid treatment 76
5.3.3.2 Porosity vs. inclination 76
5.3.3.3 Porosity vs. slenderness ratio 77
5.3.3.4 Porosity vs solids production 77
5.3.4 Time of production to collapse 78
5.3.4.1 Time of production vs. acid treatment 79
5.3.4.2 Time of production vs. porosity 80
5.3.4.3 Collapse time vs solids production, porosity, slenderness ratio 80
5.3.5 Solids production 82
5.3.5.1 Solids production for collapsed wells 83
5.3.6 Slenderness Ratio 84
5.3.6.1 Slenderness ratio vs. inclination 84
5.3.7 Perforation shot density 85
5.3.8 Analysis 85

5.3.9 Summary of well data analysis – cross plotting 88
5.4 Parameters impact on liner deformation 89
5.5 Well summary 91
5.5.1 Abandoned wells 92
5.5.2 Shut-in or producing wells 95
5.5.3 Analyses of the liner deformation parameters 106
6. Conclusions and recommendations 109
6.1 Conclusions 109
6.2 Recommendations 109
7. References 111

List of Figures

Figure 1 Valhall location 21
Figure 2 Valhall investments (Norwegian Petroleum Directorate, 2018) 22
Figure 3 Valhall reservoir schematic 23
Figure 4 Valhall historical production 24
Figure 5 Chalk influx mechanism in a pore structure 29
Figure 6 Load path of formation near wellbore in stress space 30
Figure 7 Principal stress in a thick walled cyliner 35
Figure 8 Internal stress distribution across pipe wall 37
Figure 9 Ellipses plotted for different design factors, represent different failure modes 39
Figure 10 Collapse test schematic 41
Figure 11 Sample post collapse test 42
Figure 12 Natural fracture instability 47
Figure 13 Tectonic stress instability 48
Figure 14 Mobile formation instability 49
Figure 15 Unconsolidation instability 50
Figure 16 Basic stress conditions: (a) principal stress; (b) in-situ stress; (c) triaxial stress 53
Figure 17 Example of a faulted reservoir cross section 55
Figure 18 Parameter influence on fault Re-activation (shear) 56
Figure 19 Difference in compaction of crestal and shoulder areas 57
Figure 20 Deformation mechanisms in vertical, deviated and hor. wells (Guo, et al., 2018) 59
Figure 21 Three non-uniform load cases: 1) Uni-directional, 2) Opposed line loads and 3) Opposed line loads with complete restrain to radial displacement 60
Figure 22 Shear displacement zone in overburden (Kristiansen, 2015) 67
Figure 23 Radial displacement vs. external pressure and line load magnitude for both concentric and heavy wall liner (Pattillo, et al., 1995) 69
Figure 24 Overview over collapsed heavy wall and conventional liners 72
Figure 25 Distance from collapsed point to nearest perforations 73
Figure 26 Inclination at collapse depth 74
Figure 27 Porosity at collapsed depth 75
Figure 28 Porosity and acid treatment for the collapsed wells 76
Figure 29 Cross plotting reservoir porosity and well inclination 76

Figure 30 Cross plotting reservoir porosity and slenderness ratio 77
Figure 31 Cross plotting porosity and solids production 77
Figure 32 Time from production start until collapse indication 78
Figure 33 Time until collapse vs. acid treatment 79
Figure 34 Cross plotting time until collapse with reservoir porosity 80
Figure 35 Solids production within the first year of production start-up 80
Figure 36 Solids production of wells collapsed within first two years of production start-up 81
Figure 37 Overview of solids production on the Valhall field 82
Figure 38 An overview of collapsed wells producing solids 83
Figure 39 Cross plotting time until collapse with solids production 83
Figure 40 Slenderness ratio 84
Figure 41 Cross plotting slenderness ratio and well inclination 84
Figure 42 An overview of perforation density 85
Figure 43 Location of potential collapsed wells in the Valhall field 91

1. Introduction

Valhall is one of the giant, high-porosity chalk reservoir in the southern part of the Norwegian Continental Shelf. The field has been in production since 1982 with pressure depletion and reservoir compaction as main drive mechanisms. Already since pre-production well testing and throughout the its lifetime, challenges involving well failure both in the overburden and reservoir has been encountered. This has led to several rounds of redeveloped well-design.

The main producing formation is Tor, located around 2 450 meters TVD RKB at the crest and at approximately 2 650 TVD RKB on the flanks. The Tor formation is estimated to contain 2/3 of the reserves on Valhall.

The purpose of this thesis is to get an overview over liner deformation in the reservoir at Valhall, and evaluate the causes, cases and remedial action. As the problems in overburden already have been reviewed, this thesis is focus on well deformation in the reservoir. Over 2 000 pages of well history data has been explored to find reliable data.

This thesis will first present some background information and history about the Valhall field, before describing the theory of chalk formation, steel tubes and their interaction downhole. Some liner deformation scenarios are also presented, before diving into more Valhall specific cases.

The main analysis consists of a thorough investigation of well data and different parameters which may impact the well failure with diverse severity. Data is presented in plots and cross-plots, and a summary of all well data and parameters are shown in table on a well by well basis.

At the end, conclusions and recommendations are presented.

2. Valhall

2.1 Valhall in short

This section gives a short overview of the major milestones of the Valhall field history. Exploration, development, drainage and partner ownerships are outlined. (Offshore Technology, 2016)

1967

Amoco Europe as operator of the licence (blocks 2/8 and 2/11) and the partners Amerada Hess, Texas Eastern and NOCO (20 largest Norwegian companies) hired a converted whaler to undertake the first exploration well, 2/8-1. Following severe operational problems, *including a casing collapse with extensive cost overrun*, the well was abandoned before the reservoir was drilled, (Whaley, 2009).

1969 – 1975

The second well, 2/11-1, discovered oil in the target Late Cretaceous Tor Chalk formation, but it was not commercial. The two next wells were also unsuccessful, water wet 2/8-3 and only 1 meter of oil bearing chalk in 2/8-4. In 1969, only days after the unsuccessful 2/11-1 well, Phillips drilled and discovered the billion-barrel Ekofisk field only 80 km to the north. The geology was quite different from the Amoco exploration model, a seismically structural high affected by the velocity pull-down effect of the gas. There was a strong lobby against this idea among the partnership, particularly in Amoco, but in 1974 the Valhall field was officially discovered in the well 2/8-6 which encountered a thick oil zone.

1976-82

The field was appraised by drilling the 2/8-7 and 2/8-8 wells in 1976 and declared commercial during the same year. The development plan approval for the field was granted in 1977 and installation of the platforms QP, DP and PCP started in 1979. Production from the field started in October 1982. The drilling platform (DP) had originally 25 slots but was extended to 30 slots later.

1990s

The WHP, comprising 19 well slots, was installed in April 1996 and was put on production in June. At the end of 1997, the field had 34 producing wells, and recoverable reserves were estimated at 116.8 million m^3 of oil and 27.8 billion m^3 of gas.

Amoco merged with BP in 1998 and BP Amoco was established in 1999.

2000

BP Amoco was renamed as BP in 2000. The Valhall Water Injection project, aimed at recovering an additional 155 million barrels of oil, was given the green light.

2001-2004

This period is characterized by a high activity in the development of the field with several new platformed installed. The Valhall Flank project, involving the installation of two unmanned platforms on the flank of the reservoir, was approved in 2001. Valhall South Flank platform was installed in 2002 and put on production in 2003. Both the IP and the North Flank platforms was also ready for operations in 2003. First water injection at the field started in January 2004 coinciding with production start-up from Valhall North Flank.

2005-2007

The Valhall Redevelopment project, involving the installation of the combined PH platform, was sanctioned in 2005. Power from shore was decided via a 294 km long cable to Elkem's substation at Lista. The Valhall Redevelopment project was approved by Stortinget (Norwegian Parliament) in June 2007.

2010

BP increased the ownership in Valhall to 35.95 % and Hess acquired Shell's share of 28.09 % to a total of 64.05% in September 2010. Valhall joint venture was founded.

2012

An onshore control room at Forus was opened in January for remote operations. Valhall became the world's first offshore field installation with a permanent 4D life-of-field seismic system, including approximately 10 000 sensors on the seabed.

2013

The Valhall Redevelopment project was completed, the PH platform commenced production in January and the PCP was shut down permanently in October. The new PH platform hold an oil production capacity of 19 100 Sm^3/d and gas handling capacity of 4 mill. Sm^3/d.

2016

Det norske oljeselskap, owned by the company Aker, merged with the Norwegian business of BP and the current company, Aker BP, was founded. Aker BP takes over the operatorship on Valhall.

2017

Early January 2017, Valhall and Hod passed the milestone of one billion barrels of oil equivalents produced, more than three times the volume expected at the opening of the field in 1982. Aker BP ASA submitted a Plan for Development and Operation (PDO) for Valhall Flank West. In October 2017, Aker BP entered into an agreement to acquire Hess Norge AS, making Aker BP the sole owner of Valhall. Following this transaction, Pandion Energy AS has acquired 10 percent interest in the Valhall and Hod fields.

2.1 Field development

Valhall is a fractured chalk reservoir in the Norwegian sector of the North Sea, the reservoir is in the deep, axial part of the Norwegian Central Graben, known as the Feda Graben, at the apex of a structural high known as the Lindesnes Ridge. The location of Valhall is in the most southern part of the Norwegian Continental Shelf approximately 80 km from Ekofisk. The field location is shown in Figure 1.

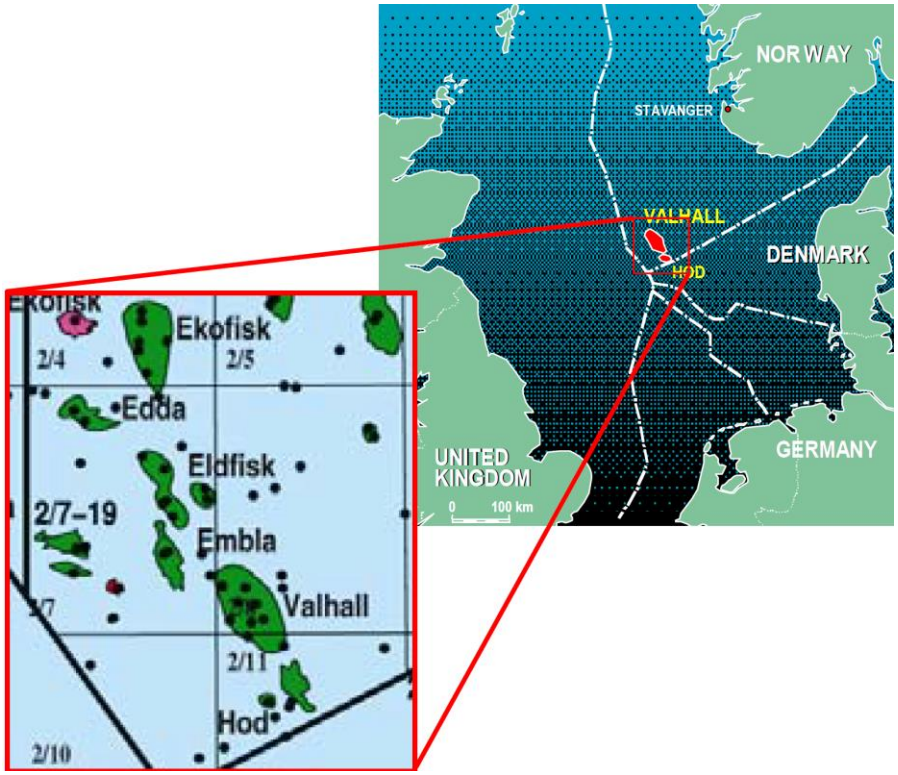

Figure 1 Valhall location

The field has been producing mainly under compaction and solution gas drive since 1982, Before introduction of water injection at the field centre in 2004, the drainage strategy of the Valhall reservoir was compaction and pressure depletion as drive mechanisms. Present, gas lift is applied to most of the production wells for production enhancement. Injection of seawater as pressure support has had a positive effect on the central crest area, but also led to problems with scale deposits on offset wells.

Figure 2 illustrates the annual and cumulative investments made to develop Valhall over the life of field. There are four periods with higher investments, the initial development (1979-1982), installation of the wellhead platform (WP) (1996-1999), the Flank project (2001-2003) and Valhall Redevelopment (2008-2012). In total, the sum of 75 bill. NOK (un-discounted) have been invested.

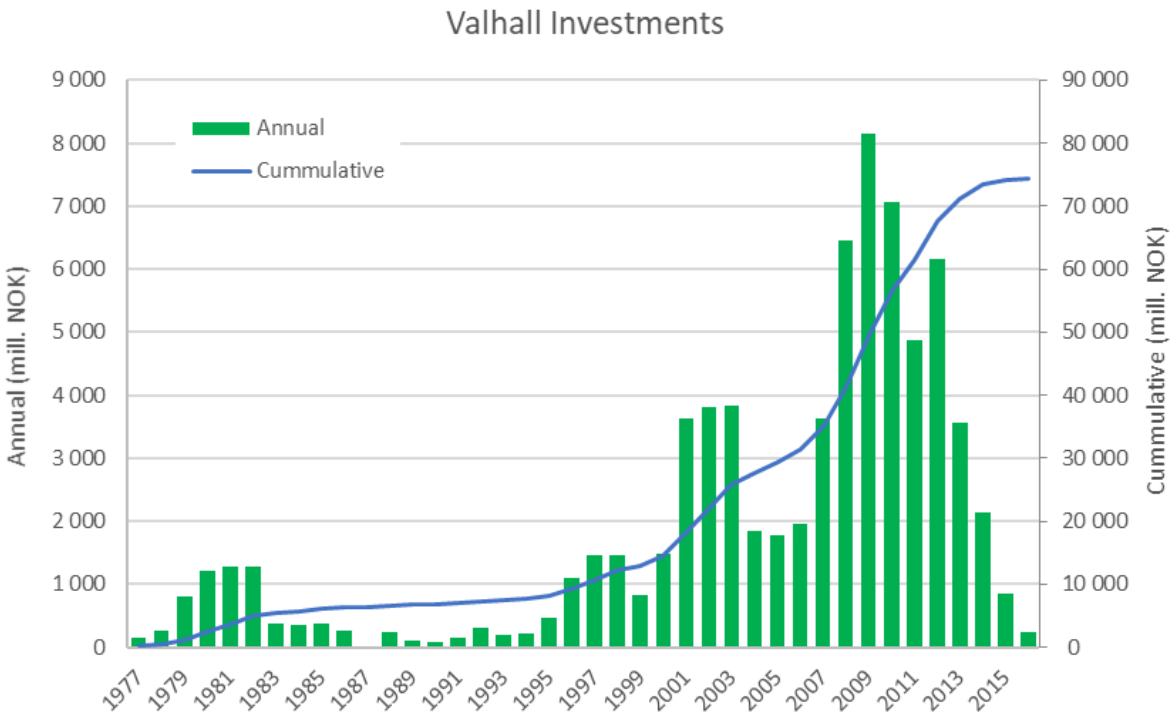

Figure 2 Valhall investments (Norwegian Petroleum Directorate, 2018)

Oil and NGL are routed via pipeline to the Ekofisk field and further to Teesside in the UK. Gas is sent via Norpipe to Emden in Germany.

2.2 Reservoir description

Valhall is currently producing from two hydrocarbon-bearing chalk formations, Hod and Tor, with most of the reserves in the latter. The formations are at around 2400 meters TVD at the crest and approximately 2650 metres TVD at the flanks, as illustrated in Figure 3.
Some properties of the Tor formation are listed below

- Reservoir thickness: 0-80 m, porosity range: 40-50 %
- Matrix permeability: 1-10 mD
- Total permeability: 1-60 mD due to natural fractures

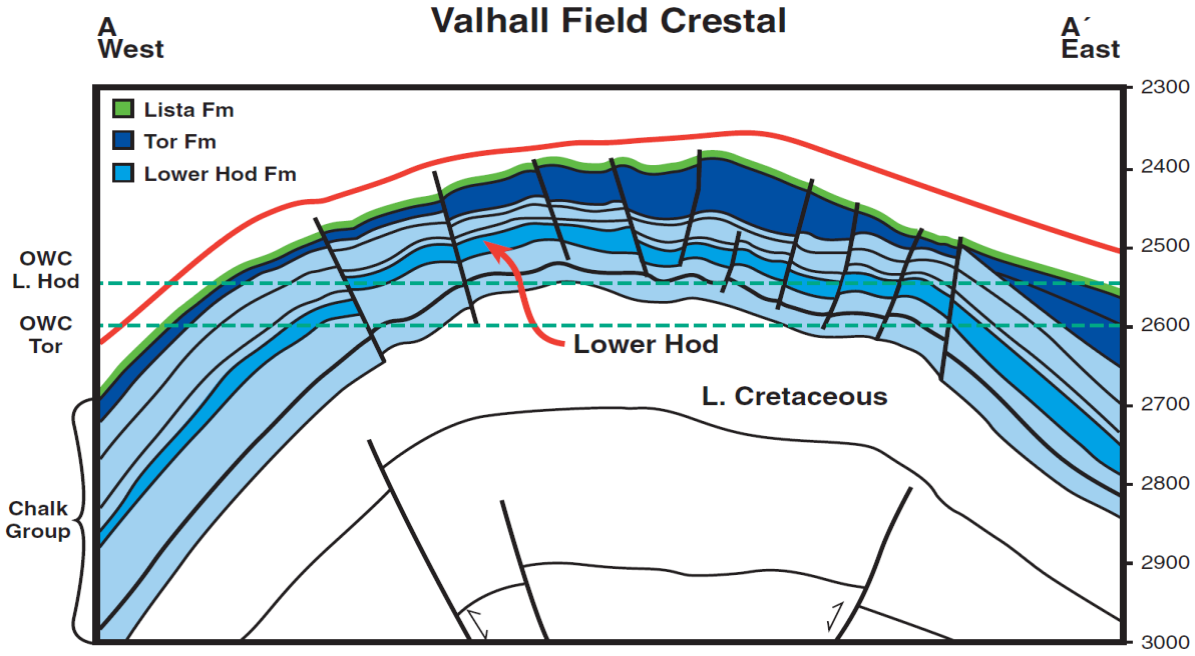

Figure 3 Valhall reservoir schematic

The Hod formation, which is of Mid-Turonian to Campanian geological age, consists of grey, partly pink to red, argillaceous chalky limestone. It varies in thickness from 200 meters at its thinnest and around 700 meters at its thickest. Majority of the chalk is laminated with some grain stone turbidites. The overlaying Tor formation, Maastrichtian to Paleocene geological age, is thinner than the Hod formation with thickness mostly under 150 meters. In some areas Tor is as thick as 250 meters in the basin which can indicate a depocenter. The formation is of good reservoir quality and consist of homogeneous white to pale grey chalk including several facies as shown below, (Kallesten, 2015).

- Hardgrounds
- Pelagic chalk
- Allochthonous deposits
- Shallow marine chalk

The Tor formation is also the main reservoir with around 66 % of the reserves. The Valhall trap is an asymmetric anticline oriented in the direction Northwest to Southeast because of basin inversion along the Lindesnes fault. The source rock is an organic rich Kimmeridge clay

from Late Jurassic, which happens to be the source of all chalk fields in the region. Although 1975 mark the official discovery of Valhall, the reservoir was penetrated for the first time in 1969. Eight more wells were drilled over the next 9 years to verify the reserves. Because of the low permeable chalk, high oil rates were inhibited initially. Production had to be enhanced through stimulation which eventually resulted in flow rates up to 1590 Sm^3/d (10 000 bopd) from the Tor formation, and 480 Sm^3/d (3000 bopd) from Hod. The history shows a production peak in 1998 and late 2004, related to commencement of water injection, with peaks above 15 900 Sm^3/d (100 000 bopd). The crestal part of Tor consist of natural fractures with matrix permeability from 1-10 mD even though much higher permeability is observed from Pressure Transient Analysis (PTA).

The expected production life has been extended several times with up to many decades, mostly because of addition of new recovery technology to enhance the recovery and increased reservoir energy due to reservoir compaction. The design of the PH platform has taken this into account, with a design life of around 40 years, and is predicted to extend the fields lifetime until the year 2025. Figure 4 displays the production history of Valhall.

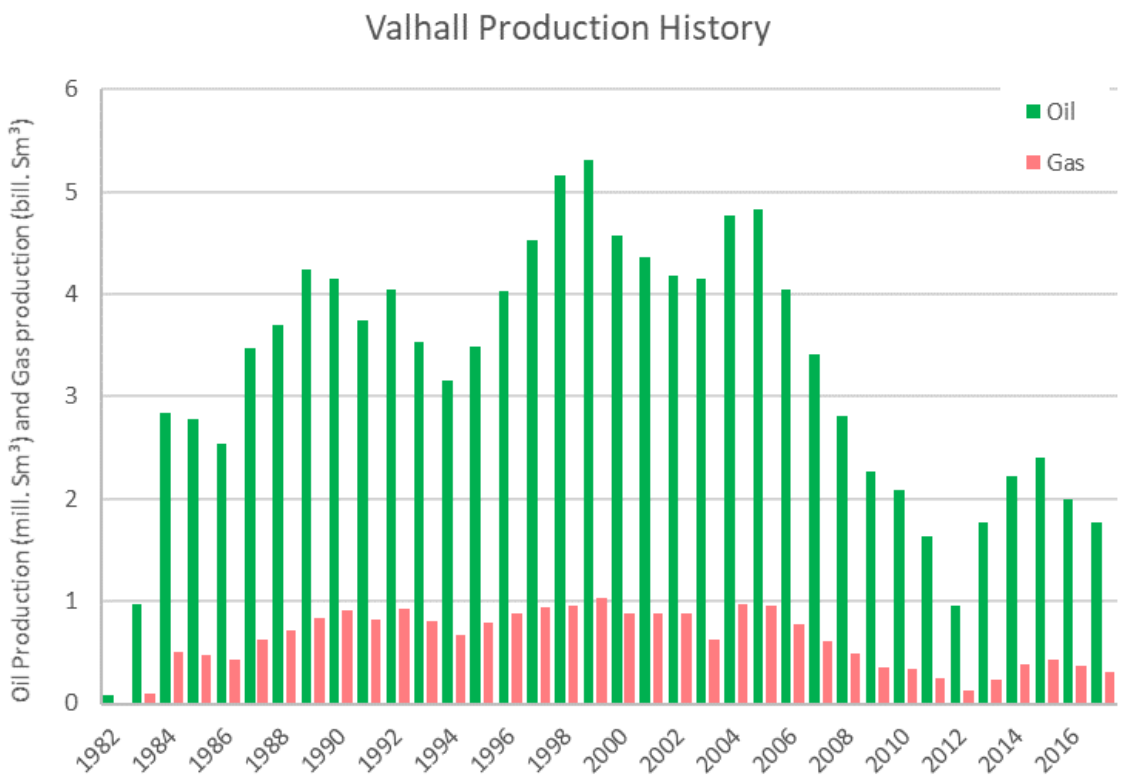

Figure 4 Valhall historical production

2.3 Well design

Initially the wells were perforated in the upper Hod formation and proppant fractured in the higher porosity Tor formation. Mitigation of solids production and well failure were focused on in the early days. From 1985 until 1990, proppant fractured gravel packs were introduced due to poor performance of the proppant fractured lower completion design. The Tor formation was fractured with proppant and then gravel packed to support the fractures. Eventually differential pressures across the gravel pack led to other problems with solids production and again, new well design strategies were needed.

The introduction of horizontal wells around 1990 gave increased reservoir exploitation. However, there were a drastically peak in well failures in this period, mainly due to failure of the stress sensitive Tor formation. In some cases, up to 80% of the horizontal section was lost within the first six months of production because of chalk influx and liner/casing collapse. In 1995, new horizontal cased and cemented reservoir sections with multiple proppant fractures was implemented. This time with heavy wall liners and 180° perforation phasing to improve on the formation stability and thereby mitigate the chalk production following collapse problem. Today, proppant fracturing is still in use, but shorter fractures and more zones is preferable in thinner reservoir sections.

3. Theory

This section will give insight information about chalk formation and its mechanics, internal stress in steel tubes and the interaction between the formation and the steel pipe. The Valhall case consists of rock mechanics inducing internal stresses in the liner, ultimately causing yield and deformation.

3.1 Rock mechanics in chalk formations

Chalk is a white porous form of sedimentary carbonate rock. It forms in deep marine conditions by debris of coccolithophorids, a planktonic organism shortly called coccoliths. These organisms are composed of an ionic salt called calcium carbonate or calcite (CaCO3). Including calcite, chalk also consists of various percentage of clay minerals, glauconite and apatite. The matrix consists of nano-fossils surrounded by mud, (0,03 mm grain size). The grains are whole or fragments of coccoliths which again is made up by calcite tablets. Rings with diameter around 20 μm is compacted together to hollow coccospheres. Which makes up for the high porosity values often seen in chalk reservoirs.

3.1.1 Solids production

Since the exploration on the Valhall field commenced, wells have shown problems with plugging due to chalk production. Some more severe than others. Great effort has been made to understand the mechanisms and addressing the challenges with influx of chalk.

3.1.1.1 Valhall challenges

As mentioned earlier, the wells on Valhall experienced severe chalk production problems. To investigate this problem, a study was conducted (Kristiansen, et al., 1996). Wells were divided into two categories:

1. Shut-down-dependent failures
2. Shut-down-independent failures

Shut-down dependent failures, or pressure gradient dependent failures are most likely related to tensile failures or liquefication. This may include

- Choke-opening increase, even at lower drawdowns than the well had already been exposed to.
- Initial drawdown period.
- Re-openings after platform shut-downs.

Regarding the wells on Valhall, they required a slower bean-up period, lot of choke adjustments to get the well back to previous production rates to minimizing risk of chalk influx.

Other causes not dependent on pressure gradients, such as shear failure which also can cause liquefication under some conditions, can cause chalk deformation and influx from stable production (magnitude of drawdown).

Kristiansen and Meling (Kristiansen, et al., 1996) concluded with

- Two distinct solids production mechanisms on Valhall. Pore pressure gradient dependent (choke opening) and drawdown dependent (stable production).
- Multiphase flow more involved in chalk production than in sands. Increasing downhole gas rate was a triggering factor.
- An in-depth analysis required good knowledge of downhole completion geometry, i.e. different perforation patterns will give different result.
- Well management important, requiring monitoring of several downhole parameters to balance production against chalk production.

Propped fractured gravel packs seemed initially stronger than horizontal wells. However, after screen fail, the well was very sensitive to pore pressure gradient resulting in well fail during re-opening after shut-downs.

3.1.1.2 Parameters affecting chalk production

Drawdown pressure

Referred to as the difference in flowing bottom hole pressure and the reservoir pressure.

$$\Delta P_{dd} = P_{res} - P_{wf} \quad (3.1)$$

Where ΔP_{dd} is the drawdown pressure, P_{res} is the reservoir pressure and P_{wf} is the flowing bottom hole pressure.

The rock matrix in the near wellbore area will be exerted to the highest stresses and deformations until the rock yields. So, to speak, the bottom hole pressure can be a measure of maximum deformation of rock matrix thus listing drawdown pressure as a main parameter in solids production.

Oil flow

The flow resistance in the oil will result in drag force on the rock matrix proportionally to the oil velocity. Depending on the magnitude, changes in the near wellbore area regarding permeability, pressure gradients and inflow area, will be observed. Understanding pressure profiles around the wellbore, will give a better insight in the parameters governing the drag force of oil.

Gas flow

Gas volume can be considered as a function of pressure, and as the reservoir pressure is creeping below the bubble point through production, the trapped gas volume is expanding and "freed" from the oil phase. Increasing gas concentrations around the well will subsequently lead to an increased pressure gradient and rapid pressure instabilities, culminating into an undrained condition in the rock matrix in some cases.

Porosity

Porosity is regarded as a measure of chalk strength, although strength variations which is difficult to discover through logging, will be present. As the pore pressure decreases, the porosity will most likely change.

Inclination and azimuth

The stress distribution around a well is directly impacted by well inclination and azimuth. In addition, in-situ stresses will also govern the magnitude and geometry of this three-dimensional stress distribution.

3.1.1.3 Chalk liquefication

As the wells are opened for production, the chalk is subjected to rapid deformation under partly drained conditions. Effective stresses are released, and stresses carried by the rock are transferred to the fluid contained in the pores. The rock becomes a suspension and if subjected to differential pressure, the chalk will flow like a paste.

Figure 5 illustrates a pore structure. By production and thus pore pressure reduction, the stresses in the reservoir are transferred from the fluid to the chalk matrix. The chalk will compact, any cementation between the grains are broken, and the chalk becomes a granular material.

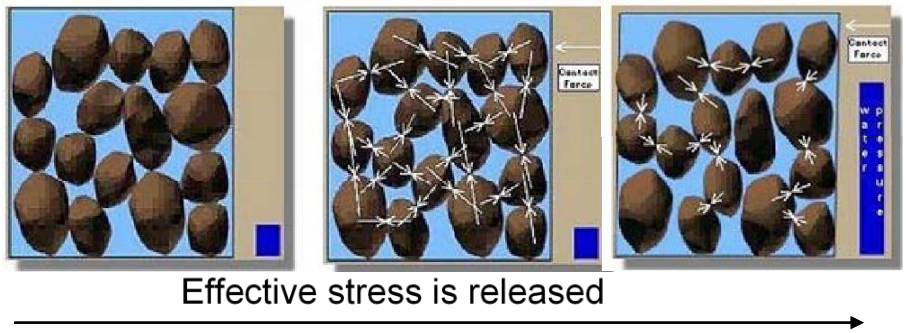

Figure 5 Chalk influx mechanism in a pore structure

3.1.1.4 Chalk influx

The mechanism for chalk production is quite similar to those for sand. During production, the flowing borehole pressure will decrease and thus increasing the matrix stresses around the wellbore. At a point the chalk will fail, leading to transport of formation fragments into the well. The literature states three basic mechanisms leading to solids production:

1. Shear or extensional failure; too high drawdown, i.e. the relative difference between well pressure and reservoir pore pressure causing unstable solids production. Drawdown pressure must be lowered to stop this problem.
2. Tensional failure; pressure gradient at perforations or wellbore surface exceeding tensional strength of the rock. This mechanism may be self-stabilizing unless too large rock volumes are affected in a short period of time, leading to plugging and ceased well flow.

3. Fines migration; movement of small particles in a flowing fluid. This is normally acceptable but can affect surface equipment and may also trigger tensional failure by pore plugging.

These three mechanisms will most likely work together in reality, thus making it difficult to decide which mechanism is accountable for the solids production.

Figure 6 (Kristiansen, et al., 2002) shows a load case for the near wellbore formation during a 2 years period from pre-drilling to production through pressure depletion. Sequence of loading is virgin - pre-wellbore depletion - completion - 2 weeks - 2 years. Exceeding the linear part of the envelope will result in shear failure of the chalk and then chalk production.

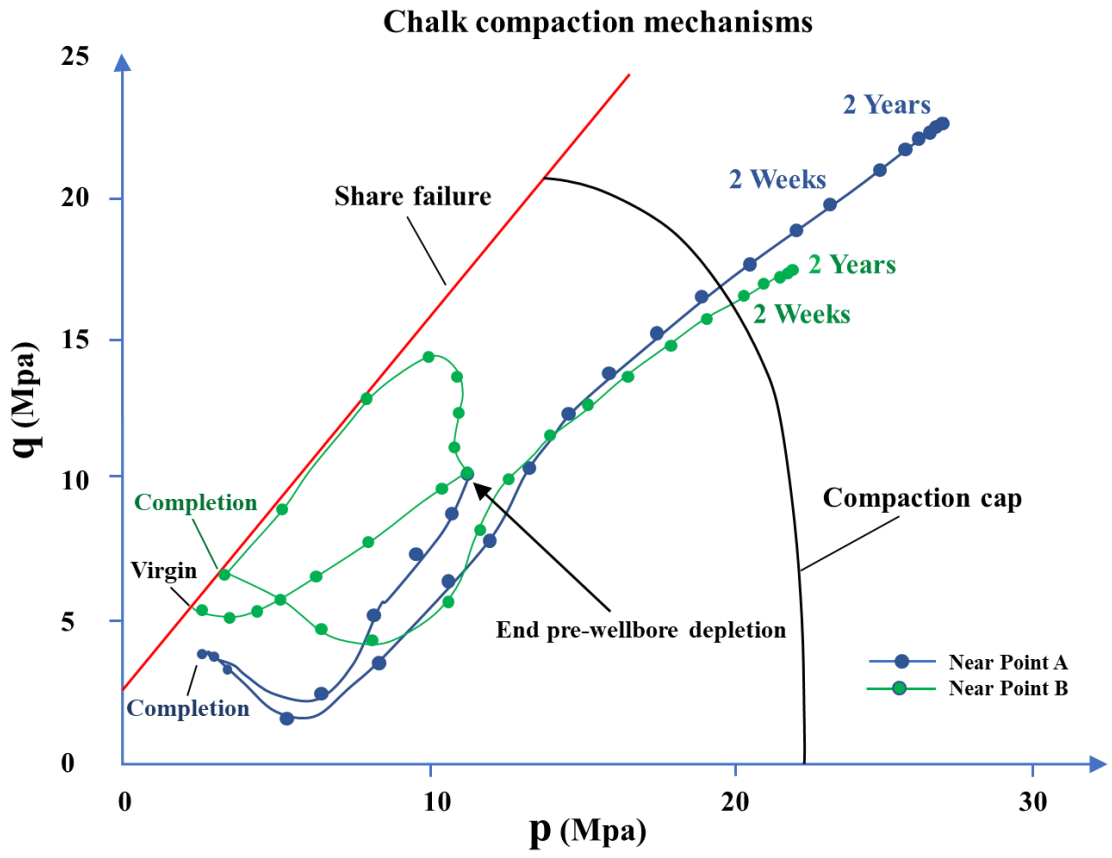

Figure 6 Load path of formation near wellbore in stress space

3.1.2 Water impact on chalk stability

The high porosity chalk on Valhall is very water sensitive. Water flooding the reservoir for improved recovery may result in fracturing of the reservoir and increasing permeability. With compaction as a main drive mechanism for production, water-induced compaction will further add to this. However, this compaction may danger well completions. In addition to compaction deformations, deformations related to the water flooding of the reservoir should also be included as a risk.

Water weakening of chalk is a known fact, and it has been shown that oil-filled chalk is stronger than water-filled. There are still uncertainties regarding the magnitude of the effect. Under some circumstances there is a notable interaction between water and chalk, and experiments conducted by (Madland, 2005) showed that chemical processes seemed to be involved. Thermodynamic-equilibrium had to be reached to emulate the in-situ deformation process.

Basically, the main approach is that pore collapse strength is a function of water saturation. Water saturated chalk is weaker than dry chalk.

$$P_{cc}(S_w = 1.0) = \kappa * P_{cc}(S_w = 0) \tag{3.2}$$

The ratio between fully saturated chalk and dry chalk is given by a parameter, κ. This parameter is again an exponential function of initial porosity and does not vary as compaction progress, (Kristiansen, et al., 2010).

$$\kappa = e^{(-2,3(\emptyset_{ini}-0,27))} \tag{3.3}$$

Although water will weaken the chalk, the discussion is how it will affect the compaction of the chalk during water flooding. It is interesting to note that the implementation of water injection on the Valhall field may be increasing the total compaction and/or accelerate the process. Reservoir temperature also plays a role here, where higher temperature will result in magnified compaction. The Valhall reservoir temperature is around 90°C, the Ekofisk reservoir temperature is 130°C in comparison.

Water breakthrough triggering to solids production and subsequently liner deformation in the S-3 well, is a great example of water weakening of chalk. (Kristiansen, 2018)

3.2 Tubular deformation modes

Steel tubes used in oil fields is subjected to many different loads during its lifetime. The design must be robust enough to withstand these loads without losing integrity and then compromise the operation. To prevent this, a tubing or casing design is preferably based on the maximum potential load condition expected. These loads are differentiated into; burst, collapse, tension and triaxial loads. When exposed to different loads, the steel tubes develop internal stresses which in worst case can lead to yield and failure of the pipe.

3.2.1 Burst

When the internal pressure of the pipe is much higher than the external pressure, we have a scenario where the pipe may burst. This is typical in cases where we have a gas kick, an influx of formation fluid with very low density. If gas fills the whole well from top to bottom, the internal pressure at the wellhead will be the reservoir/formation pressure where the influx took place minus the gas column. The external pressure on the other hand will only be exerted by the hydrostatic formation pressure outside of the pipe, which is low at shallow depths. If the burst load is large enough, the material will fail, and the pipe will lose its integrity.
The minimal internal yield pressure of a pipe can be derived from Barlow's equation:

$$P_b = 0{,}875 * [\frac{2 * \sigma_y}{D}] \tag{3.4}$$

σ_y is the yield stress, often found in tables depending on wall thickness of pipe and steel grade of material. D is the outer diameter of pipe, and 0,875 is a safety factor from API standards.

3.2.2 Collapse

A collapse scenario is when the external pressure exceeds the internal pressure significantly. Pipe collapse is undesirable, since a restricted wellbore severely reduces the accessibility of the well when running equipment and in worst case can lead to side-tracking or even well abandonment. During cementing, collapse loads on the pipe may occur. Especially when cementing all the way to surface. At the bottom of the pipe, we have an outside pressure equal to the hydrostatic pressure of wet cement, while the internal pressure is caused by the lighter mud column. Axial loads also affect the collapse strength of the pipe. If the pipe is in

compression, collapse resistance increases, but if the pipe is in tension, collapse resistance decreases.

The collapse strength of pipe is usually a function of material yield strength and the ratio of diameter to wall thickness (D/t) and is differentiated by four collapse regimes.

1. Yield strength collapse
2. Plastic collapse
3. Transitional collapse
4. Elastic collapse

3.2.2.1 Yield strength collapse

Using Lamé thick wall elastic solution we can find yield at the inner wall. This in fact, does not represent a collapse pressure. The tangential stress at the inner wall will exceed yield strength of the material long before a collapse failure occurs. For a thick-walled cylinder, collapse pressure can be estimated from:

$$P_{yc} = 2\sigma_y \left[\frac{(D/t) - 1}{(D/t)^2}\right] \tag{3.5}$$

P_{yc} – yield strength collapse pressure
D – nominal outer diameter of pipe
t – wall thickness of pipe
(D/t) – slenderness ratio

3.2.2.2 Plastic collapse

This collapse criterion is based on empirical data. The minimum collapse pressure for plastic range of collapse is calculated by:

$$P_{pc} = \sigma_y \left[\frac{A}{(D/t)} - B\right] - C \tag{3.6}$$

Where P_{pc} is plastic collapse pressure and A, B and C are all factors that can be found in a table. Applicable slenderness ratio can be found in the same table.

3.2.2.3 Transitional collapse

Obtained from a numerical curve fit between plastic and elastic regimes. Minimum collapse pressure in the transitional zone is calculated with:

$$P_{tc} = \sigma_y \left[\frac{F}{(D/t)} - G \right] \tag{3.7}$$

Factors F and G and applicable D/t ratio range found in table.

3.2.2.4 Elastic collapse

Based on theoretical elastic instability failure, this criterion is applicable for thin walled (D/t > 25±) cylinder and does not take yield strength into consideration. The minimum collapse pressure can be calculated as:

$$P_{ec} = \frac{46{,}95 * 10^6}{(D/t) * [(D/t) - 1]^2} \tag{3.8}$$

3.2.3 Axial strength

The pipe body axial strength is determined by its cross-sectional area and the yield strength, expressed with a formula as illustrated below:

$$F_y = {}^{\pi}/_{4} (D^2 - d^2)\sigma_y \tag{3.9}$$

When exerted to axial strain the pipe will become more susceptible to deformation by radial stress. If the axial load exceeds the yield strength of the pipe, this will cause a tension failure.

3.2.3.1 Tension and compression

Bending, tension and compression stresses will change casing properties and performance. Collapse resistance is reduced for a pipe in tension and increased if the pipe is in compression.

3.2.4 Combined stress effects

All the previously presented pipe-strength equations have been uniaxial. This means that only one of the stresses acting on the tubular has been nonzero. A downhole pipe is often exposed to axial load (tension or compression) at the same time as external and internal pressure. These

combined stresses generate a triaxial load, referred to as the principal stresses. These are axial, tangential and radial stress. (Departement of Petroleum Engineering, 2017)

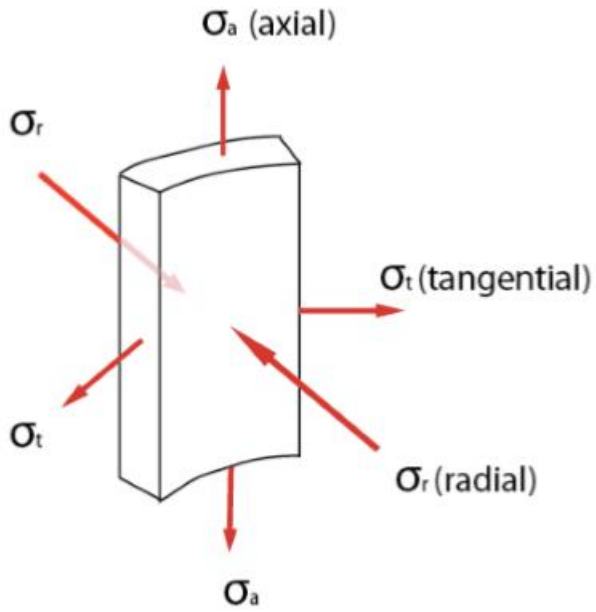

Figure 7 Principal stress in a thick walled cyliner

Under these conditions with combined loads, the most common way to calculate pipe-strength is with the use of Von Mises theory. Von Mises, also called Triaxial or Equivalent stress theory, is actual not a true stress, but a theoretically value which allows the 3D stress state of the pipe to be compared with a uniaxial failure criterion.

$$\sigma_{VME} = \frac{1}{\sqrt{2}} * \sqrt{(\sigma_z - \sigma_\theta)^2 + (\sigma_\theta - \sigma_r)^2 + (\sigma_r - \sigma_z)^2} \geq \sigma_y \qquad (3.10)$$

Uniaxial yield strength is compared to yielding condition. Where

σ_y – minimum yield stress, psi

σ_{VME} – triaxial stress, psi

σ_z – axial stress

σ_θ – tangential or hoop stress

σ_r – radial stress

As seen from the equation, yield failure is indicated when the Von Mises stress exceeds the minimum yield stress. Tangential and radial stresses is calculated with Lamé equation for thick walled cylinder:

$$\sigma_\theta = \frac{(1 + {r_o}^2/r^2)}{({r_o}^2 - {r_i}^2)} * {r_i}^2 * P_i - \frac{(1 + {r_i}^2/r^2)}{({r_o}^2 - {r_i}^2)} * {r_o}^2 * P_o \quad (3.11)$$

$$\sigma_r = \frac{(1 - {r_o}^2/r^2)}{({r_o}^2 - {r_i}^2)} * {r_i}^2 * P_i - \frac{(1 - {r_i}^2/r^2)}{({r_o}^2 - {r_i}^2)} * {r_o}^2 * P_o \quad (3.12)$$

Where

P_i – Internal pressure

P_o – External pressure

r_i – Inner wall radius

r_o – Outer wall radius

r – Radius at where the stress occurs

If the pipe is not exerted to bending or buckling loads, the axial stress is considered constant across the entire wall cross-sectional area.

$$\sigma_a = \frac{F_a}{A} + \frac{P_i * {r_i}^2 - P_o * {r_o}^2}{{r_o}^2 - {r_i}^2} + \sigma_z * (\Delta T) \quad (3.13)$$

F_a is the actual axial force, working on the entire wall cross-sectional area, A. Pressure loads, and temperature elongation is added to the equation.

Real axial force is the actual force working on the pipe, while the effective force is the considered force when the pressure effects are ignored.

$$F_e = F_a + P_i * A_i - P_o * A_o \quad (3.14)$$

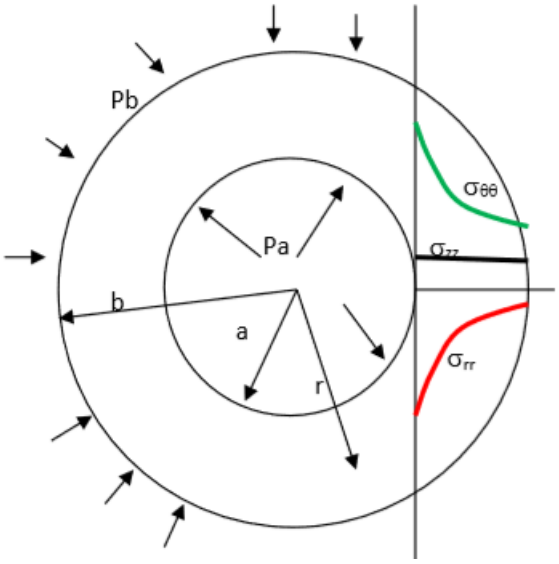

Figure 8 Internal stress distribution across pipe wall

There are four loads that determine the combined stress limit in a tubing, which is P_i, P_o, F_a and T – torque (Departement of Petroleum Engineering, 2017). The pressure difference, $\Delta P = P_i - P_o$, is calculated to determine if it's collapse or burst condition. Positive indicates burst and negative pressure difference indicates collapse.

Maximum equivalent stress is often located at the inside surface of the pipe. By letting $r = r_i$, the equation is simplified and gives radial and hoop stresses as:

$$\sigma_r = -P_i \tag{3.15}$$

$$\sigma_\theta = \frac{{d_o}^2 + {d_i}^2}{{d_o}^2 - {d_i}^2} * P_i - \frac{2 * {d_o}^2}{{d_o}^2 - {d_i}^2} * P_o \tag{3.16}$$

Which again can be written as

$$\sigma_\theta = (\beta - 1) * P_i - \beta * P_o \tag{3.17}$$

Where

$$t = {}^1/_2\,(d_o - d_i) \rightarrow \beta = \frac{2 * {d_o}^2}{{d_o}^2 - {d_i}^2} \approx \frac{{d_o}^2}{2t * (d_o - t)}$$

Tri-axial stress intensity design factor is given by:

$$SF = \frac{\sigma_y}{\sigma_{VME}} \rightarrow SF = \frac{\sqrt{2} * \sigma_y}{[(\sigma_a - \sigma_\theta)^2 + (\sigma_\theta - \sigma_r)^2 + (\sigma_r - \sigma_a)^2]^{1/2}} \quad (3.18)$$

By inserting for radial and hoop stress above you get two dimensionless parameters:

$$x = \frac{(P_i + \sigma_2)}{\sigma_y} \quad (3.19)$$

$$y = \frac{\beta(P_i - P_o)}{\sigma_y} \quad (3.20)$$

The term for design factor, using the dimensionless parameters, can now be written as:

$$SF = \frac{\sigma_y}{\sigma_{VME}} = \frac{1}{\sqrt{x^2 - xy + y^2}} \quad (3.21)$$

Solving for y, one gets:

$$y = \frac{x}{2} \pm \sqrt{\frac{1}{SF^2} - \frac{3}{4}x^2} \quad (3.22)$$

This equation is that of an ellipse shown in Figure 9, where the negative sign defines compression for collapse and the positive defines tension for burst (Aasen and Aadnøy, University of Stavanger).

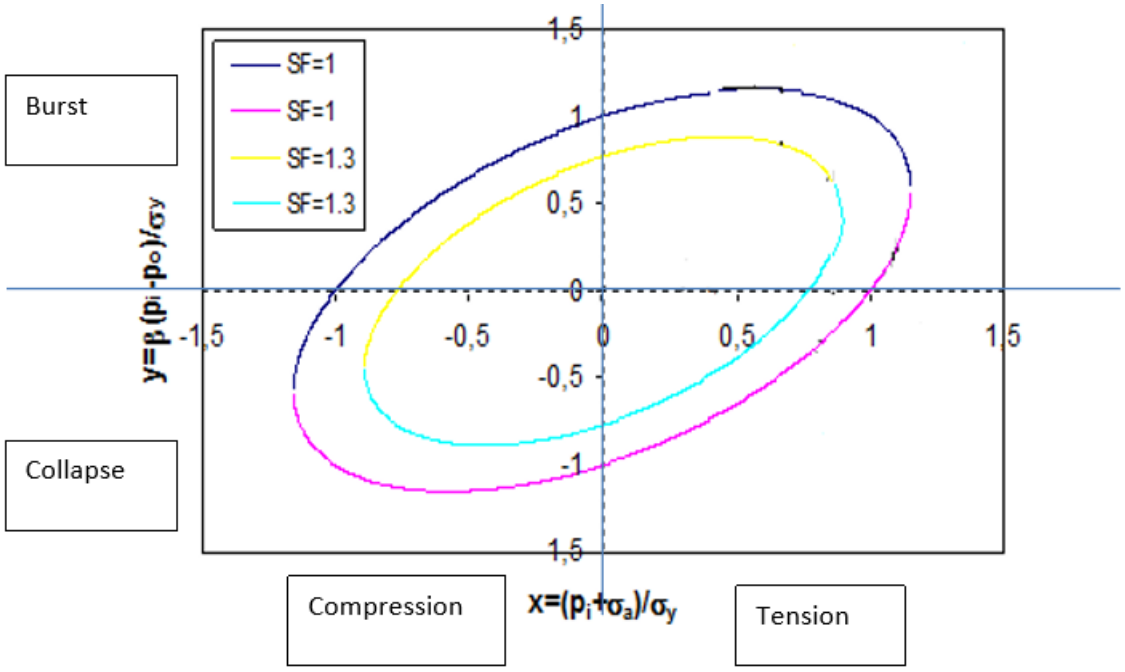

Figure 9 Ellipses plotted for different design factors, represent different failure modes

3.2.5 Bending

In a well, bending stress acting on the casing or tubing is usually caused by doglegs and/or buckling of pipe. When calculating bending stress in a pipe, beam theory can be applied.

$$\sigma_b = \frac{M * y}{I} \tag{3.23}$$

Where σ_b is the bending stress, M is calculated bending moment, y is vertical distance from neutral axis and I is the area moment of inertia around neutral axis. The area moment of inertia of a pipe is given by

$$I = \frac{\pi}{4} * ({r_o}^4 - {r_i}^4) \; or \; \frac{\pi * ({d_o}^4 - {d_i}^4)}{64} \tag{3.24}$$

The bending stress caused by doglegs will be greater at the outside diameter and can be calculated by

$$\sigma_{DL} = \pm \frac{E * D}{2 * R} = \pm \frac{\pi * E * DL * D_o}{432000} \tag{3.25}$$

Positive, tensile, at outside of bend. Negative, compression, at inside of bend. Where E is elastic modulus, D_o – outside diameter, R – radius of curvature, DL – dogleg severity (°/100ft). With increased dogleg severity, increased tensile stress is induced on the pipe.

3.2.6 Buckling

If the pipe is exerted to a sufficiently high compressive load, contributed by either thermal or pressure loads, it might become unstable and deformation may initiate. Because of confinement, i.e. the borehole, the pipes usually coil in a helical shape in vertical wells and form an S-shape in more deviated wells.

Casing buckling is not normal under production conditions, but increased temperature can lead to large enough loads to induce buckling. A stress check of the pipe using a triaxial analysis including bending stress should be conducted to hinder plastic deformation. Deformation due to buckling only occurs when the triaxial stress exceeds the yield stress and is prone to happen in unsupported intervals.

For a vertical well, the critical buckling force is given by Euler's equation, (Dawson, et al., 1984):

$$F_c = -k\pi^2 \frac{EI}{L^2} \tag{3.26}$$

Where E is the Young's modulus for steel, I is the pipe cross-sectional moment of inertia defined in the previous section, L is the length of the pipe, and k is a parameter that varies with conditions at either end of the pipe. Max value of k is set to 4, corresponding to both ends being fixed hindering lateral displacement.

For inclined wells, the critical buckling force is derived from Dawson and Paslay, (Dawson, et al., 1984):

$$F_c = -\sqrt{\frac{4EIw_c \sin\alpha}{r_c}} \tag{3.27}$$

Where E and I is the same as mentioned above, w_c is the effective weight per unit length, r_c is the radial distance clearance between the hole and outer diameter of casing, and α is the inclination angle compared to vertical direction.

3.2.1 Perforated pipes structural strength

Horizontal wells to drain the reservoir in an efficient way by enlargement of the contact area by fracturing techniques are commonly used on Valhall. Horizontal lower completions may consist of perforated liners. Mechanical and structural degradation of the perforated pipe against the demanding loads is investigated in this Section such as high torque, bending, tension and compression (Mantovano, et al., 2016). It is important to note that the perforation density on Valhall is in the range 6 – 12 SPF and this experiment is performed with pre-drilled liner having a slot density of 60 – 120. Hence, the results obtained is very conservative compared to a liner in Valhall.

A analytical and experimental study of collapse pressure of pre-drilled pipes was performed to evaluate the effect of lateral perforations on the radial resistance of pipes under external pressure. A variation of geometric configurations, relation diameter/pipe thickness (D/t), distance between perforations, number of perforation on the circumferential and longitudinal directions and hole diameter were evaluated.

The experimental and numerical results show that the D/t relationship, initial imperfections (like ovalization) and material properties have important influence on the pipes resistance, although the pre-drilled diameter and the axial space between them are the variables with most influence on the collapse resistance. The collapse pressure differences of pipes with slots and pipes without was observed to a reduction of collapse pressure close to 10%, but some geometrical parameters of slots could alter this.

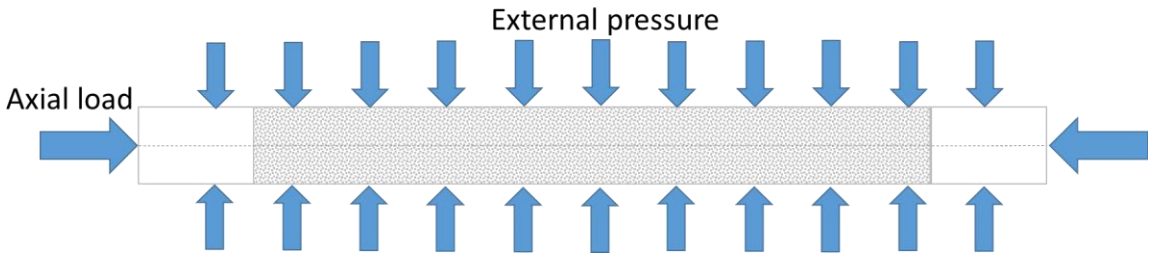

Figure 10 Collapse test schematic

A compressive load of 50% of yield was applied and held constant while the external pressure increased until specimen collapse occurs. Table 1 summarizes the collapse results.

Slot density (Slots per foot)	Axial load (kips)	Collapse Pressure (psi)
60	222	2857
60	226	2955
180	222	2094
180	230	2094
180 - Seamed	217	2077
180 - Seamed	217	2086

Table 1 Collapse testing results

The deformed perforated pipe after collapse testing is shown in Figure 11.

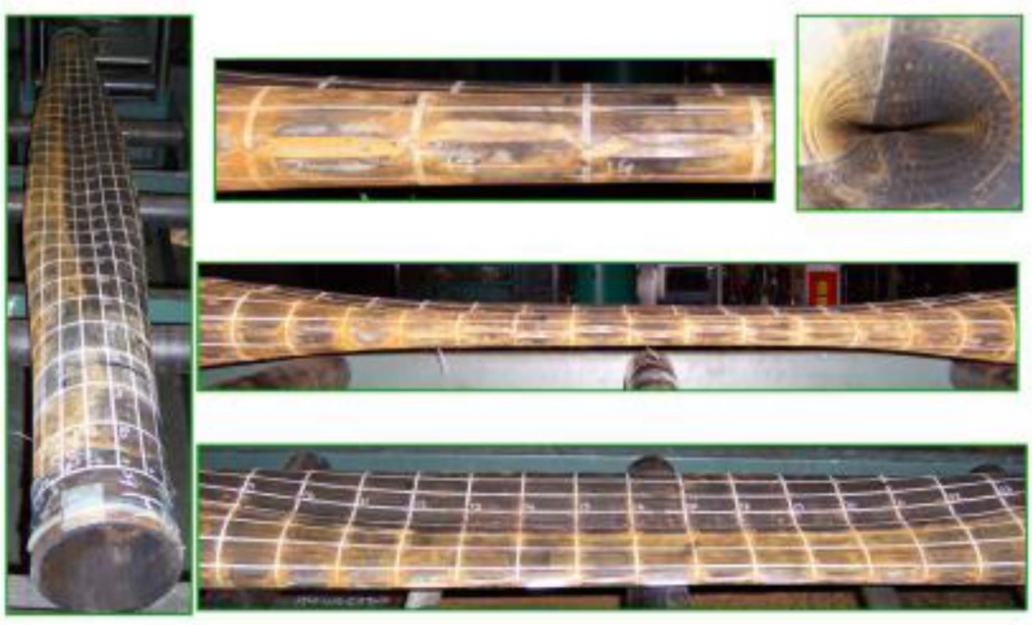

Figure 11 Sample post collapse test

The results in this laboratory testing of collapse resistance of a pre-drilled liner clearly shows that the weakening of the liner due to perforations is negligible.

3.3 Tubular failure due to rock deformation

Different petroleum activities may lead to rock deformation which can exert new load conditions not accounted for in the traditional casing design. As well as on Valhall, this has concern has been observed in other cases all around the world. Usually for instances involving reservoir compaction and subsidence, solids production, tectonic loading, salt flow, earthquakes or large thermal fluctuations. (Kristiansen, et al., 2000)

Rock volume changes surrounding the wellbore can lead to casing or liner deformation. These volumetric changes are a result of internal stress changes in the rock because of pressure and temperature changes during production and injection. If the cap rock or reservoir is weak enough, such volume changes can be substantial enough to deform casing or liner.

Pore pressure changes is the main reason leading to stress changes in the rock, where production is reducing the pore pressure and injection is increasing it. The total stress and pore pressure are connected through the effective stress law (Kristiansen, et al., 2000):

$$S = \sigma - \propto P_p \tag{3.28}$$

Where σ is the total stress, $\propto$ is Biot's constant and P_p is the pore pressure.

Biot's constant is given by:

$$\propto = 1 - \frac{K_{fr}}{K_s} \tag{3.29}$$

Where K_{fr} is the bulk modulus of rock framework and K_s is the bulk modulus of solids.

For weak, high porosity rocks and soil one can set $\propto = 1$ because of $K_s \gg K_{fr}$.

Changes in the effective stress, S, will subsequently lead to volumetric deformation of rock as following:

$$\Delta\varepsilon_v = \frac{\Delta S}{M_r} \tag{3.30}$$

M_r, the rock deformation modulus, has typically a constant value for elastic deformation (M_e) with gradually reducing value as the rock behaves more plastically ($M_{e\text{-}p}$), until it reaches as certain plastic strain where it will have a constant reduced value (M_p). With increased plastic deformation M_p will start to increase again due to work hardening effects. Strain rate dependent deformation is also present along with plastic and elastic strain in many rocks. Giving the following volumetric strain:

$$\varepsilon_v = \varepsilon_{ve} + \varepsilon_{vp} + \varepsilon_{vp(t)} \tag{3.31}$$

Where ε_{ve} is instantaneous elastic volumetric strain, ε_{vp} – instantaneous plastic volumetric strain and $\varepsilon_{vp(t)}$ – time dependent plastic volumetric strain, often referred to as creep. This creep can be expressed as:

$$\varepsilon_{vp(t)} = C \log\left[1 + \frac{t}{D_m}\right] \tag{3.32}$$

Where C and D_m are material constants.

Thermal changes can be included through a relation as:

$$\Delta S = \frac{E}{1-\upsilon}\alpha_T \Delta T \tag{3.33}$$

Where E is the Young's modulus, υ is the Poisson's ratio, α_T is the thermal expansion coefficient and ΔT is the temperature change.

Load distributions induced by these volumetric rock changes in the reservoir will lead to volumetric deformations some distance away from initial volume change. Volumetric deformations in rock masses containing joints, fractures and faults, may induce slip on these weak planes. Slip can be predicted by the Mohr-Coulomb criteria:

$$\tau_{max} = \sigma_n \tan \varphi \tag{3.34}$$

Where σ_n is the normal stress on the weak planes, and φ is the frictional coefficient of the planes. So, when τ exceeds $\sigma_n \tan \varphi$, we get slip.

Rock deformation and these shear displacements on weak planes will be transferred to the well, through the rock, cement and into the steel. The magnitude of deformation transferred is depend on the properties of the rock, cement and bond strength between the cement and the steel and the rock. Accurate estimations of pipe load due to rock deformation is very difficult to obtain. Hugely because of the uncertainty of strain needed to induce debonding and also the frictional load parameters after debonding has happened.

3.4 Compaction of the formation

Soft reservoirs with high porosity and high compressibility is often susceptible to compaction when the reservoir is depleted. When reservoir pressure is reduced, the rock matrix lacks "support" from the pores and must support more weight of the overlaying formations. Plastic deformation of the reservoir will occur if the compressive strength of the rock is exceeded. This can ultimately lead to large reduction in porosity and permeability which is an irreversible process. The basics of reservoir compaction can be expressed as a simple 1D analytical estimate (Settari, 2002):

$$\varepsilon_z = \frac{\Delta h}{h} = \frac{\left[\frac{\propto (1 - v - 2v^2)}{1 - v}\right] * \Delta P}{E} \quad (3.35)$$

Assumed that there is uniaxial compaction, elastic vertical strain and no arching (constant vertical stress). Where h is initial reservoir thickness, Δh - change in thickness, α – biot's constant, v – Poisson's ratio, ε_z – vertical strain, ΔP – pressure depletion and E – modulus of elasticity.

Vertical strain can also be expressed by introducing a uniaxial compaction coefficient, C_m.

$$\varepsilon_z = \frac{\Delta h}{h} = C_m * \Delta P \quad (3.36)$$

For linearly elastic behaviour:

$$C_m = \left[\frac{1 + v}{1 - v}\right] * \frac{C_b}{3} \quad (3.37)$$

C_b – drained bulk compressibility.

This model assumes that all the vertical displacement in the reservoir is transferred to the surface. In reality the compaction is smaller at the edges due to constraining effects of the side burden. This will create a bowl-shaped reservoir, called a subsidence bowl. However, the estimate presented above can be used at the centre of large reservoir with soft overburden. For smaller reservoir the transfer ratio, R_T, between surface subsidence and reservoir compaction can be notable lower than 1. Total compaction can then be estimated from equation 3.36 (Settari, 2002) as:

$$\Delta h = h * Cm * \Delta P, \Delta h_s = R_T * h * Cm * \Delta P \quad (3.38)$$

Where R_T = Δhs/Δh,

Compaction is a common phenomenon on the NCS and DCS and is abundant in over pressurised and thick chalk reservoir such as Ekofisk, Eldfisk, Dan, Tyra, Gorm as well as Valhall. Field development where compaction is a factor tends to become more complex than for conventional reservoirs. Detailed compaction analysis should be included in the

development as it can affect the recovery forecast, drilling program, permeability, stimulation and platform and well design. Seafloor subsidence as the most apparent consequence of compaction, will make issues for the field installations and pipelines.

As seen from the equations above, the magnitude of compaction depends on the thickness of the reservoir. This means that we will have more compaction in thick layers of reservoirs than in thin. Variation in compaction and subsidence in areas with different reservoir thickness, can subsequently lead to re-activation of faults i.e. basin/crest/flanks. This can further threaten the production liner integrity.

Although reservoir compaction imposes some problems to the production, it also contributes with an incredible additional drive mechanism for production as well. In some cases, overcoming the problems and turning into improved profits.

3.5 Wellbore instability mechanisms

The following section is most applicable for consideration of wellbore stability during drilling, but these mechanisms may also be valid to liner deformation conditions.
Wellbore instability is usually caused by a combination of factors which may be broadly classified as being either controllable or natural in origin. These factors are listed below, (Pasic, et al., 2007):

- Naturally fractures and faulted formations
- Tectonic and high in-situ stress
- Well trajectory (inclination and azimuth)
- Transient reservoir pressures
- Mobile formations and unconsolidated rock
- Physical/chemical rock-fluid interaction

The next sections give an overview of the general causes of instabilities that may induce liner collapse.

3.5.1 Naturally fractures and faulted formations

A natural fracture system is often near faults and the formation can be broken into large or small pieces. Hole collapse problems may become quite severe if weak bedding planes intersect a wellbore at unfavourable angles. Such fractures in shales may provide a pathway for fluid invasion resulting in a possible time-depended strength degradation, softening and ultimately to hole collapse. Figure 12 highlight a situation where natural fractures onset instability in the well.

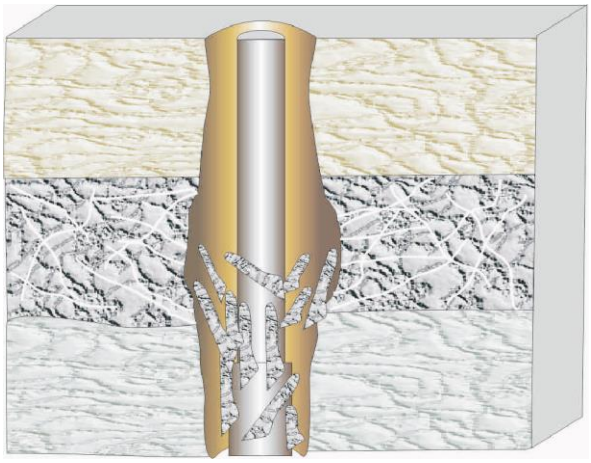

Figure 12 Natural fracture instability

As the Valhall reservoir is naturally fractured, this situation can be related to, i.e. the risk of solids production through near wellbore pressure fluctuations.

Reactivation of faults may occur due to injection or compaction, any changes in the stresses may induce fault reactivation. Pore pressure and stress changes over time are very dependent of the chosen drainage strategy and can to some extent be controlled. Well locations, well counts and lower completion designs also play an important part in the risk of reactivation of faults.

Because of high chalk porosity and large pressure depletion through years of production, compaction is a serious issue on the Valhall field. In contrast to the Ekofisk field, fault-reactivation might not be as abundant on Valhall, owing to more intricate reservoir complexity and thickness.

3.5.2 Tectonic and high in-situ stress

Highly stressed formations with a significant difference between the near wellbore stress and the restraining pressure within the well may induce instabilities. Tectonic stresses build up in areas where the formation is compressed or stretched due movement at a much larger scale. The formation in these areas may buckle due to the pressure of the moving tectonic plates. Figure 13 illustrate this mechanism.

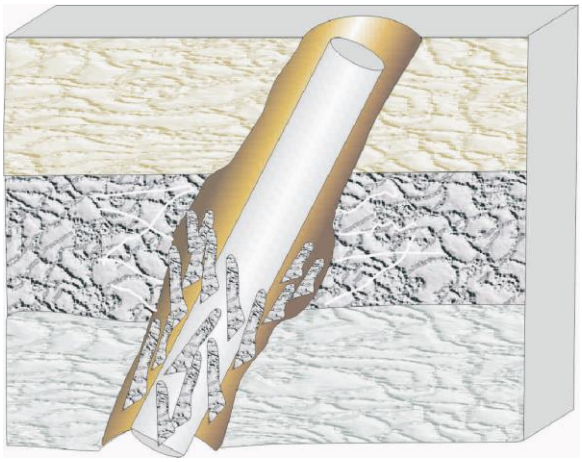

Figure 13 Tectonic stress instability

This scenario is more likely to happen at slip planes between different formations with differences in geomechanically properties and can be considered a top of the reservoir problem, bordering the cap rock. The transition from List to Tor formation is vulnerable to this mechanism.

Anomalously in-situ stresses may impact the formation instability and is often found near faults or in the inner limbs of a fold/pinch-out. These stress concentrations occur in particularly stiff rocks such as quartz sandstones or conglomerates.

3.5.3 Well trajectory (inclination and azimuth)

Inclination and azimuthal orientation of a well with respect to the principal in-situ stresses can affect the risk of collapse and/or fracture breakdown to a large degree. This is particularly true for estimating the fracture breakdown pressure in tectonically stressed regions where there is strong stress anisotropy.

This effect can be related to the high risk of chalk production due to stress anisotropy in horizontal wells at Valhall.

3.5.4 Transient reservoir pressures

Pressure and temperature changes in the reservoir as a function of production and injection will affect the in-situ stress. Depletion of the reservoir leading to a higher effective overburden stress is a typical well instability mechanism. Temperature cooling gives changes in the mechanical properties in the formation and may induce fracturing.

3.5.5 Mobile formations and unconsolidated rock

The mobile formation squeezes into the wellbore because it is being compressed by the overburden forces. Mobile formations behave in a plastic manner, deforming under pressure. An example on this is reactive shale layers that are sensitive to water diffusion. The deformation results in an unstable situation in the well, ref. Figure 14.

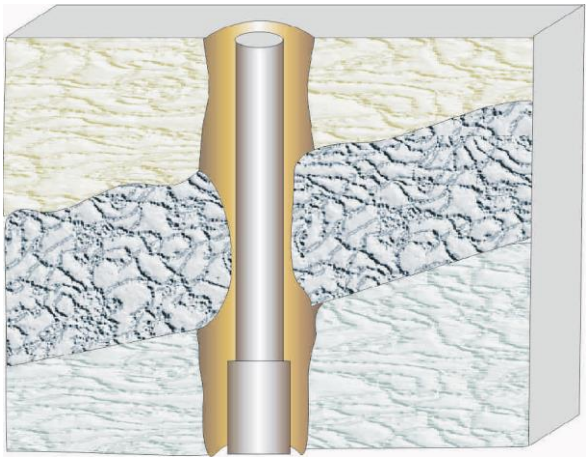

Figure 14 Mobile formation instability

Liquefication of chalk on Valhall is an example of such moblie formation, where the formation matrix turns into a granular material which might flow like a paste.

An unconsolidated formation will tend to be dissolved into individual grains because it has little or no bonding between particles. The collapse of formations is caused by removing the supporting rocFigure 15 shows an unconsolidated formation being unstable and collapse into

the well. The un-bonded formation (sand, gravel, etc.) cannot be supported by hydrostatic pressure and then falls into the hole and packs off.

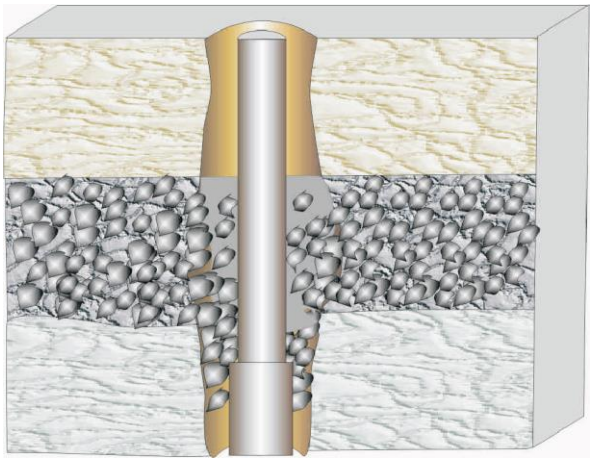

Figure 15 Unconsolidation instability

This is related to the loss of chalk cohesion during compaction, which is a severe problem on Valhall.

3.5.6 Physical/chemical rock-fluid interaction

There are many physical/chemical fluid-formation interaction phenomena that modifies the near wellbore strength or stress. These include hydration, osmotic pressures, swelling, dispersion, rock softening and strength changes. The significance of these effects depends on many factors including the nature of the formation such as mineralogy, stiffness, strength, pore water composition, stress history and temperature. Typical fluids/chemicals that is used in stimulation operation is scale dissolver, scale inhibitor, acids, breakers, etc.

This is linked to the water-weakening of chalk following increased risk of chalk liquefication and influx in the Valhall wells.

4. Liner and casing deformation scenarios

A casing with restricted access due to a substantial reduced internal diameter is usually referred to as a casing failure or collapse. This well condition often results in decreased production rates, increase in solids production, build-up of annular pressure and naturally suffer from the loss of moving intervention tools past the failure point. A casing failure may not be discovered at immediately, especially if the failure/collapse do not plug the well and no decrease in production rate is observed. but is usually discovered when performing workover or run a logging survey. As there are many different reasons for plugging of a well, like a fish stuck in hole or fill, a dump bailer is run to collect a sample of the potential plugging material. A confirmed failure is solved with different actions, these may include:

- In a worst-case scenario, the well may be shut-in and abandoned due to severe problems related to casing collapse
- Side-track well above failure/collapse depth
- Milling through obstruction
- Using special tools to restore original pipe diameter
- Or if little to none reduction in productivity is observed, no remedial action may be needed
- Use of acids to dissolve the obstruction

Most commonly the well is either shut-in or side-tracked. Casing failure in overburden and liner failure in the reservoir are often differentiated. Plugging and side-tracking of wells in the overburden with no access to reservoir might be necessary. Side-tracking is more problematic in the reservoir due to reduced hole size, but only a major problem if the well is no longer producing.

Liner deformation resulting in an unpassable obstruction of the wellbore leads to huge problems in relation to further reservoir management. Reservoir surveillance is constrained by well access and to clean-out and sufficient logging cold be performed. Nevertheless, not reaching the wells total depth will to a large extent impair the wells ability to drain the desired reserves and optimize production. Mitigation measures like water and gas injection, gas lift, reservoir stimulation, fracturing, monitoring and re-perforating is made impossible and will,

as mentioned earlier, relentlessly reduce the wells productivity. From an economical point of view, the cost of workovers of a troubled well must be considered against the benefit in terms of increased production of the failed well.

4.1 Shear failures

Petroleum activities inducing downhole pressure and temperature changes can lead to rock shear and displacement of large rock volumes. This movement of rock volumes can ultimately lead to shearing of casing. If the pressure integrity is lost or the distortion is too large to lower workover tools and production tubing downhole, the liner has lost its function. This is referred to as a liner failure. Pressure integrity is lost from one of two mechanisms, thread popping or physical rupture. With the former more common, especially if the joints are located near slip planes. Formation slip usually occurs over one single thin plane and as a distributed zone of a few meters (Bruno, et al., 2001). Observations shows three critical shear-induced well damages:

- Localized horizontal shear at weak lithology interfaces in overburden during reservoir compaction or heave
- Localized horizontal shear at the top of production or injection interval, because of temperature and pressure leading to volume changes
- Liner buckling and shear within the producing interval, mainly along perforations because of axial buckling when lateral constraint is removed. Or occasionally due to shearing at a lithological interface

4.1.1 Formation-induced shear

Stress and pressure changes in the formation through depletion, injection, heating and other reservoir management activities reduce the rock strength and may lead to shear failure. Due to the fact that geomaterials in rock formations seldom are of homogenous or isotropic nature, these shear movements transpire along planes. This effect is mainly occurring around planar features such as bedding planes, joints and faults. Regardless if these features are pre-existing or not, as the rock yields under large induced shear stresses, shear strains will induce slip along specific planes. Liner shear occurs when the stresses induced by the displacing rock mass overcomes the material strength of the steel pipe.

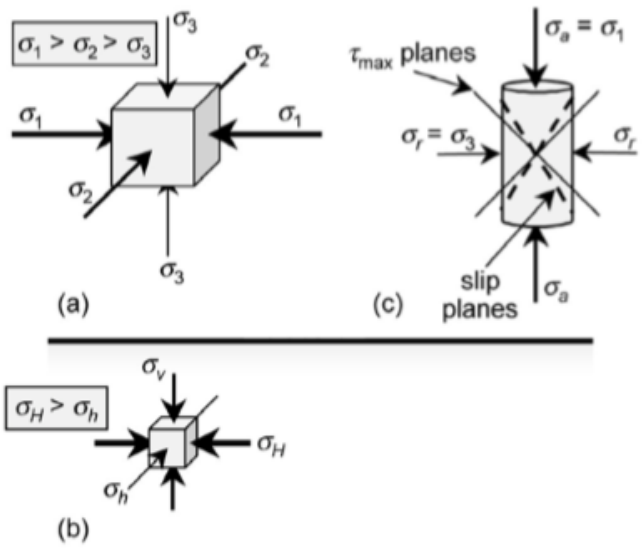

Figure 16 Basic stress conditions: (a) principal stress; (b) in-situ stress; (c) triaxial stress

Slip planes tend to develop along interfaces between materials of different stiffness, existing discontinuities or weakness planes (Bruno, et al., 2001). Even in homogenous intact rock, slip on single planes will be present if subjected to large enough shear stresses. They will very often befall around interfaces between two materials, because shear strain trigger naturally slip concentrate where there is a contrast in deformation properties. Delamination will happen in the weakest formation near the interface.

Rock strength and stress/strain behaviour are the two terms for estimating formation shear. There are three basic stress definitions shown in Figure 16:

- Principal compressive stresses at a point (σ_1, σ_2 and σ_3)
- In-situ stresses, common used in petroleum engineering defined with respect to ground surface (σ_H, σ_h and σ_v)
- Triaxial stress

Natural shear stresses are highest on planes 45° from the principal-stress planes, defining maximum shear stress as:

$$\tau_{max} = \frac{\sigma_1 - \sigma_3}{2} \tag{4.39}$$

Mohr-Coulomb criterion (see equation 3.32) is a common slip criterion for a geomaterial. The effective stress, transferred by matrix forces, is the key factor in formation shear. This effective stress, σ', is also affected by fluid pressure including depth of burial and boundary loads. Higher fluid pressure means lower effective stress. This is further described in Section 3.3.

There are many other criteria, but they all use the same principle of relating the maximum permissible shear stress to the effective stress in a geomaterial.

4.1.2 Fault shear

Changes in reservoir pore pressure affect the formation stress state. Depletion gives lower and injection higher horizontal total stress. Temperature changes such as cooling changes the mechanical properties and stresses in the rock and gives lower fracturing pressure and higher stiffness.

Key elements for the estimation of fault stability are the initial conditions like throw, smear, sand-sand contact, seismic features, etc. In addition, the influence over the field life for the parameters listed below is crucial.

- Reservoir compaction
- Seismic effects
- Dynamic pressure and temperature
- Well count and locations
- Stress changes
- Mechanical properties

An example of a faulted reservoir is illustrated in the seismic map in Figure 17, it should be noted that this is an example of a seismic map for a sandstone reservoir.

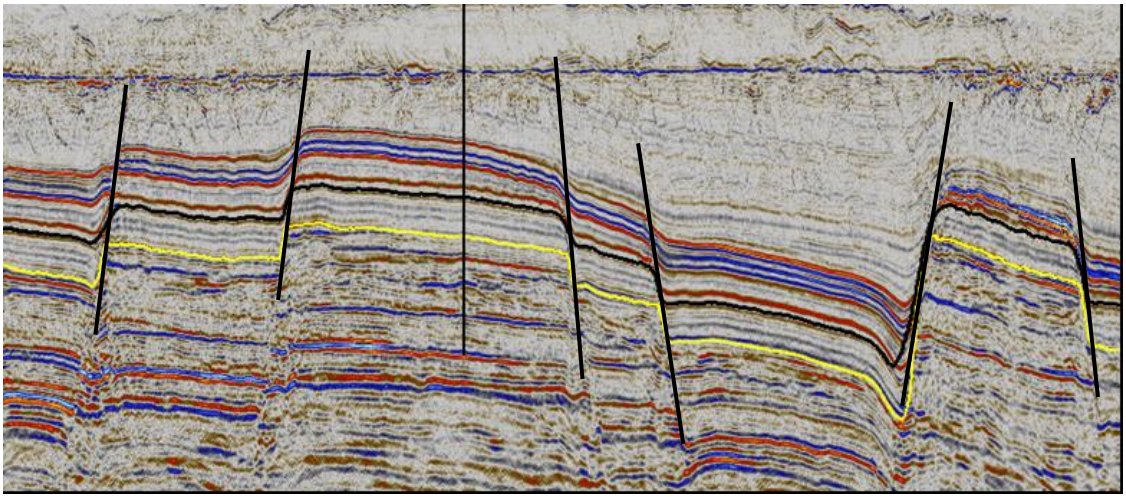

Figure 17 Example of a faulted reservoir cross section

Re-activation of fault depends on stress state relative to Mohr-Coulomb failure line. Stress (normal and shear) changes over time in pressure and temperature, i.e. the stress path may get closer to or further away from failure.

Key parameters to evaluate in that respect are:

- Mechanical properties (stiffness, friction angle and cohesion for fault)
- Location and relative orientation of faults and injectors
- Close evaluation of injector placement exposing faults to injection
- Direct link to the constrain value of the σ_h of the cap rock
- Bottom hole pressures and temperatures

An overview of the most dominating factors influencing the risk of fault re-activation is illustrated in Figure 17.

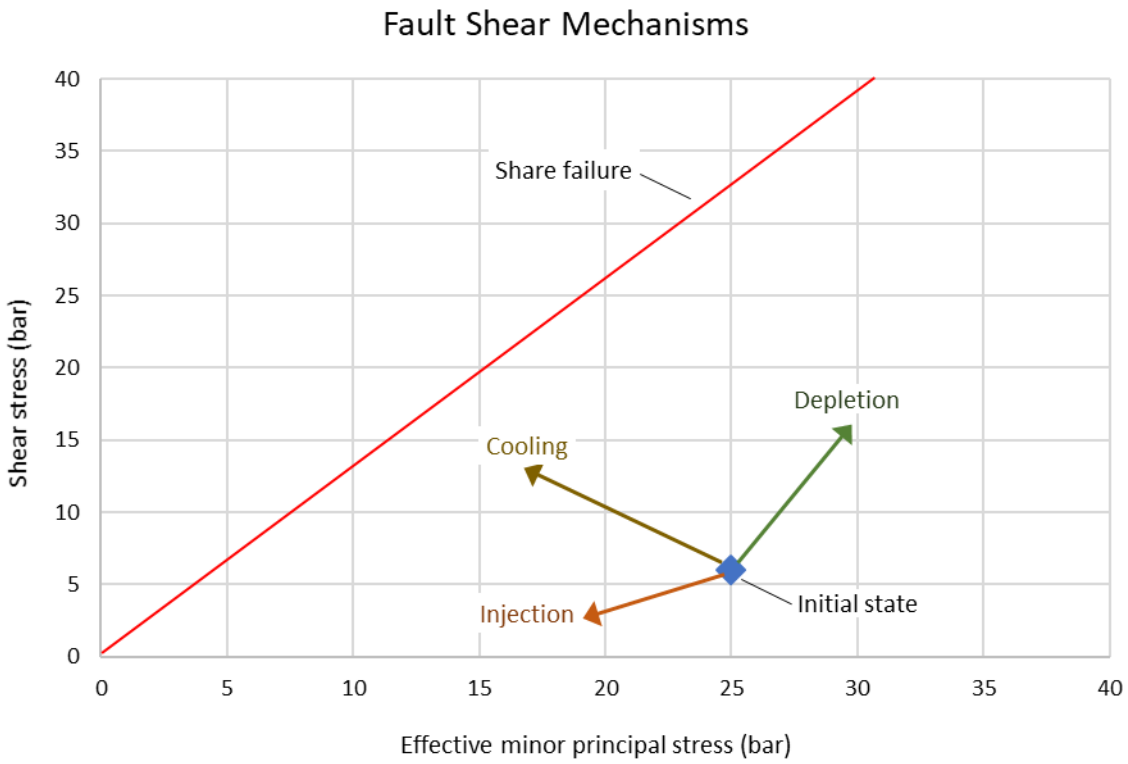

Figure 18 Parameter influence on fault Re-activation (shear)

The example of predict fault re-activation for a set of conditions shows the risk. Stress state changes for depletion, cooling and injection are illustrated with different arrows and colours. They point in dissimilar directions and to some extent counteract.

4.1.3 Injection shear

There are two main mechanisms that can lead to injection induced shear. Increasing reservoir pressure resulting in reduced effective normal stress or reservoir expansion leading to shearing near bounding interfaces where stresses are concentrated. Reduction in effective stress means volumetric expansion which the more impermeable seal rocks do not encounter. Large shear stresses are imposed on this interface between the reservoir and bounding strata. If this shear stress exceeds interface strength, it causes slip and thereby liner shear. Injection pressure tend to migrate upwards along cement-rock-casing boundaries, especially if cement shrinkage has occurred during setting. Pressurization of a weak zone at a higher elevation may lead to increased chances of shearing, predominantly in cases where there are large in-situ stress differences (large, natural shear stresses). (Bruno, et al., 2001).

4.1.4 Production shear

Production of fluid leads to reduction in the reservoir volume and an increase in effective stresses. Shear-stress concentration like the reservoir pressuring case occurs, but the rock displacement would be along the opposite direction. If reservoir compressibility is large enough, this may damage the liner. Reservoir depletion causing volume shrinkage, can lead to a remote lateral unloading and creating a normal fault mechanism in reservoirs in tectonically relaxed areas where initial lateral-stress is low. This mechanism is especially dominant in the presence of pre-existing faults. (Bruno, et al., 2001).

4.1.5 Compaction shear (under fault shear?)

Because of the characteristic downward and inward motion of compaction and difference in thickness of crestal parts and outer flanks of a reservoir, different effective stress changes will be experienced in the different reservoir sections. Thicker crestal parts will be subjected to an increase in minimum horizontal stress, whilst the thinner remote flanks will encounter a reduction in horizontal stress. This will subsequently give a shear stress increase in the rock masses above the shoulders and increasing the potential of high-angle fault mechanisms to develop on the flanks. Re-activation of thrust faults is also probable as horizontal stresses increases and potentially developing a thrusting mechanism, shown in Figure 19. The probability of casing/liner shear is highest on the shoulders, because of the high shear stress present.

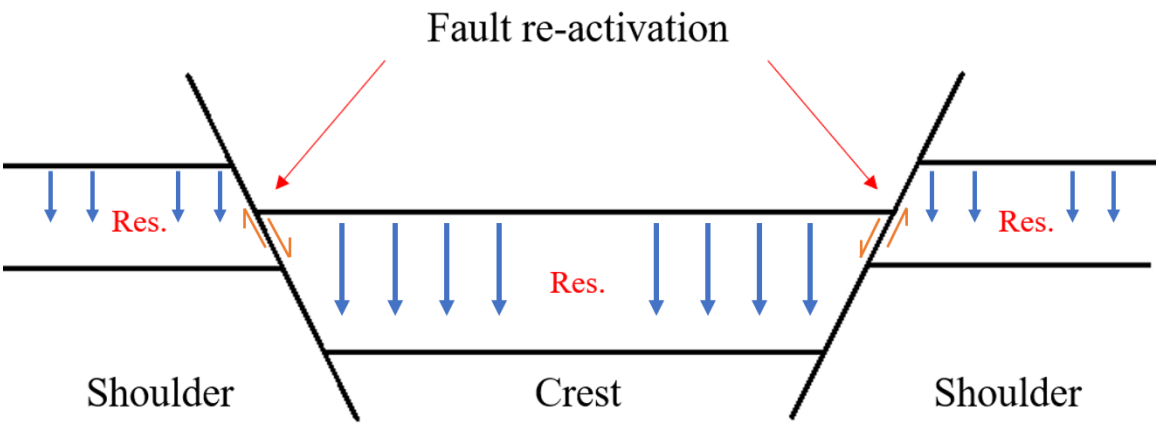

Figure 19 Difference in compaction of crestal and shoulder areas

Valhall has complex reservoir geology and does not show a distinct thicker crest with bordering thinner flanks. In fact, Valhall have a handful of thicker sub-basins scattered across the field, with thinner flanks around these sub-basins.

4.2 Collapse failures

4.2.1 Compaction-induced collapse

Liners may experience buckling and collapse as a result of axial compression with the greatest risk at unsupported intervals. Perforated areas with chalk production, poor cement support or at connections are some of the most exposed areas.

An estimate of axial strain induced on liner by reservoir compaction can be expressed as (Guo, et al., 2018):

$$\varepsilon_a = \varepsilon_c cos^2 \alpha \tag{4.40}$$

Where ε_c is compaction strain and α is the wellbore inclination.

This equation assumes uniform reservoir compaction and no slip at interfaces between liner /cement, and cement/formation. As there are different deformation mechanisms on a pipe, this may have limited applicability. (Guo, et al., 2018).

Only wellbore inclination will govern deform mechanisms, but the strain magnitude induced on the liner can vary with compaction strain, slenderness ratio and material grade. 3 different inclinations with different deformation mechanism, shown in Figure 20 are categorized:

1. Vertical – the liner deformation is accommodated by axial shortening and radial expansion
2. Deviated – deformation characterized by bending in the dip direction. Where the deformation is maximized in the reservoir compaction direction. Axial shortening is reduced, and radial deformation is enhanced as the well inclination increases
3. Horizontal – deformation is mainly accommodated by axial shortening at the top and bottom, and elongation on the sides

Up until plastic yielding, maximum liner strain is lower than compaction strain. After yielding has occurred, continued compaction strain will, however, increase the liner strain to a larger magnitude than that of the compaction strain itself. Studies (Guo, et al., 2018) has showed that slenderness ratio and liner grade are secondary compared to reservoir depletion magnitude, rock compressibility and well inclination when in their effect on liner deformation,
Ref. Figure 20.

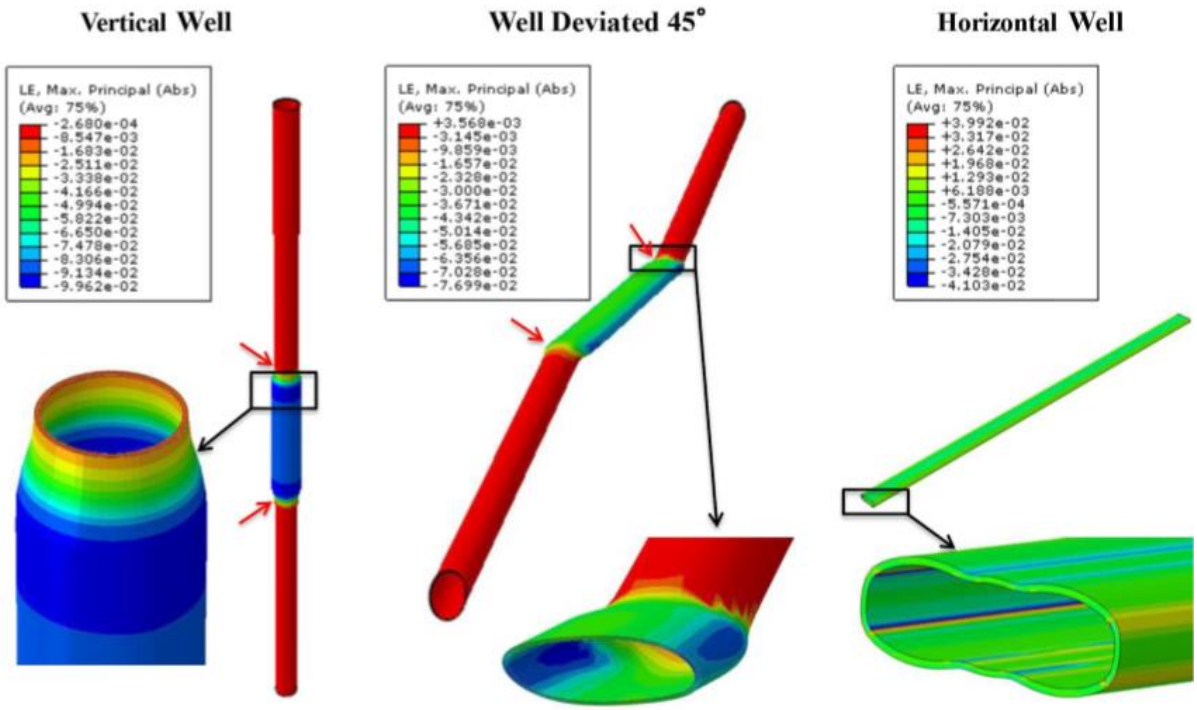

Figure 20 Deformation mechanisms in vertical, deviated and horizontal wells (Guo, et al., 2018)

4.2.2 Non-uniform load

Normally, collapse strength of casing and liners are based on outside hydrostatic-pressure on pipe. Such values are tabulated for maximum permissible API tolerance for initial deformation. However, hydrostatic collapse loading will not always be the case.

Collapsed or plastically flowing formations like weak or liquefied chalk, may lead to a non-uniform load. Production liners experiencing chalk production and thus losing lateral support while still be compressed vertically by the overlaying formations, may be subjected to this type of non-uniform load, meaning the outer loads is not uniformly distributed along the outer pipe circumference. Usually, three load cases are distinguished to compute these loadings, shown in Figure 21.

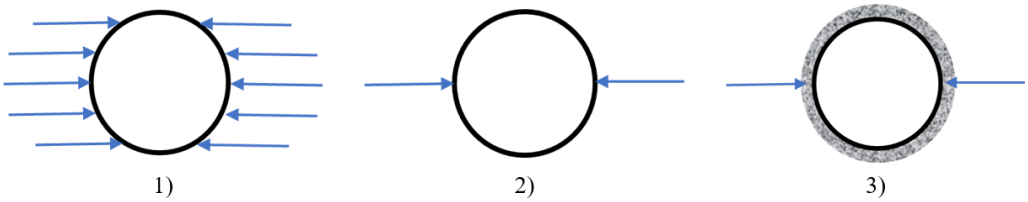

Figure 21 Three non-uniform load cases: 1) Uni-directional, 2) Opposed line loads and 3) Opposed line loads with complete restrain to radial displacement

Critical failure of the liner can be determined in two ways; failure by collapse caused by elastic instability or yielding of material. For slenderness ratios up to 32, plastic yielding occurs at lower values than required for elastic collapse.

According to (Nester, et al., 1955), if the stress distribution in the liner wall is considered strictly elastic, the maximum distortion strain energy criterion states that plastic yielding occurs at the point where principal stresses surpass material yield stress for uni-axial load.

$$(\boldsymbol{\sigma_1 - \sigma_2})^2 + (\boldsymbol{\sigma_2 - \sigma_3})^2 + (\boldsymbol{\sigma_3 - \sigma_1})^2 > \boldsymbol{2\sigma_y}^2 \tag{4.41}$$

σ_1, σ_2 and σ_3 are the three principal stresses and σ_y is the yield strength for uni-axial loading.

One of the principal stresses, σ_3, is axial stress. If there are no applied axial loading and vertical displacement is restricted, which means axial strain is zero, then

$$\sigma_3 = v(\sigma_1 + \sigma_2) \tag{4.42}$$

Where υ is Poisson's ratio.

Inserting equation 3.23 into 3.22, one gets (Nester, et al., 1955):

$$|\sigma_1 - \sigma_2| = 1{,}13\sigma_y \left(1 - 0{,}08\sigma_1 \frac{\sigma_2}{{\sigma_y}^2} + \cdots\right) \tag{4.43}$$

Here is v set to 0,3 and σ_y is the same for tension and compression. Yielding occurs first at the points where one of the principal stresses are equal to σ_y and the other principal stress are relatively small. Correction terms in parenthesis can be neglected and effectively increased yield strength of 13 percent due to axial constraint can be assumed.

4.2.2.1 Uni-directional load, uniform along diameter

Mathematical theory of elasticity is used to compute the elastic stress distribution in the liner wall. Tangential and radial stresses, as well as shear stress inside liner wall, is a function of r and θ in general. Which sequentially is certain partial derivations of the general solution to the Airy stress function, (Nester, et al., 1955):

$$\sigma_r = \frac{1}{r} * \frac{\partial \emptyset}{\partial r} + \frac{1}{r^2} * \frac{\partial^2 \phi}{\partial \theta^2}$$

$$\sigma_\theta = \frac{\partial^2 \phi}{\partial r^2}$$

$$\tau_{r\theta} = \frac{1}{r^2}\frac{\partial \theta}{\partial \theta} - \frac{1}{r}\frac{\partial^2 \phi}{\partial r \partial \theta}$$

Where ϕ, the stress function, in this case is given by:

$$\phi = A_0 \ln r + 3_o r^2 + C_o r^2 \ln r + \left(A_2 r^2 + B_2 r^4 + {}^{C_2}/_{r^2} + \zeta_2\right) \cos 2\,\theta \qquad (4.44)$$

By equating values for σ_r and $\tau_{r\theta}$ at boundaries r = a and r = b, we can determine coefficient for this stress equation:

At r = a: $\sigma_r = -P \; and \; \tau_{r\theta} = 0$
At r = b: $\sigma_r = -\frac{P}{2}(1 - \cos 2\theta) \; and \; \tau_{r\theta} = -\frac{P}{2}(1 - \sin 2\theta)$

Then it's necessary to find the position where

$$|\sigma_1 - \sigma_2| = \sqrt{(\sigma_\theta - \sigma_r)^2 + 4{\tau_{r\theta}}^2}$$

is maximum so criterion for yielding from eq. 3.23 can be applied. $|\sigma_1 - \sigma_2|$ should be max near inner wall at θ = 0 or 180 degrees, or at 90 or 270 degrees. Here, τ should be zero and $\sigma_1 - \sigma_2$ almost equal to $\sigma_\theta - \sigma_r$.

Then the computations at r = a result in:

$$\sigma_\theta - \sigma_r = -(P_o - 2P_i)\left[\frac{K^2}{4(K-1)}\right] - P\left[K^2(3K-2)\frac{K-2}{8(K-1)^2}\right]\cos 2\theta \qquad (4.45)$$

Where K is the slenderness ratio (D/t) of the liner.

$|\sigma_\theta - \sigma_r|$ is maximal at 0 and 180 degrees if $P_i < 0{,}5P_o$ and maximal at 90 and 270 degrees if $P_i > 0{,}5P_o$. For either of those internal pressure conditions:

$$|\sigma_\theta - \sigma_r|_{max} = \left(\frac{K^2 P_o}{K-1}\right) * \left[\frac{\in}{4} + \frac{(3K-2)(K-2)}{8(K-1)}\right] = Pf(\in, K) \tag{4.46}$$

Where $\in = \left|\frac{P_o - 2P_i}{P_o}\right|$. Applying this to eq. 3.23 the outcome is:

$$\frac{P_o}{\sigma_y} = \frac{1{,}13}{f(\in, K)} \tag{4.47}$$

This is the curve of fail resistance for these loadings. If $\in = 1$, which means P_o or $P_i = 0$, equation 3.28 reduces to:

$$\frac{P_o}{\sigma_y} = \frac{8}{3} 1{,}13 \frac{(K-1)^2}{K^2}(K^2 - 2K + 2) \cong \frac{3{,}0}{K^2} \tag{4.48}$$

Equation 3.29 defines failure resistance for case 1. Noted that the liner is only slightly stronger for $\epsilon = 0$. The gain in failure resistance is approximately 11% for thick-walled liners and only a tiny 1% for thin-walled liners.

The curved-beam analysis, which involves minor simplifying assumptions, results in:

$$\frac{P_o}{\sigma_y} = \frac{8}{3} \frac{1{,}13}{(K^2 - 1)} \tag{4.49}$$

Analysis of the theory of elastic stability gives the following equation for elastic collapse curve:

$$P_o = 1{,}4P_i + \frac{8\pi E}{9{,}02}(1 - v^2)(K-1)^3 \tag{4.50}$$

Where E is Youngs modulus. For steel (E = $30*10^6$ psi), this can again be reduced to:

$$\frac{P_o}{\sigma_y} = 1{,}4\frac{P_i}{\sigma_y} + \frac{92 * 10^6 psi}{\sigma_y}(K-1)^3 \tag{4.51}$$

Which lies well above the plastic yielding curve at K=32, even for $\sigma_y = 110\ 000$ psi. When considering this case, the elastic collapse criterion for steel, given as:

$$P_o = P_i + \frac{66 * 10^6\ psi}{(K-1)^3} \tag{4.52}$$

The equation above indicates that the pipe is more stable against elastic collapse than hydrostatic load on the outside.

4.2.2.2 Concentrated opposed line loads

Different from case 1, the distributed external load, P_o, is replaced by two opposed line loads, F, at $\theta = 90°$ and $\theta = 270°$ respectively, shown in Figure 21.

To compute this case, it is easier to use the curved-beam theory. Here the tangential stress, σ_θ, is produced by the bending moment from outside load and hoop stresses induced by both outside load and internal pressure are calculated as functions of θ.

Maximum absolute value of $\sigma_\theta - \sigma_r$ equal to $\sigma_\theta + P_i$ at r = a is set to $1{,}13\sigma_y$, giving (Nester, et al., 1955):

$$\frac{F}{D}\sigma_y = \frac{1{,}13}{\left[(K-1)(0{,}96K - 0{,}32) + \frac{1}{2}\zeta(K+1)\right]} \tag{4.53}$$

Where $\zeta = \frac{P_i D}{F}$. For ζ =1, the liner is 13% weaker for K=6 and only 2% weaker for K=32. F is the outside loading force in pounds per unit axial length.

Elastic collapse curve for this case is given by

$$\frac{F}{D} = \left(\frac{\pi}{2}\right) P_i + \frac{\pi E}{(1-v^2)}(K-1)^3 \tag{4.54}$$

And for steel

$$\frac{F}{D}\sigma_y = 1{,}57\frac{P_i}{\sigma_y} + \frac{104 * 10^6 psi}{\sigma_y}(K-1)^3 \tag{4.55}$$

Equation 3.35 is well above equation 3.33 even for yield strength up to 110 000 psi and K-value equal 32.

For case 2, opposed line loads, the liner will only resist about half the load as for case 1, much because bending moment is doubled when considering loading on a line and not distributed.

4.2.2.3 Opposed line loads, complete restrain in perpendicular direction

This analysis is developed in a similar manner as for case 2 using theory of bending of curved beams. Constraints at $\theta = 0° \; and \; 180°$ is replaced by a pair of opposing reaction line loads, Q. Using an expression for liner strain energy per unit length, U, the magnitude of Q can be determined. Since displacement is not present at the lines of application,

$$\frac{\partial U}{\partial Q} = 0$$

And if only strain energy caused by bending is considered

$$Q = 0{,}918F$$

Where F is defined as in case 2. The failure resistance curve is given by:

$$\frac{F}{D}\sigma_y = 1{,}13\left[(K-1)(0{,}45K - 0{,}61) + \frac{1}{2}\zeta(K+1)\right] \tag{4.56}$$

And the elastic collapse curve can be written as:

$$\frac{F}{D} = 0{,}82P_i + 2{,}61\frac{\pi E}{(1-\upsilon^2)}(K-1)^3 \tag{4.57}$$

This is also much higher than the yielding curve. Constraint in lateral direction has doubled the liner strength. The failure resistance curves of case 1 and 3 are approximately superimposed.

4.3 Liner deformation challenges on Valhall

Valhall wells can be divided roughly into four categories in terms of liner deformations, (Kristiansen, et al., 2000):

1. The production interval with perforations
    a. Often very rapid deformations
    b. Chalk production in combination with compaction results in buckling in deviated and vertical wells
    c. Chalk production in combination with compaction results in cross-sectional collapse in highly deviated and horizontal wells
    d. Potential shear deformations along faults and induced hydraulic fractures during compaction or chalk production
2. The interval between the perforations and the cap rock
    a. This section is often left un-perforated and is used as a contingency when the top perforated interval is no longer accessible after a chalk influx
    b. Un-perforated, this section has a relatively low frequency of deformations, especially in horizontal wells
    c. When the section is perforated, it acts as a normal production interval
3. The section at the top of reservoir/cap rock transition
    a. The production liner is often placed as close to top reservoir as possible
    b. Casing deformations are most frequent in this part of the overburden and can be found anywhere from top chalk to Middle Eocene
    c. There also seems to be a relation between chalk production and liner deformation in the deeper part of the cap rock (discussed more later)
4. The section through the shallower overburden
    a. The deformations have a higher frequency in the deeper part

The shallowest deformation to date has been found around 500 meters above the top of the reservoir.

4.3.1 Compaction-induced deformation

Due to high porosity zones, over-pressured reservoir and large production drawdown, Valhall has experienced significant compaction. This have ultimately affected the wells integrity negatively both in the overburden and the reservoir, leading to casing and liner failures.

Liner deformation within the reservoir can mostly be observed around perforated intervals and are associated with solids production and lateral stress reduction because of depletion. In vertical wells, this phenomenon is called column buckling and is caused by the compaction forces exerting axial loading on the pipe. Adding in the fact that lateral constrain is removed because of cavities around the pipe made by chalk production, a non-uniform load case is developed on the pipe ultimately leading to buckling and deformation.

The greatest stress anisotropy in a normal fault regime, assuming equal horizontal stresses, is experienced in a horizontal wellbore. As the production start-up is closer to the chalk failure conditions due to the large stress anisotropy, horizontal wells have larger risk of chalk production. Like the vertical case, the wellbore is exerted to compaction forces leading to a non-uniform loading case resulting in cross-sectional ovalling and deformation.

4.3.2 Overburden

Although this is not the focus of this thesis, the following is a short summary of overburden well failures encountered on Valhall is given in this Section.

Collapsed wells in the overburden was a substantial problem at the Valhall field throughout the 80’s and 90’s. Reservoir compaction has played a part here, as the overburden also have experienced subsidence resulting in shear movements in weak rock. This load case has tested the wells shear displacement capacity along shear zones of about 1 meter in thickness, measured from calliper data, shown in Figure 22.

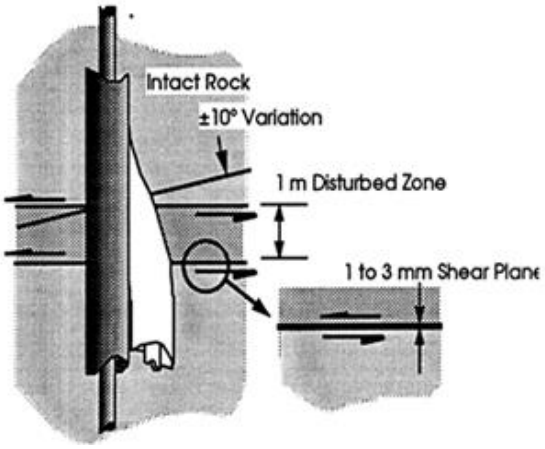

Figure 22 Shear displacement zone in overburden (Kristiansen, 2015)

Extending well life through the challenging subsurface at Valhall has been assessed, and based on field data, laboratory data and numerical modelling, these well design considerations listed in (Kristiansen, 2015) has been used:

1. Avoid well locations where too large shear stresses are going to build-up over the life of the well
2. Increased wellbore diameter with no cement between wellbore wall and outer pipe
3. Increased steel grade of inner pipe in a concentric configuration with cement between the two pipes
4. Increased steel grade of outer pipe in a concentric configuration with cement between the two pipes
5. Increased t/D ratio of inner pipe in a concentric configuration with cement between the two pipes
6. Increased t/D ratio of outer pipe in a concentric configuration with cement between the two pipes
7. Using sealed casing connections
8. Minimize pressure differential between pore pressure and internal pressure in the inner pipe

The main feature that contributed the most to increased shear displacement and thus extending well life on Valhall, was the cemented concentric liner lap. This configuration provided a significant displacement tolerance in excess of the maximum limit.

Studies performed (Kristiansen, 2014) showed that no wells drilled after 1999, has failed in the overburden. Estimates also showed that the life expectancies of the wells were increased from 6-10 years in the old wells to 16-24 years for the new wells, and even higher for those drilled outside the crestal area.

4.3.3 Non-uniform load case on Valhall

As mentioned in section 4.3.1, the wells on Valhall experiencing solids production will have large washouts on the outsides of the liner in the affected areas. This will ultimately lead to a non-uniform load exerted on the liner due to the heavily compaction forces from the overburden and the loss of lateral constrain.

4.3.4 Remedial action

At the same time as the shear displacement problem in overburden was addressed, another challenge also had to be dealt with. The estimation of the well performance of the horizontal wells implemented in the early 90s, was too optimistic. Well failure rate increased significantly after these wells were installed at Valhall. A new well design had to be developed to deal with the chalk influx problems and the resulting load case.

4.3.4.1 Concentric cemented liners

The first concentric liners were installed in 1992 in the horizontal A-28 well. A 9 5/8" production casing was set just inside the Tor formation. The outer liner was a 7", 29 ppf, grade N-80 with a 5", 18 ppf, grade Q-125 liner cemented inside. Chalk influx created problems shortly after production start and liner collapse was detected within the first year.

A new concentric liner was also tested a year later in the deviated A-24 well. This well was completed with same liner properties as A-28 except the inner string had grade P-110 instead of Q-125. Possible collapse was met just half a year after production start-up.

Taking the long horizontal section in the A-28 into account, it is difficult to perform a good cement job in the annulus between the two liners, i.e. to get 100 % cement displacement. Most likely the cement job performed has not been satisfying resulting in the concentric liners

loosing substantial collapse resistance. The collapse was also in a perforated area across a fault. Adding these factors in to the load case, it ultimately lead to liner collapse.

A plot of radial displacement versus external pressure and line load for concentric liners can be seen in Figure 23 Radial displacement vs. external pressure and line load magnitude for both concentric and heavy wall liner .

4.3.4.2 Heavy wall liners

The new option, after failure of the concentric liners, were heavy wall liners. The idea was simple, increasing wall thickness thus increasing both collapse and buckling resistance. Thicker walled liners also have higher resistance to radial displacement, shown in Figure 23. Slenderness ratio in these liners were reduced to under 6. Two options were tested, 6 5/8" outer diameter liner with 66 ppf and 5 ½", 46 ppf liner. Some medium thick liners were also tested, like the 5" 26,7 ppf used in the S-3 well on the southern flank where less risk of chalk influx was anticipated. Well failure rates decreased drastically after the implementation of these thicker liners around 1995. In addition, these wells were completed with 180° perforation phasing. Perforations were oriented in vertical direction, thus increasing wellbore stability during production.

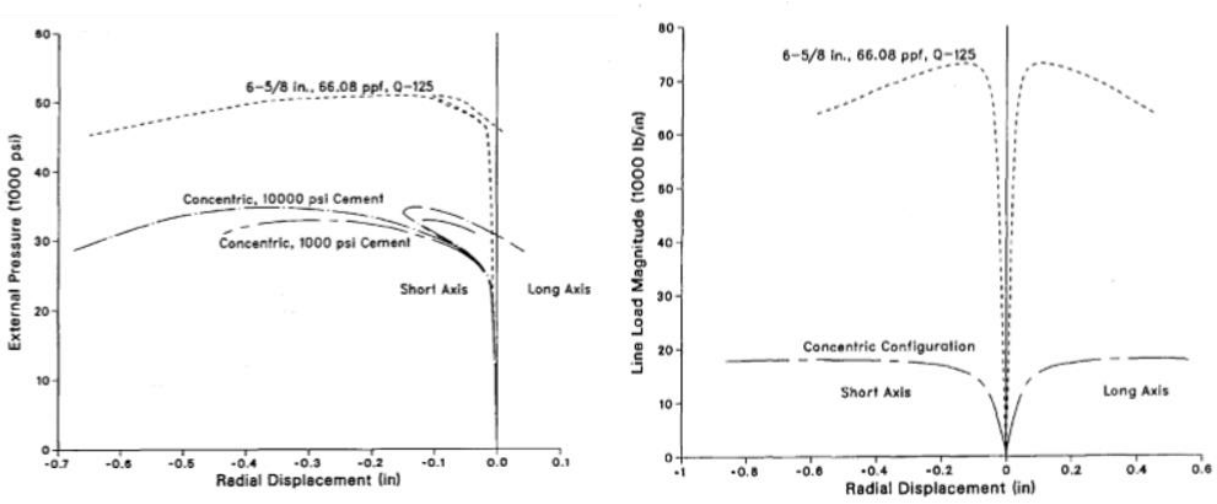

Figure 23 Radial displacement vs. external pressure and line load magnitude for both concentric and heavy wall liner (Pattillo, et al., 1995)

As this thesis later show, some of these heavy wall liners may have deformed in later years. This may indicate a more dynamic load case in the reservoir than first anticipated, which should be further investigated.

4.3.4.3 Well management

After the observation of several horizontal wells troubled with chalk production and in worst case collapse, a profound focus on well management was developed. Detailed guidelines for opening and shut-down was provided. Experience was passed on to offshore production staff, as well as full time well performance monitoring onshore. Sand (solids) detectors were mounted and remotely operated chokes were installed. Every well got an individual drawdown schedule depending on wellbore stability, solids production, completion quality, reservoir properties and response. The main strategy was to drawdown the well quickly the first days of opening to clean up the fractures and then gradually decrease the drawdown.

The acid fractured lower Hod wells usually required 3-4 months until the chokes could be fully opened, while the multiple proppant fractured Tor wells often needed a full year before operating at separator pressure. (Barkved, et al., 2003).

4.3.5 Valhall vs. Ekofisk

The Ekofisk field was the first oil discovery on the Norwegian sector. Located 20 km north of the Valhall field, the giant chalk reservoir can be referred to as Valhall's "big brother". Ekofisk was discovered in 1969, ordinary production started in 1972 and water injection was implemented already in 1986 (Norwegian Petroleum Directorate, 2018).

Casing failure on Ekofisk was believed to be a direct consequence of reservoir pressure depletion and resulting increase in effective rock stress. This was before reservoir-compaction was confirmed. Both thicker and concentric liners were unsuccessfully installed in the lower completion.

Due to the abundant use of deviated wells and acid stimulation creating washouts around the liner, deformation on the Ekofisk field can be heavily related to non-uniform load from compaction forces. Less support to the liner in the horizontal direction is the basis for non-uniform load.

Main differences between Ekofisk and Valhall is:

- Higher reservoir temperature
- More use of acid stimulation
- Larger subsidence
- Water flooding for a longer period
- Deviated wells more commonly completed

Higher reservoir temperature, larger subsidence and water flooding is the main reasons for more extensive compaction forces and well deformation problems on Ekofisk than Valhall.

5. Valhall failures - well data analysis

5.1 Data collection

To search for potential collapsed wells on the Valhall field, over 150 wells were analysed looking for a restriction, obstruction or a hold up point that could indicate failure. The focus was in the reservoir area, since the overburden problems have already been assessed. Well data listed in the summary found in Section 5.5, are collected from the Valhall well history book for both abandoned and current wells. In total, more than 2 000 pages of well history has been searched through. Some data were also provided by Tron Golder Kristiansen, Engineering Geology Manager at Aker BP. These wells were analysed, and quality checked up to several times to provide reliable data.

5.2 Heavy wall liner vs. conventional liners

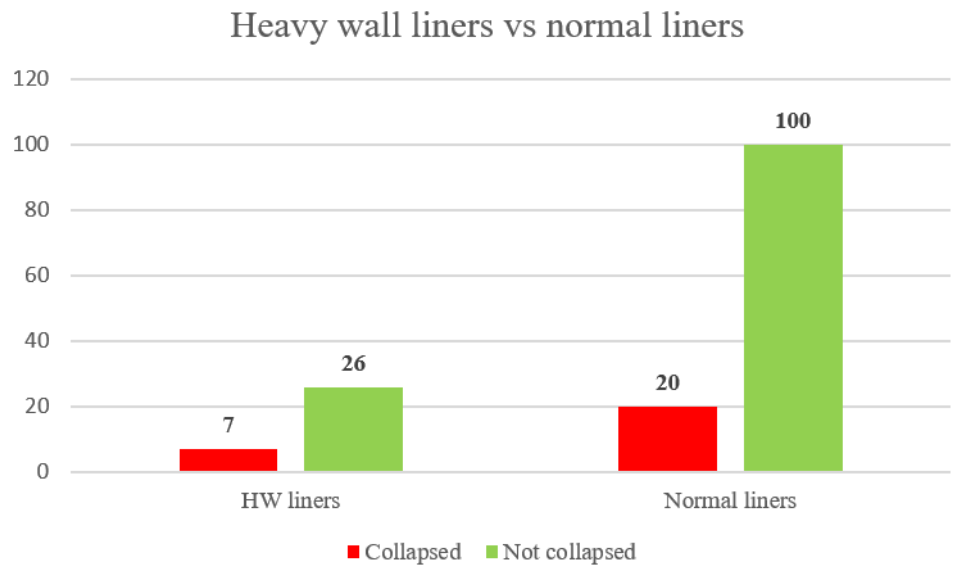

Figure 24 Overview over collapsed heavy wall and conventional liners

Of the 153 wells examined, 33 of these are installed with heavy wall liners. In this case, two liner designs are HW:

- 5 ½”, 45,5 ppf with slenderness ratio of 5,9
- 6 5/8”, 66 ppf with slenderness ratio of 5,93

Figure 24 shows that 7 of the 33 HW liner has strong evidence of deformation, this compares to a failure rate of 21,2 %. In comparison 20 of the 120 (17,5%) wells completed with slim liners has potentially deformed. These are staggering numbers, considering that the heavy wall liners were thought to not have failed yet.

5 of the 7 collapsed HW liners had experienced solids production, a strong indication of non-uniform load. Even though the initial HW design were estimated to bear the loads in the reservoir. The safest theory is that of kinetic energy release. Due to extensive chalk influx, the cavities around the liner grown large enough until a point where all the overlaying mass comes crushing down in a matter of seconds, deforming the liner instantly.

5.3 Analysis of dependencies of well deformation parameters

5.3.1 Distance to perforations

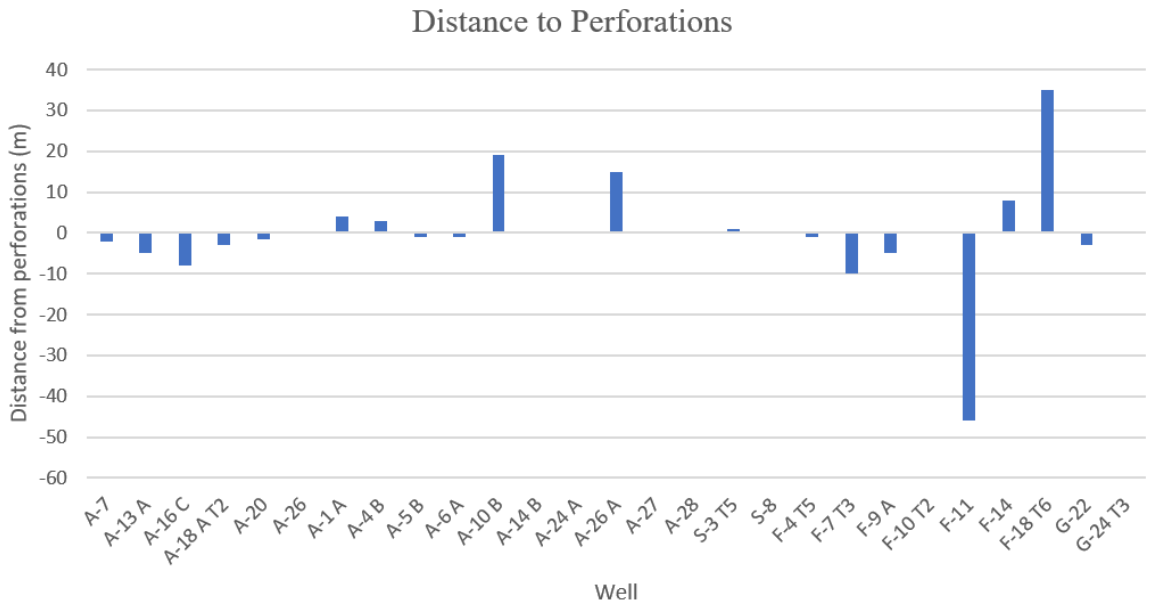

Figure 25 Distance from collapsed point to nearest perforations

Evaluation distance from collapsed depth to perforations is shown in the diagram above, it clearly shows that most of the wells are collapsed at a point within 5 meters of the perforation interval. 20 out of 27 collapsed wells is in the vicinity of 5 meter from the perforation interval, and 8 of those are collapsed inside the interval. In addition, because of some inaccuracy in the measured depth during the intervention when restriction was met, the rather small offsets of 1-

3 meters suggests that this number can be even higher. This plot presents clearly indicates that there is higher risk of collapsed liner in the producing interval at Valhall.

5.3.2 Inclination at collapse depth

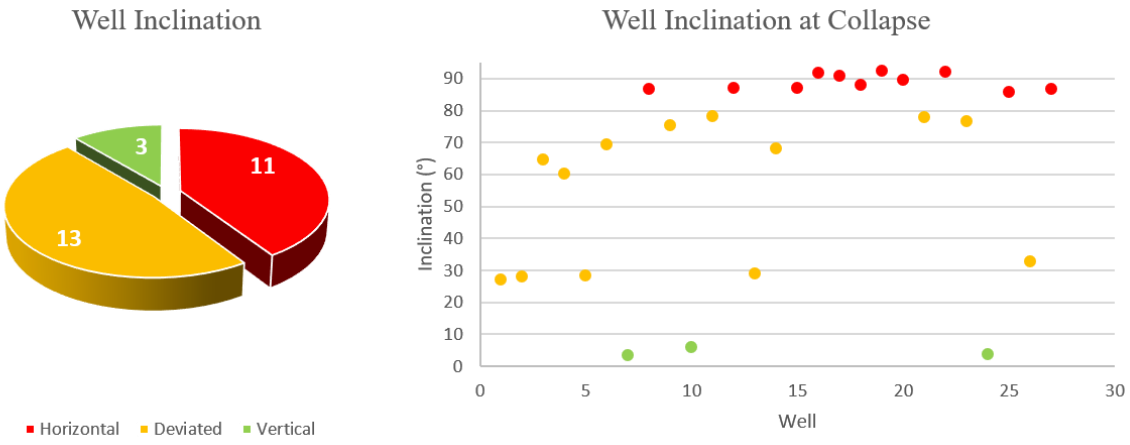

Figure 26 Inclination at collapse depth

The wells are divided into three categories; vertical, deviated and horizontal. Vertical wells have been considered as less than 25° inclination, deviated between 25-85°, and horizontal are high-angle wells with more than 85°. The well inclinations plotted are measured at collapse depth.

Of a total of 27 wells, 11 were horizontal, 13 deviated and 3 vertical. However, 19 of the wells had inclination above 60°. This might be an indication that high-angle wells have a higher risk of collapse at Valhall.

5.3.3 Porosity at collapsed depth

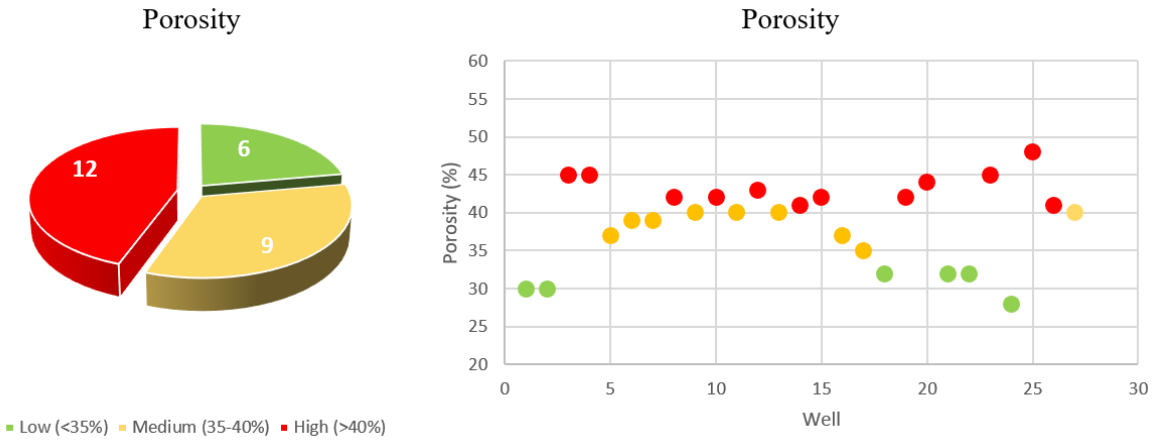

Figure 27 Porosity at collapsed depth

Valhall is considered as a high porosity chalk field with up to and even above 50% porosities in some cases. It is no doubt that these high porosities are contributing to the massive reservoir compaction and subsequently seafloor subsidence experienced on Valhall. Reservoir compaction is also leading to more strain exerted on the liners and is a plausible reason for collapse.

The wells have been divided into 4 categories; low (under 35%), medium-low (35-37%), medium-high (38-40%) and high porosity (above 40%). This seems reasonable since porosities around 40% is normal at the Valhall field. Porosity is measured at collapse depth.

Of all collapsed wells, 6 were in the low porosity range, 3 in medium-low, 6 in medium-high and 12 in the high porosity zone. It seems that high porosity wells are more likely to collapse, but again, porosity alone is not a driving mechanism for liner collapse.

5.3.3.1 Porosity vs. acid treatment

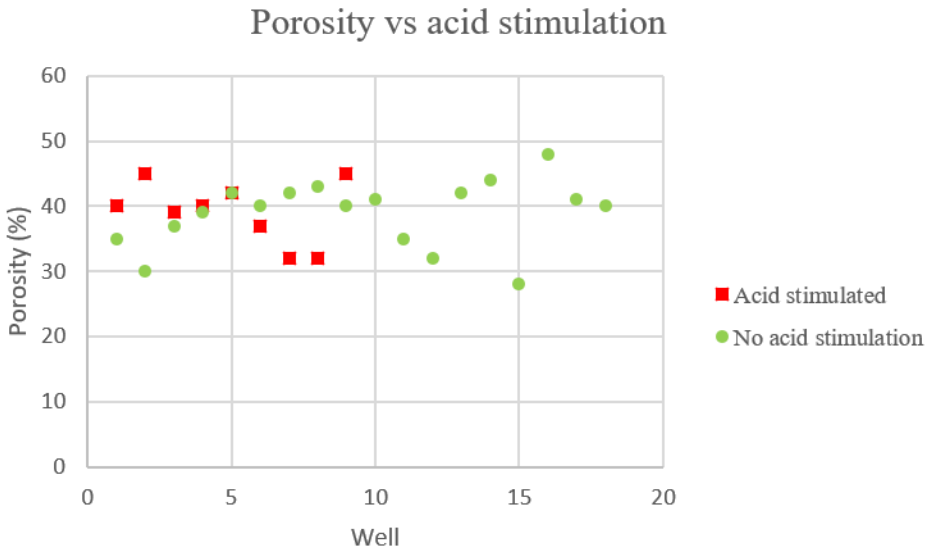

Figure 28 Porosity and acid treatment for the collapsed wells

10 wells of 18 in the medium-high to high porosity range, were acid treated before collapse discovery. In additional 3 wells, acid was pumped during the intervention where restriction was met. As noticed, 10 out of the 13 wells that were acid stimulated before collapse was discovered, had porosities above 38%, a relationship is possible.

5.3.3.2 Porosity vs. inclination

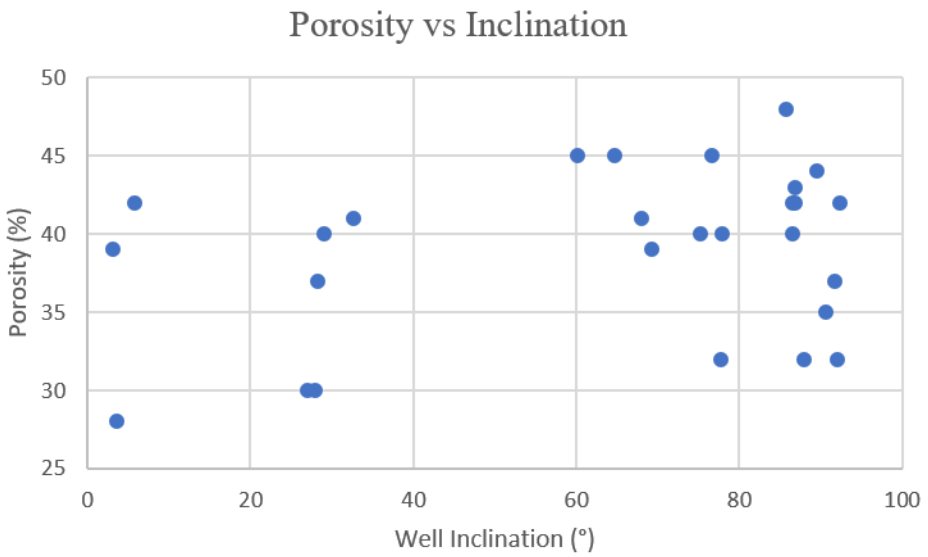

Figure 29 Cross plotting reservoir porosity and well inclination

Judging from the cluster in the upper right corner, high angle wells with high porosity have a larger risk of collapse.

5.3.3.3 Porosity vs. slenderness ratio

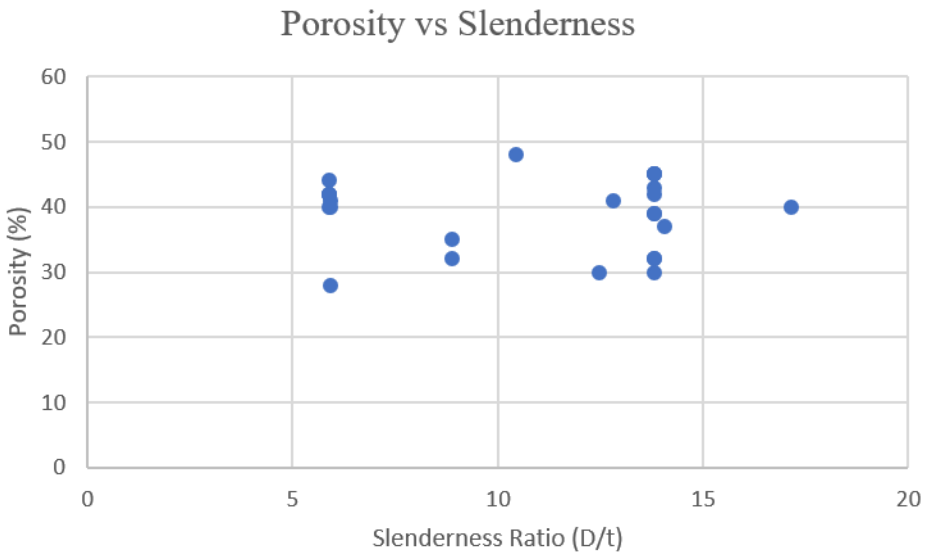

Figure 30 Cross plotting reservoir porosity and slenderness ratio

There seems to be no correlation between reservoir porosity and liner slenderness. Reservoir porosity has not been a factor in the liner slenderness design.

5.3.3.4 Porosity vs solids production

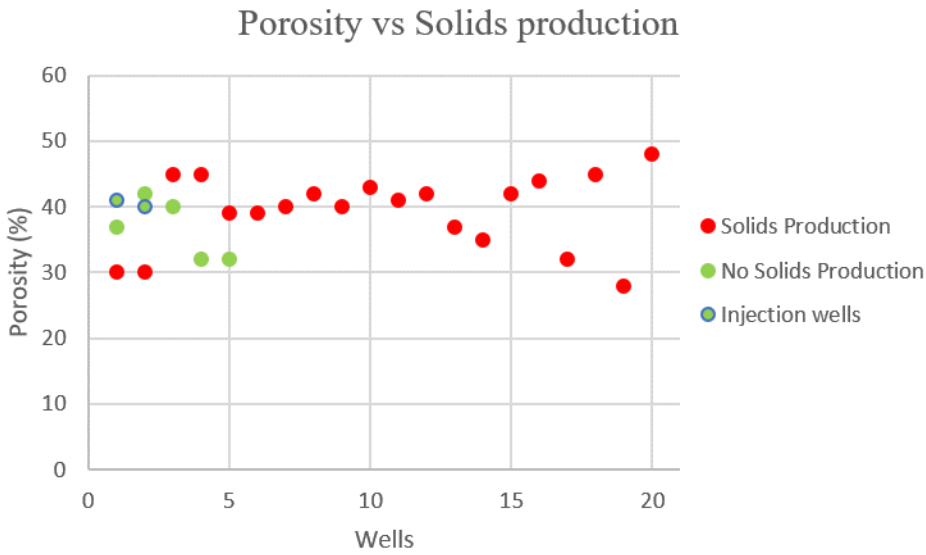

Figure 31 Cross plotting porosity and solids production

A many of the high porosity wells has experienced solids production. This indicates that wells producing from high porosity zones are prone to solids production. However, the solids producing wells in the plot above, is scattered across both high and low porosity. It cannot be clearly determined that high porosity affects solids production.

5.3.4 Time of production to collapse

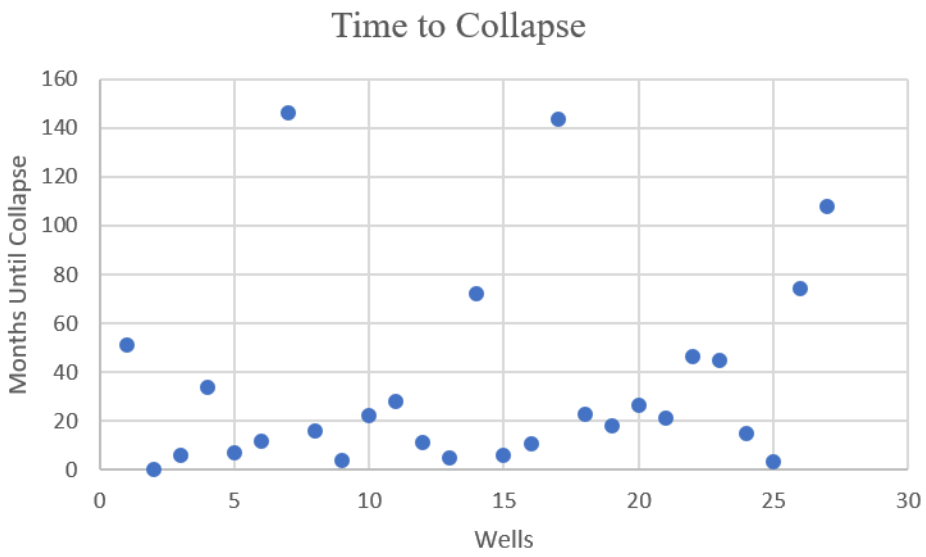

Figure 32 Time from production start until collapse indication

The plot shows how long time it took (in months since production start), until restriction/ obstruction was discovered for each well. Collapse may not be discovered until an intervention is conducted, and for some cases, where the well is still producing with the liner deformation it will logically take even longer time until collapse may be confirmed.

In 16 out of the 27 inspected wells, restriction was observed within the first 24 months since production start-up. 19 within the first 36 months. The remaining 8 wells had a production "life-time" of approximately 4 years or longer. One well, which showed problems with chalk production from the start-up, even ceased flowing after a couple of days.

5.3.4.1 Time of production vs. acid treatment

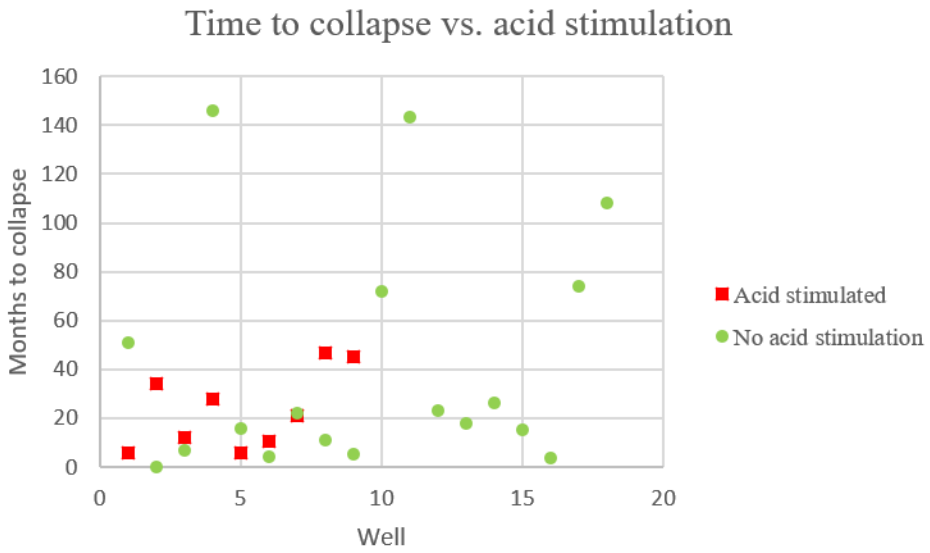

Figure 33 Time until collapse vs. acid treatment

This plot presents an overview of acid treated wells compared to time until collapse discovery. 21 out of the 27 wells were acid treated. 13 of these were stimulated before collapse and 5 were treated after collapse discovery. 6 wells were never exposed to acid. In 3 wells, acid was pumped when restriction was met, even though it safe to say that collapse most likely happened before acid was circulated.

It's difficult to conclude from this plot, as there are a variety of treated and non-treated among the early collapsed wells. Considering the long producing wells, there are approximately half and half regarding treated and non-treated. Probably there are other factors that contribute more to encourage liner collapse.

5.3.4.2 Time of production vs. porosity

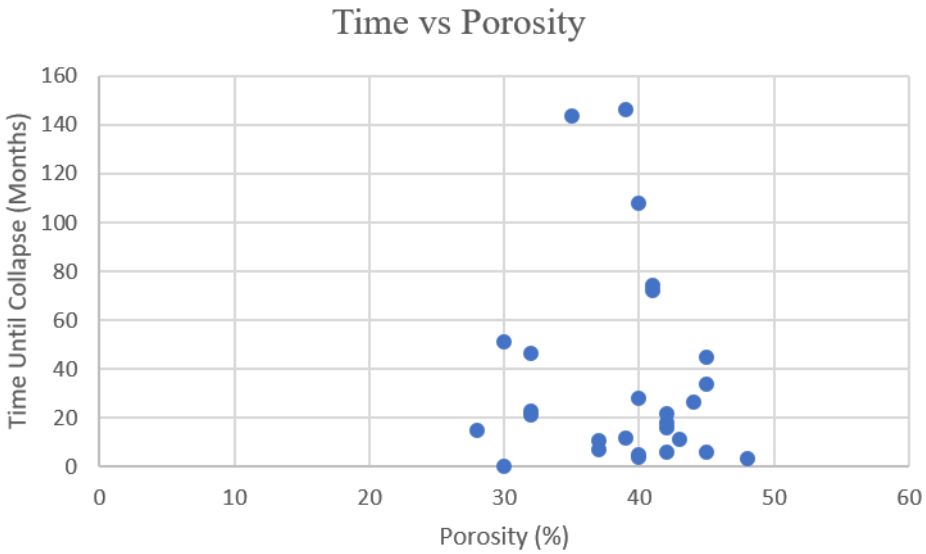

Figure 34 Cross plotting time until collapse with reservoir porosity

From this plot there seems to be a possibility that wells in higher porosity reservoir sections tend to collapse at an earlier stage than wells in lower porosity formation.

5.3.4.3 Collapse time vs solids production, porosity and slenderness ratio

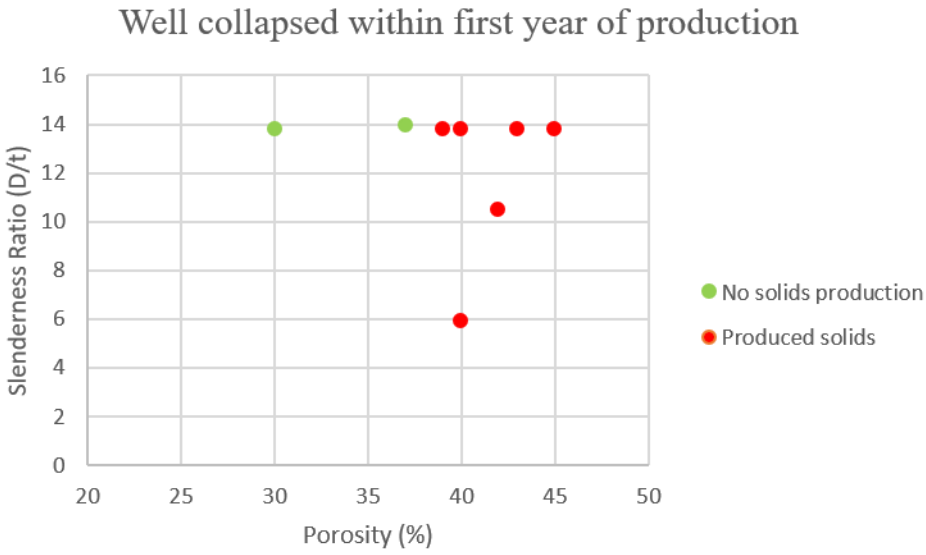

Figure 35 Solids production within the first year of production start-up

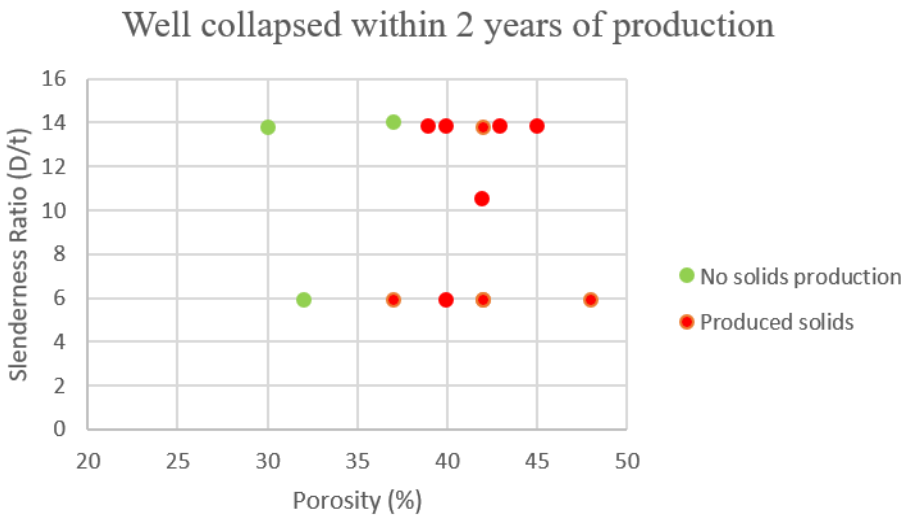

Figure 36 Solids production of wells collapsed within first two years of production start-up

Looking at Figure 35, it seems that wells completed with thinner liners who experienced solids production are collapsing at an earlier stage than others. However, the next figure shows that also heavy wall liners are collapsing relatively fast if experiencing problems with chalk production.

5.3.5 Solids production

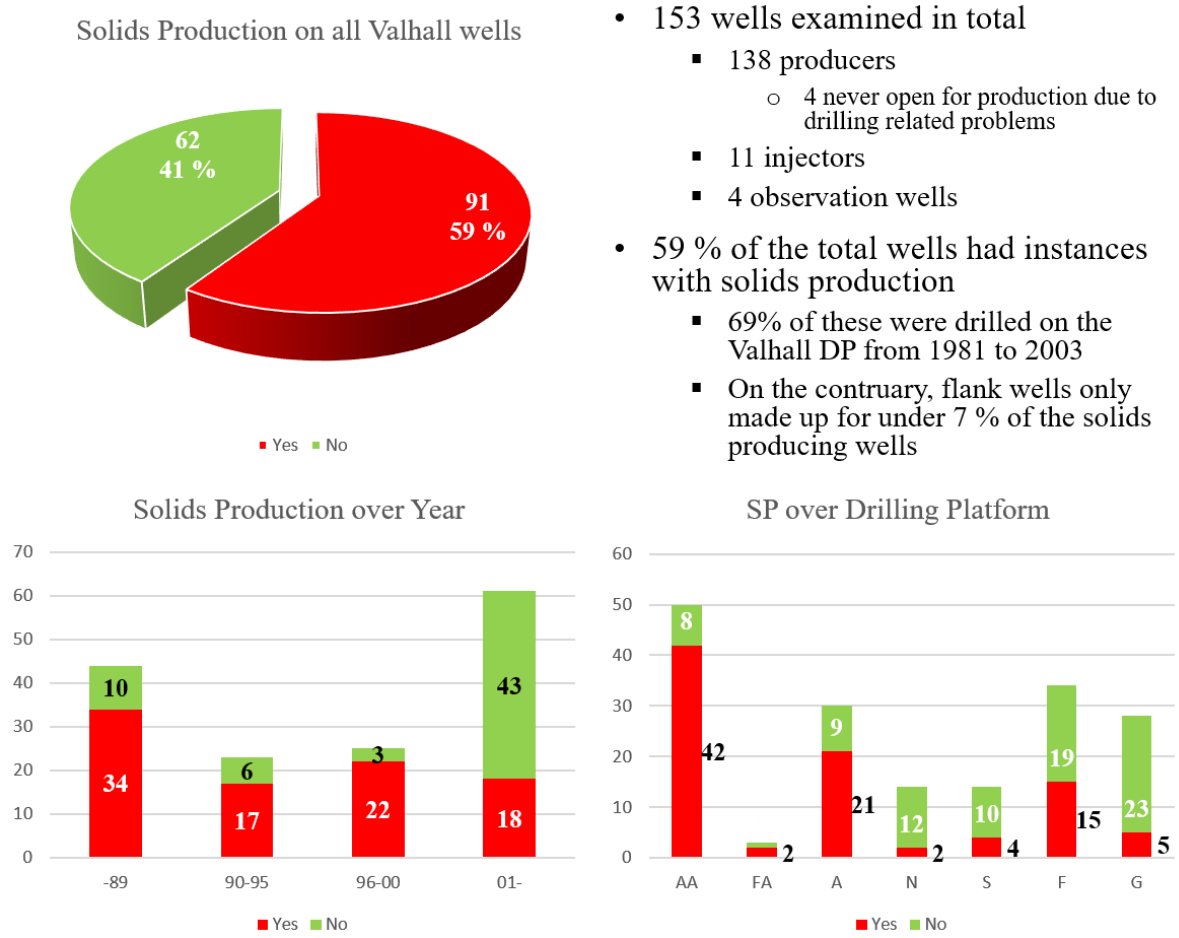

Figure 37 Overview of solids production on the Valhall field

Chalk production has been a serious issue on the Valhall wells, with 59% of the total drilled wells having some instances, some more severe than others, with solids production. 44 of total 53 abandoned wells were affected, which corresponds to 83 %. This indicates that solids production is a huge treat regarding well failure. However, it must be noted that the rate of solids producing wells has been drastically reduced since 2001. This is mainly because broad experience has led to newer and better completion and well management strategies.

5.3.5.1 Solids production for collapsed wells

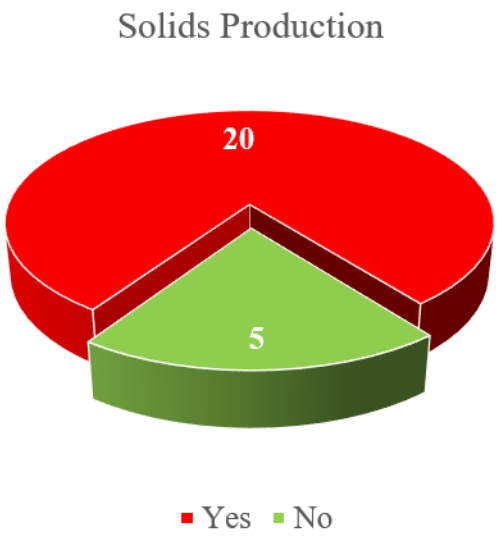

Figure 38 An overview of collapsed wells producing solids

20 out of 25 producers had problems with solids production. Some of them even had severe problems, leading to well shut-in. This is a clear indication of a possible relation between solids production and liner collapse.

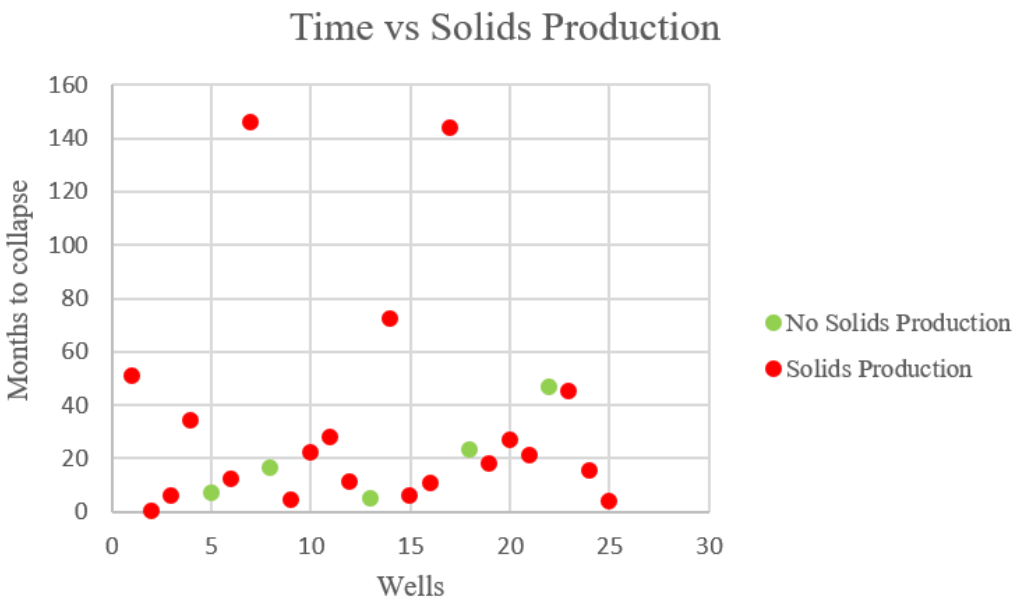

Figure 39 Cross plotting time until collapse with solids production

There is no indication of relation between chalk production and time until liner collapse. 20% of the examined production wells did not experience problems with chalk production, but as seen from the plot above, they collapsed relative early as well.

5.3.6 Slenderness Ratio

Figure 40 Slenderness ratio

14 of 25 wells, not including the wells with two concentric liners, have a slenderness ratio (D/t) of 12 or higher. According to equations from section 3.2.2, increased ratio will give reduced collapse resistance. Liners with thinner wall thickness tends to be more prone to collapse.

5.3.6.1 Slenderness ratio vs. inclination

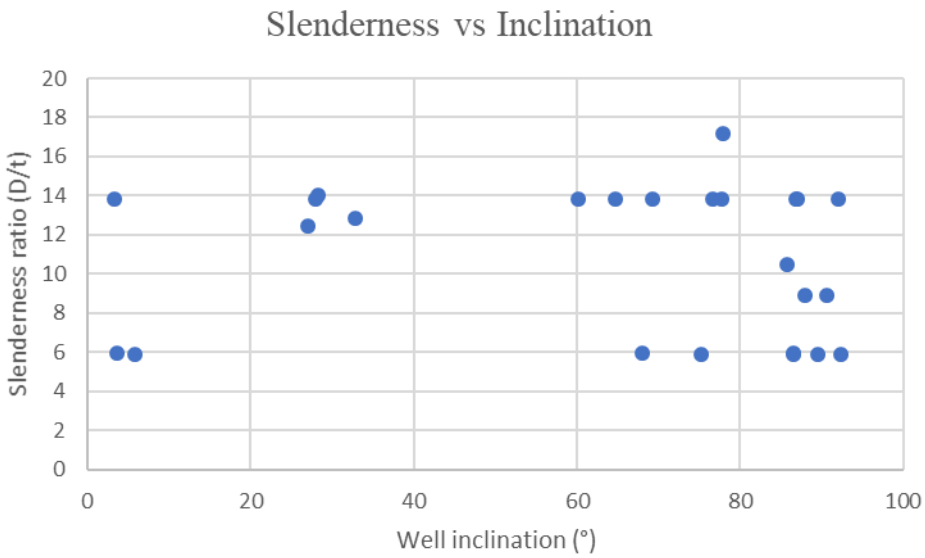

Figure 41 Cross plotting slenderness ratio and well inclination

It is difficult to see a relation between liner slenderness and well inclination concerning liner collapse. Slenderness ratio has not been an important design factor for inclined wells.

5.3.7 Perforation shot density

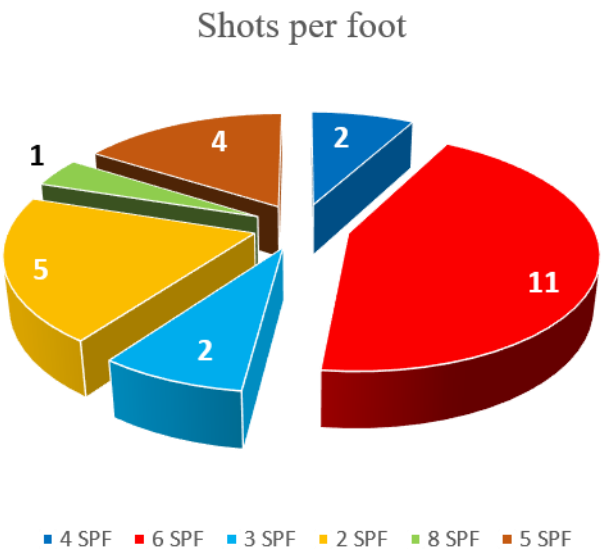

Figure 42 An overview of perforation density

There is an overweight of wells perforated with 6 shots per foot among the collapsed wells. The rates are ranging from 2 to 8 SPF, and even the highest rate of 8 is no way near the amount of shots per foot needed to impair the structural integrity or collapse resistance of the pipe. From Section 3.2.1, the marginal effect of perforations on the liner strength is shown. The low shot densities on Valhall are likely to have little effect on the liner deformation issue.

5.3.8 Analysis

Distance to perforations

This has not a direct impact on liner deformation alone but can indicate the reason for collapse. Wells collapsed at a reasonable distance outside of the perforated interval and they are most likely deformed because of formation or fault shear. Deformation caused by non-uniform load due to loss of lateral constrain can be ruled out.

Inclination

The plots conclude that there is a higher rate of high-angle wells, over 60° well inclination, which have collapsed. This is evidentially related to the fact that highly deviated wells are more prone to produce solids due to larger stress anisotropies around the wellbore. 83% of the high inclined wells had problems with chalk production.

As for the distance to perforations, well inclination at collapse depth has no direct impact on its own, it rather governs the liner deformation mechanism. Deformation in vertical wells is accommodated by axial shortening and radial displacement. Excessive axial strain will lead to buckling of the pipe. Deviated wells deform via bending in the liner dip direction, and a combination of axial shortening and liner ovalization. In highly inclined wells, deformation is assisted by radial reduction in the vertical direction and elongation in the horizontal direction.

Porosity

Wells completed in high porosity zones are be more prone to deformation. This can be linked to the fact that high porosity chalk is weaker than low porosity chalk. Compaction is also larger in higher porosity formation, subsequently inducing higher compaction strain on the liner.

Acid treatment seems not to be related to porosity, due to the reason that both acid treated, and non-acid treated wells have deformed in both high and low porosity zones. Cross-plotting porosity against well inclination, there seems to be an abundance of highly inclined wells in high porosity zones that have deformed.

Porosity and slenderness ratio of the liner do not have a relation, most likely because reservoir porosity has not been included in the well design. Most of the high porosity wells experienced solids production, but again so did most of the deformed wells. There might be some relation that higher porosity wells have a greater risk of chalk influx.

Slenderness ratio

A large amount of the deformed wells had a high slenderness ratio, i.e. thinner liners are more prone to deformation. This is evidentially because of the lower collapse resistance in thin walled liners.

However, it must be noted that 6 of the failed wells were heavy wall liners implemented in a new well design from 1999. It was the engineers in BP's perception that they had not failed yet, still there are clear indications of collapse from data collected in this Thesis. 5 out of 6 HW liners have experienced chalk influx. This suggests that the forces from non-uniform load when creating large cavity around the wellbore are more severe or maybe dynamic than first estimated. It can also be shearing due to a fault re-activation, then the wall thickness does not matter when large rock volumes are being displaced in matter of seconds. Slenderness ratio has not been a factor in the well design for highly deviated wells.

Time

Deformation of wells is likely to happen within the first 40 months of production. From cross-plotting it seems that thin liners in high porosity zones are deforming earlier than the rest. Although, it must be considered that many of the HW liners also deform with in the first 24 months. This can again be related to the load being more dynamic than static. Acid treatment seemed to be unaffected to the time until deformation occurred.

Solids production

84% of the producers had problems with solids production, this shows that chalk influx plays a big role in liner deformation on Valhall. In total 59% of all the wells, experienced solids production. This has been a huge challenge on Valhall and seems to also be a part of the liner deformation problem in the reservoir.

Perforation shot density

High shot density will weaken the collapse resistance of the liner. However, the densities used on Valhall are not large enough to play a significant role in the deformation. Perforation density can therefore be ruled out as main contributor to the investigated liner deformation.

5.3.9 Summary of well data analysis – cross plotting

The parameters examined do not seem to have a huge impact on the deformation on their own. However, a combination of several, it looks like a recipe for collapse. It is worth mentioning that both porosity and solids production seem to have a larger impact than the other parameters.

Analyses of highly deviated wells that have deformed within or close to the perforated interval have experienced instances of chalk influx and/or being stimulated with acid. These are all indications of a collapse due to non-uniform loading. Vertical wells with identical problems as above, have most likely deformed because of buckling as a result of lateral constrain loss. Based on the location of the failure, non-uniform load can certainly be ruled out if the distance to perforations is more than 5-10 meters. Deformations between or below perforation zones are harder to reveal but the failure mode is fault shear. These shear failures may be the reason to some of the HW liner deformation. Another reason for HW liners collapse can be found in the load case. Cavities around the pipe created by chalk influx around the liner/or acid, can eventually be large enough triggering the compacted overburden to crash and instantly collapse the liner in a matter of seconds. When these enormous forces are released in such a short time, it will be almost impossible to resist deformation, even for the heavy wall liners.

5.4 Parameters impact on liner deformation

The following section categories some of the most relevant parameters that influence on liner deformation in the Valhall field. The parameters are chosen based on the theory behind liner and liner deformation scenarios, analysis of the vast amount of data gathered and valuable input from a Rock Mechanics advisor at Aker BP. Deformation scenarios are described in Section 4. In addition to the above mentioned, trends in the cross plots of well-data in section 5.3 has been accounted for.

The 6 parameters in question are:

- Inclination
- Porosity
- Distance to perforation
- Slenderness ratio
- Solids production
- Acid Stimulation

The parameters are then categorised and ranked based on the impact they have on liner deformations, the categorization consist of 3 different levels red, yellow and green colour coding. A short theoretical description of all parameters is included for information.

Deformation Parameter Impact		
Parameter	**Theoretical Description**	**Impact**
Inclination	- Vertical wells is exerted to axial shortening and as a result, radial expansion. - Deviated wells will bend in the casing dip direction with maximum bending strain in the concave area. The liner deformation is accommodated by axial shortening combined with cross-sectional ovalling. - Axial shortening is reduced and radial deformation is boosted as well inclination increases, i.e. maximized liner deformation is in the direction of reservoir compaction. - Horizontal wells is mainly accommodated by radial shortening in vertical direction and elongation in horizontal direction, i.e an elliptical cross section.	Horizontal > 85° Deviated 25-85° Vertical < 25°
Porosity	High porosity weakens the formation and makes it more ductile and vulnerable to liquefication and subsequently solids production. The effective strain on the liner is also reliant on high porosity, because a weaker formation induces higher compaction strain on the liner. On the contrary, lower porosity gives stronger and more brittle formation.	High >40% Medium 35-39% Low < 35%
Solids Production	Fast production ramp-up gives a rapid reduction in pore pressure, leading to transferred stresses from the fluid phase to the chalk matrix. Cementation between the individual grains becomes weakened and the chalk turn into a granular material, called chalk liquefication. Solids production is characterized by heavy influx of liquefied chalk due to rapid changes in flowing bottom hole pressure and drawdown. For deviated/horizontal wells, localized washouts of chalk will remove lateral constrain and thus increase the effective vertical/radial stresses. This state gives high risk of axial compaction collapse. Vertical wells with no lateral constrain due to washouts will suffer from increased buckling collapse risk.	YES NO
Slenderness Ratio	Slenderness ratio is a very important factor for collapse resistance of the liner. Slenderness ratio dictates the most likely collapse regime. Lower slenderness ratio gives higher collapse strength.	Thin > 12 Medium 6-12 Thick < 6
Distance to Perforations	The distance between the collapsed area and perforations may be a good indication of the deformation mechanism. If the collapse has occurred outside of the perforation intervals, then axial compaction due to non-uniform load can be out-ruled. Collapse may be caused by fault movement. Negative signed distance is referring to deformations occurring at a shallower depth than perforations.	Inside 0-5 m Near 5-10 m Far > 10 m
Acid Stimulation	The acid treatments dissolve minerals in the chalk formation and create higher porosity and permeability giving higher productivity. In addition, the acid dissolves the chalk formation completely around liner, forming a cavity. The risk of solids production and washout around wellbore is hugely increased. Hence removing lateral constrain and increased collapse risk.	Initially Before Non

Table 2 Parameters impact on deformation

5.5 Well summary

All the wells have been undertaken an assessment with the parameter categorization as outlined in the Section above. The parameters impact is tabulated together with some key information, which is presented on a well by well basis. This structured means gives an overview of and the complex and comprehensive data set gathered. Figure 43 below, shows the potential collapsed wells and their location in the Valhall field.

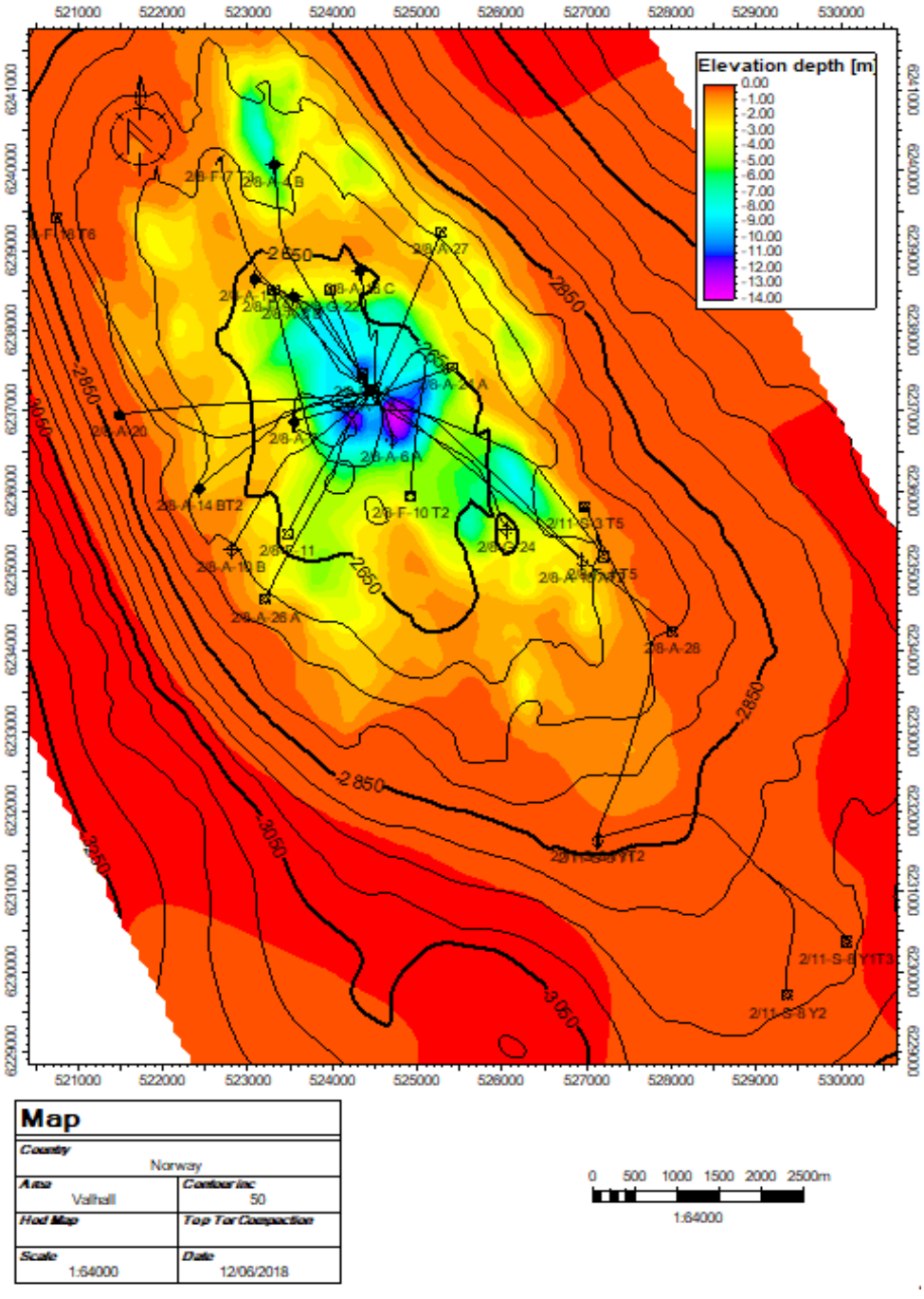

Figure 43 Location of potential collapsed wells in the Valhall field

5.5.1 Abandoned wells

The following 6 abandoned wells are those who have shown high potential of collapse.

2/8-A-7 (1983) Abandoned	**Deviated fractured Hod producer. Porosity around 30%.**			
General	Top Hod (m MD)	TD (m MD)	Collapse depth (m MD)	Inclination @ collapse
	2668	2856	2668	27°
Perforations:	Top perforation @ 2670 m. 3 3/8" guns, 8 SPF, 90° phasing.			
Liner	OD (") / Grade	Weight (ppf)	Wall thickness (")	Slenderness ratio
	7 / N-80	29	0,561	12,47
Well History	Hydraulic fractured without acid stimulation. Production start-up was in October 1983. Well restriction and possible collapse, was discovered 6th of February 1988. Several instances of solids production led to well cease flowing and abandoned.			

Inclination	Porosity	Distance to perforation	Slenderness Ratio	Solids Production	Acid Stimulation
27°	**30%**	**-2m**	**12,48**	**YES**	**NO**

Table 3 A-7 impact assessment

2/8-A-13A (1987) Abandoned	**Deviated hydraulic fractured Hod producer. Porosity around 30%.**			
General	Top Hod (m MD)	TD (m MD)	Collapse depth (m MD)	Inclination @ collapse
	3273	3471	3270	28°
Perforations:	327 5- 3290 m. 3 3/8" guns, 3 SPF, 120° phasing.			
Liner	OD (") / Grade	Weight (ppf)	Wall thickness (")	Slenderness ratio
	5 / P-110	18	0,362	13,81
Well History	The well was hydraulic fractured through perforations in Upper Hod. Production start-up February 1987 and washed down to a restriction at 3270m a couple of days later. The well flowed around 1000 bopd in the beginning then steadily declining, produced chalk/mud.			

Inclination	Porosity	Distance to perforation	Slenderness Ratio	Solids Production	Acid Stimulation
28°	**30%**	**-5m**	**13,81**	**YES**	**NO**

Table 4 A-13 A impact assessment

2/8-A-16C (1991) Abandoned	**Deviated Tor producer with three perforation intervals. Porosity up to 45%.**			
General	Top Tor (m MD)	TD (m MD)	Collapse depth (m MD)	Inclination @ collapse
	2854	3389	2864	64,7°
Perforations:	2865,5 - 3127,5 m. 3 3/8" guns, 3 SPF and 120° phasing.			
Liner	OD (") / Grade	Weight (ppf)	Wall thickness (")	Slenderness ratio
	5 / P-110	18	0,362	13,81
Well History	An acid stimulation was performed prior to production start-up in December 1991, following stimulations two times in July 1992 and again in January 1993. A possible shallower hydrate plug and a mechanical restriction at 2864 m (MD) was observed in June 1992. The liner collapsed at 2858m (MD), confirmed 18th of January 1993.			

Inclination	Porosity	Distance to perforation	Slenderness Ratio	Solids Production	Acid Stimulation
64°	**45%**	**-1,5m**	**13,81**	**YES**	**YES**

Table 5 A-16 C impact assessment

2/8-A-18AT2 (1986) Abandoned	**Deviated fractured Tor producer. Porosity approximately 45%.**			
General	Top Tor (m MD)	TD (m MD)	Collapse depth (m MD)	Inclination @ collapse
	4296	4457	4300	60,1°
Perforations:	4303 - 4315 m. 3 3/8" guns, 2 SPF, 180° phasing oriented.			
Liner	OD (") / Grade	Weight (ppf)	Wall thickness (")	Slenderness ratio
	5 / P-110	18	0,362	13,81
Well History	An acid fracture operation was done before production started 5th of October 1986. After only two days, the well ceased flowing due to chalk production followed by a diesel clean-out. Plugged with chalk again on 7th of February 1987. Another acid stimulation was performed in July 1987. A fracture job in Tor formation was conducted on 18th of August 1988, washed down and reamed to 4323 m MD. The workstring was twisted off below RN-nipple, suspected liner damage at 4300 m MD. No fracture job was conducted, and the well was left shut-in.			

Inclination	Porosity	Distance to perforation	Slenderness Ratio	Solids Production	Acid Stimulation
60,1°	**45%**	**-3m**	**13,81**	**YES**	**YES**

Table 6 A-18 AT2 impact assessment

2/8-A-20 (1988) Abandoned	Deviated propant fractured Tor producer. Porosity around 37%.			
General	Top Tor (m MD)	TD (m MD)	Collapse depth (m MD)	Inclination @ collapse
	4019	4334	4018	28,3°
Perforations:	4019,5-4031 m. 3 3/8" guns, 2 SPF, 180° phasing. Re-perforated: 3 3/8" guns, 6 SPF, 60° phasing.			
Liner	OD (") / Grade	Weight (ppf)	Wall thickness (")	Slenderness ratio
	7" / L-80	35	0,498	14,05
Well History	Well was fractured with 167 000 lbs proppants and gravel packed 8th of August 1988 and production started the 18th. March 10th, 1989; impression block stopped at top of screens at 4018 m MD. Indications of possible screen collapse. 27th of April; well shut-in, appeared to have died. Sidetracked on May 24th, 1989.			

Inclination	Porosity	Distance to perforation	Slenderness Ratio	Solids Production	Acid Stimulation
28,3°	**37%**	**-2m**	**14,05**	**NO**	**NO**

Table 7 A-20 impact assessment

2/8-A-26 (1992) Abandoned	Deviated proppant fractured Tor producer. Reservoir porosity approximately 39%.			
General	Top Tor (m MD)	TD (m MD)	Collapse depth (m MD)	Inclination @ collapse
	3745	5330	3774	69,3°
Perforations:	3774-3784 m. 3 3/8" guns, 6 SPF, 60° phasing.			
Liner	OD (") / Grade	Weight (ppf)	Wall thickness (")	Slenderness ratio
	5 / P-110	18	0,362	13,81
Well History	Stimulated with acid prior to production start-up 20th of April 1992. Ceased flowing due to solids production on 18th of September and stimulated October 1992. This sequence was repeated in January and April 1993. Acid wash down to 4017 m MD was performed each time. Tor formation was fracture stimulated 11th September 1993. Ceased flowing again and chalk/proppant was produced to surface. A solid restriction was encountered on 25th of March 1994. Well re-perforated and proppant fracture stimulated once more on March 24th, 1995. Indications of tubing collapse led to shut down in January 1996, a restriction at 3208 m MD was observed.			

Inclination	Porosity	Distance to perforation	Slenderness Ratio	Solids Production	Acid Stimulation
69°	**39%**	**0m**	**13,81**	**YES**	**YES**

Table 8 A-26 impact assessment

5.5.2 Shut-in or producing wells

The following wells have shown restrictions or obstruction indicating a collapsed wellbore during production, some wells are still producing and others shut-in for P&A.

2/8-A-1A (1993) Abandoned	**Vertical proppant fractured Tor producer, 39% porosity.**			
General	Top Tor (m MD)	TD (m MD)	Collapse depth (m MD)	Inclination @ collapse
	2458	2528	2478	3,2°
Perforations:	2468,7-2477,1 m. 3 3/8" guns, 6 SPF, 60° phasing, big hole.			
Liner	OD (") / Grade	Weight (ppf)	Wall thickness (")	Slenderness ratio
	5 / Q-125	18	0,362	13,81
Well History	Proppant fractured before production start 21'st of November 1993. Fractured, and re-fractured in May 95 and October 1996. Tagged fill at 2473 m and worked string down to 2478 m in the operation October 1996, recovered a mix of formation, cement and fracture sand. Water breakthrough indirectly from G-18 in July 2006. Unable to go deeper than 2221 m when running WL operation in August 2006.			

Inclination	Porosity	Distance to perforation	Slenderness Ratio	Solids Production	Acid Stimulation
3°	**39%**	**4m**	**13,81**	**YES**	**NO**

Table 9 A-1 A impact assessment

2/8- A-4B (1994) Unknown status	**Horizontal proppant fracture Tor producer, observation well. Porosity around 42%.**			
General	Top Tor (m MD)	TD (m MD)	Collapse depth (m MD)	Inclination @ collapse
	3633	4420	3743	86,6°
Perforations:	3738-3740 m. 3 1/2" guns, 6 SPF, 180° phasing.			
Liner	OD (") / Grade	Weight (ppf)	Wall thickness (")	Slenderness ratio
	6 5/8 / Q-125	66	1,123"	5,90
Well History	Proppant fracture stimulated three zones before production start-up in September 1995. Acid stimulated 1'st of October 1996, and again in April 2001. Could not wash through obstruction at 3741,1 m MD in January 1997. Indications of pinched/collapsed liner.			

Inclination	Porosity	Distance to perforation	Slenderness Ratio	Solids Production	Acid Stimulation
87°	**42%**	**3m**	**5,90**	**NO**	**NO**

Table 10 A-4 B impact assessment

2/8- A-5B (1997) Producer	Horizontal proppant fractured Tor producer. Porosity 40%.			
General	Top Tor (m MD)	TD (m MD)	Collapse depth (m MD)	Inclination @ collapse
	2665	3468	2783	75,3°
Perforations:	2781,25-2782 m. 3 1/8" guns, 5 SPF, 180° phas., 26 shots in 5 zones.			
Liner	OD (") / Grade	Weight (ppf)	Wall thickness (")	Slenderness ratio
	5 1/2 / Q-125	45,5	0,932"	5,90
Well History	Well was propped fractured and put on production 7th of January 1998. Tried to wash through obstruction at 2783 m MD with 15 % HCl, no progress. Scale squeeze operation was done during November 2006. A-5B was converted to waste injector on February 4th, 2011. Prepared for P&A in August 2015.			

Inclination	Porosity	Distance to perforation	Slenderness Ratio	Solids Production	Acid Stimulation
75,3°	**40%**	**-1m**	**5,90**	**YES**	**NO**

Table 11 A-5 B impact assessment

2/8- A-6A (1998) Unknown status	Vertical fractured Tor producer. Porosity 42%.			
General	Top Tor (m MD)	TD (m MD)	Collapse depth (m MD)	Inclination @ collapse
	2650	2729	2665	5,9°
Perforations:	2666-2684 m. 2 3/4" guns, 2 SPF, 180° phasing.			
Liner	OD (") / Grade	Weight (ppf)	Wall thickness (")	Slenderness ratio
	5 1/2 / Q-125	45,5	0,932"	5,90
Well History	Production start-up 28th of July 1998 after fracture stimulation. Possible FISH left in hole. Tag at 2667 m MD in June 2000. Tried to mill and pump acid through with no progress. Scale squeeze operation in conducted in May 2007. Well temporary P&A 22nd of June 2016.			

Inclination	Porosity	Distance to perforation	Slenderness Ratio	Solids Production	Acid Stimulation
5,9°	**42%**	**-1m**	**5,90**	**SEVERE**	**NO**

Table 12 A-5 B impact assessment

2/8-A-10B (1993) Unknown status	**Horizontal, 300 m perforated section in Tor. Acid stimulated in horizontal section and propped fracture stimulated in deviated section. Porosity 40%.**			
General	Top Tor (m MD)	TD (m MD)	Collapse depth (m MD)	Inclination @ collapse
	3172	4588	3212	78°
Perforations:	3282 m (fractured 3190-3193 m), 6 SPF, 60° phasing.			
Liner	OD (“) / Grade	Weight (ppf)	Wall thickness (“)	Slenderness ratio
	7 / L-80	29	0,408	17,16
Well History	Well was opened gently on 6th of January 1994 and encountered early signs of chalk production. Acid stimulated 1st of March 1995 and fracture stimulated 30th of January 1996. Restriction observed at 3212 m MD on 2nd of May 1996, acid circulated. Nitrified acid stimulation performed on 27th of June 2005. Well suddenly ceased flowing in July the same year. Bull-headed 6,5 bbls acid in April 2006. Permanently plugged and abandoned in August 2015.			

Inclination	Porosity	Distance to perforation	Slenderness Ratio	Solids Production	Acid Stimulation
78°	**40%**	**19m**	**17,16**	**YES**	**YES**

Table 13 A-10 B impact assessment

2/8-A-14B T2 (1992)	**Horizontal acid matrix stimulated Tor producer. Porosity 43%.**			
General	Top Tor (m MD)	TD (m MD)	Collapse depth (m MD)	Inclination @ collapse
	3015	3235	3084	86,9°
Perforations:	3045 - 3584 m. 3 3/8” guns, 6 SPF, 60° phasing.			
Liner	OD (“) / Grade	Weight (ppf)	Wall thickness (“)	Slenderness ratio
	5 / P-110	18	0,362	13,81
Well History	Production started 16th of July 1992. Acid pumped 13th of October same year. Well ceased flowing in February 1993 due to chalk influx. Tagged fill at 1175 m and cleaned out to hard spot at 3084 m MD June 17th, 1993. Possible liner collapse. Several chalk fills observed and washed down to obstruction at 3078 m MD. Acid spotted across perforations on July 9th, 1993. Acid matrix stimulation performed on March 23rd, 1995. Cleaned wellbore down to 3147 m MD with acid on April 16th, 1996. Several liner collapse erosion marks on CT. Restriction tagged at 3046 m MD on 3rd of October 1997, bull-headed acid. Environmental plug set March 2015. The well has died 9 times due to solids influx, last clean-out indicated further development of liner restriction/collapse. Liner damage at 3046 m MD.			

Inclination	Porosity	Distance to perforation	Slenderness Ratio	Solids Production	Acid Stimulation
86,9°	**43%**	**40m**	**13,81**	**YES**	**NO**

Table 14 A-14 BT2 impact assessment

2/8-A-24A (1993)	Deviated proppant fracture stimulated Tor producer with dual concentric liner. Porosity 40%.			
General	Top Tor (m MD)	TD (m MD)	Collapse depth (m MD)	Inclination @ collapse
	2698	-	2730	29°
Perforations:	3045 - 3584 m. 3 3/8" guns, 6 SPF, 60° phasing.			
Liner	OD (") / Grade	Weight (ppf)	Wall thickness (")	Slenderness ratio
	7 / N-80	29	0,408	17,15
	5 / P-110	18	0,362	13,81
Well History	Fracture stimulated, direct water-based resin coated on 14th July 1993. Opened well to production. Made several attempts to pass obstruction at 2731 m MD without success. Tagged at 2730 m MD on January 13th, 1998. Acid wash of proppant fracture performed on 15th of August 2000. Eventually dead and unable to produce due to plugged wellbore. P&A candidate.			

Inclination	Porosity	Distance to perforation	Slenderness Ratio	Solids Production	Acid Stimulation
29°	**40%**	**15m**	**17,15/13,81**	**NO**	**NO**

Table 15 A-24 A impact assessment

2/8-A-26A (1996)	Horizontal proppant fractured Tor producer. Porosity 41%.			
General	Top Tor (m MD)	TD (m MD)	Collapse depth (m MD)	Inclination @ collapse
	3549	4389	3586	68°
Perforations:	3565 - 3566,5 m. 3 1/8" guns, 5 SPF, 180° phasing.			
Liner	OD (") / Grade	Weight (ppf)	Wall thickness (")	Slenderness ratio
	6 5/8 / Q-125	65,8	1,118	5,93
Well History	Fracture stimulated in 3 zones prior to production start 3rd of May 1996. Well unstable due to solids production. Tagged hard spot at 3586 m MD, pumped acid pill but no progress on 22nd of May 2002. Attempted to pass obstruction with mill and acid on 1st of April 2004, not able to pass. Perforated new zone above obstruction. Zone 1-4 isolated with mechanical plug, only producing from the shallowest zone 5.			

Inclination	Porosity	Distance to perforation	Slenderness Ratio	Solids Production	Acid Stimulation
68°	**41%**	**15m**	**5,93**	**YES**	**NO**

Table 16 A-26 A impact assessment

2/8-A-27 (1991)	Horizontal proppant fractured Tor producer. Porosity 42%.			
General	Top Tor (m MD)	TD (m MD)	Collapse depth (m MD)	Inclination @ collapse
	3370	3904	3434	86,9°
Perforations:	3385 - 3605,5 m. 3 3/8" guns, totally 395 shots.			
Liner	OD (") / Grade	Weight (ppf)	Wall thickness (")	Slenderness ratio
	5 / P-110	18	0,362	13,81
Well History	Acid fracture stimulated prior to production start, September 1991. Ceased flowing due to solid influx after a month. Pumped acid on 9th of November 1991. Well ceased flowing again in February 1992 due to chalk influx. Managed to wash down to 3430 m MD with acid, solid obstruction. Well died after shut-down in July 1992, milled down to obstruction at 3433 m MD, injected more acid. Ceased flowing again in August 1992, plugged. Washed down to 3428 m MD, pumped more acid. Acid treatments occurred in November 1992, January 93, April 93, March 95, August 96, December 96, May 2001 and May 02. As from November 2005, the well is considered dead. Possible liner deformation in horizontal section.			

Inclination	Porosity	Distance to perforation	Slenderness Ratio	Solids Production	Acid Stimulation
86,9°	**42%**	**45m**	**13,81**	**YES**	**YES**

Table 17 A-27 impact assessment

2/8-A-28 (1992)	Horizontal perf. Tor producer with concentric liner. Porosity 37%.			
General	Top Tor (m MD)	TD (m MD)	Collapse depth (m MD)	Inclination @ collapse
	4275	5900	4687	91,8°
Perforations:	4550 - 5185m. 3 3/8" guns, 6 SPF, 60° phasing.			
Liner	OD (") / Grade	Weight (ppf)	Wall thickness (")	Slenderness ratio
	7 / N-80	29	0,362	17,16
	5 / P-110	18	0,408	13,81
Well History	Production started on 6th of October 1992. Well plugged by solids on March 10th, 1993. Restriction at 4687m (MD) was discovered July 21st, 1993, after around 10,5 months of production. Well history data shows that the well was cleaned out with seawater prior to production start-up and underwent acid stimulation in March 1995 and August 2000 after collapse indications.			

Inclination	Porosity	Distance to perforation	Slenderness Ratio	Solids Production	Acid Stimulation
91,8°	**37%**	**0m**	**13,81/17,16**	**YES**	**YES**

Table 18 A-28 impact assessment

2/11-S-3T5 (2004)	Horizontal proppant fractured (10 zones) Tor producer. Porosity 35%.			
General	Top Tor (m MD)	TD (m MD)	Collapse depth (m MD)	Inclination @ collapse
	3630	5898	5081	90,7°
Perforations:	10 zones in the interval 3675-5800 m. 3,3" guns, 4 SPF, 180° phasing.			
Liner	OD (") / Grade	Weight (ppf)	Wall thickness (")	Slenderness ratio
	5 / Q-125	26,7	0,563	8,88
Well History	Well handed to production in June 2005. Producing from all zones from 10th of August 2005. Gas lift valves installed in August 2013 and producing with GLV for the first time on 27th of September the same year. Performed clean-out on 22nd of May 2017, milled down to obstruction at 5081 m. Several failed attempts to pass. Observed chalk/proppants in return from 4400 m MD. Cyclic producer from November 2006.			

Inclination	Porosity	Distance to perforation	Slenderness Ratio	Solids Production	Acid Stimulation
90,7°	**35%**	**1m**	**8,88**	**YES**	**NO**

Table 19 2/11-S-3 T5 impact assessment

2/11-S-8 (2006)	Horizontal MLT Tor producer with two branches. Porosity 32%.			
General	Top Tor (m MD)	TD (m MD)	Collapse depth (m MD)	Inclination @ collapse
	3375	Y1 - 5256	3734	88°
Lower completion:	Y1 is an open hole lateral while Y2 is an uncemented liner. Swell packers at 4014,4, 4188,8 and 5159,3 m MD. Perf. valve at 4078,5 has 24 holes with diameter 0,625".			
Liner	OD (") / Grade	Weight (ppf)	Wall thickness (")	Slenderness ratio
	5 / Q-125	26,7	0,563	8,88
Well History	Production started on 12th of May 2006. Attempted to run PLT and perform WSO on April 6th, 2008. Obstruction at 3668 m MD, worked tractor down to 3734. Unable to pass several times.			

Inclination	Porosity	Distance to perforation	Slenderness Ratio	Solids Production	Acid Stimulation
88°	**32%**	**0m**	**8,88**	**NO**	**NO**

Table 20 2/11-S-8 impact assessment

2/8-F-4T5 (1996)	Horizontal proppant fractured Tor producer. Porosity 42%.			
General	Top Tor (m MD)	TD (m MD)	Collapse depth (m MD)	Inclination @ collapse
	3827	4917	4028	92,3°
Perforations:	4029,5 - 4031m. 5 SPF, 180° phasing, 6 zones w/ 26 shots.			
Liner	OD (“) / Grade	Weight (ppf)	Wall thickness (“)	Slenderness ratio
	5 ½ / Q-125	45,5	0,932	5,90
Well History	Fracture stimulated in all 6 zones prior to production start-up on 2nd of March 1997. Well produced solids. Unable to flow after SD on March 1st, 1998. September 2nd, 1998: Tag several times at 4536 m MD. Pumped acid, no progress. September 4th: restrictions seen at 4314m, 4172m and at 4035 m MD. 5th of September 1998: calliper logs suggest liner deformation at 4035 m and possible collapse at 4512 m MD. Well ceased flowing without warning in June 2001, chalk influx. Solid tag at 4028 m MD on 4th of July 2001. Pumped acid, no go. Several instances of solids production. Obstruction observed at 3188 m, no go with acid (24th Oct 92).			

Inclination	Porosity	Distance to perforation	Slenderness Ratio	Solids Production	Acid Stimulation
92,3°	**42%**	**-1m**	**5,90**	**YES**	**NO**

Table 21 F-4 T5 impact assessment

2/8-F-7T3 (1997)	Horizontal proppant fractured Tor producer. Porosity 44%.			
General	Top Tor (m MD)	TD (m MD)	Collapse depth (m MD)	Inclination @ collapse
	3821	5066	4235	89,6°
Top Perforation:	4245 m. 3 1/8” guns, 5 SPF, 180° phasing.			
Liner	OD (“) / Grade	Weight (ppf)	Wall thickness (“)	Slenderness ratio
	5 ½ / Q-125	45,5	0,932	5,90
Well History	Fractured stimulated in all 5 zones prior to production start on 10th of August 1997. Indications of solids production in Jan-Feb 1998. Suddenly ceased flowing on 12th of October 1999. Tagged fill and washed down to obstruction at 4235 m MD. Pumped acid and tried to mill through (21st Oct-99), still no go. Scratch marks on mill indicated liner collapse. Well converted to SW injection well on 25th of January 2004.			

Inclination	Porosity	Distance to perforation	Slenderness Ratio	Solids Production	Acid Stimulation
89,6°	**44%**	**-10m**	**5,90**	**YES**	**NO**

Table 22 F-7 T3 impact assessment

2/8-F-9A (2001)	**Horizontal Lower Hod producer. Perforated in 42 one-feet clusters with acid fracture stimulation. Porosity 32%.**			
General	Top Hod (m MD)	TD (m MD)	Collapse depth (m MD)	Inclination @ collapse
	3089	5109	3190	77,8°
Top Perforation:	3195 m, one-feet clusters. 2,5" guns, 2 SPF, 180° phasing.			
Liner	OD (") / Grade	Weight (ppf)	Wall thickness (")	Slenderness ratio
	5 / L-80	18	0,362	13,81
Well History	Perforated acid clusters with acid fracturing, 42 in total with 43,8 m average spacing. Opened well to production on 3rd of August 2001, well not fully open until 18th of November same year. Acid re-fracture on 24th of May 2002 and 28th of February 2003. 5th of May 2003: bailer returned with 99% chalk from tag at 3190 m MD. Another acid re-fracture on 6th of February 2005, well is now cyclic. Clean-out down to 3181 m MD due to chalk influx, unable to go deeper than 3184 m MD on 22nd of July 2015.			

Inclination	Porosity	Distance to perforation	Slenderness Ratio	Solids Production	Acid Stimulation
77,8°	**32%**	**-5m**	**13,81**	**YES**	**YES**

Table 23 F-9 A impact assessment

2/8-F-10T2 (1999)	**Horizontal Lower Hod producer. Perforated in 48 one-feet clusters with acid fracture stimulation. Porosity 32%.**			
General	Top Hod (m MD)	TD (m MD)	Collapse depth (m MD)	Inclination @ collapse
	2842	4348	3179	92,1°
Perforations:	3031-4290 m, 48 one-feet clusters. 2 ¾" guns, 2 SPF, 180° phasing.			
Liner	OD (") / Grade	Weight (ppf)	Wall thickness (")	Slenderness ratio
	5 / Q-125	18	0,362	13,81
Well History	Perforated and acid stimulated in 48 clusters, 3031-4290 m MD, 26,2 m average spacing. Well opened to production on 10th of June 1999. Acid re-fracture performed on 24th of January 2000 and April 13th, 2001. Cyclic producer from august 2001 due to water loading. Tagged solid obstruction at 3179 m MD on 29th of April 2003, no go.			

Inclination	Porosity	Distance to perforation	Slenderness Ratio	Solids Production	Acid Stimulation
92,1°	**32%**	**-5m**	**13,81**	**NO**	**YES**

Table 24 F-10 T2 impact assessment

2/8-F-11 (1998)	**Horizontal Lower Hod producer. Initially fractured and later acid fracture stimulation. Porosity 45%.**			
General	Top Hod (m MD)	TD (m MD)	Collapse depth (m MD)	Inclination @ collapse
	2807	4388	2908	76,6°
Top Perforations:	2954 m. 3 3/8" guns, 6 SPF, 180° phasing.			
Liner	OD (") / Grade	Weight (ppf)	Wall thickness (")	Slenderness ratio
	5 / Q-125	18	0,362	13,81
Well History	Well handed over to production on April 20th, 1998. Acid wash on lower Hod fractures performed on April 16th, 2000. Pumped acid pill at 2890 m MD on January 16th, 2002. Tagged at 2908 m MD, 1/3 of lead impression block completely undamaged, straight line shear from across surface centre to outer bottom edge of lead. Indication of liner collapse. Acid bullhead on lower Hod fractures performed on 1st of March 2003. Cyclic producer from June 2009, possible lifting problems or influx failure.			

Inclination	Porosity	Distance to perforation	Slenderness Ratio	Solids Production	Acid Stimulation
76,6°	**45%**	**-46m**	**13,81**	**YES**	**YES**

Table 25 F-11 impact assessment

2/8-F-14 (1998)	**Vertical Tor producer, proppant re-fractured in 1 zone. Porosity 28%.**			
General	Top Tor (m MD)	TD (m MD)	Collapse depth (m MD)	Inclination @ collapse
	2470	2635	2621	3,6°
Perforations:	2593 - 2613 m. 2 ¾" guns, 2 SPF, 180° phasing.			
Liner	OD (") / Grade	Weight (ppf)	Wall thickness (")	Slenderness ratio
	6 5/8 / Q-125	65,8	1,118	5,92
Well History	Fracture stimulated prior to production start in May 1998, poor initial performance. 4th of January 1999: well unstable due to solids production (proppant), choked back. Ceased flowing on April 2nd, 1999. Bailer sample indicated scale 2 m above top of perforations. Milled through down to solid tag at 2621 m MD. Scale squeeze operation performed in August 1999. Well died, most likely due to a combination of water loading and proppant/chalk accumulation in wellbore. Unsuccessful acid cleanout on 9th of January 2000, solid tag at 2590 m MD. Milled through on 14th of July 2000 and wash down to 2620 m MD. Sat bridge plug and perforated new zone 2578-2584 m MD, in July 2000. New zone fracture stimulated. Continuous problems with solids production, attempted to mill through solid tag at 2589 m MD on 20th of April 2005 without success. Well now used for pressure monitoring in water flood area. Unstable performance since 2003 with instances of chalk influx.			

Inclination	Porosity	Distance to perforation	Slenderness Ratio	Solids Production	Acid Stimulation
3,6°	**28%**	**8m**	**5,92**	**YES**	**NO**

Table 26 F-14 impact assessment

2/8-F-18T6 (1999)	Horizontal Tor producer, proppant fractured in 12 zones. Porosity up to 48%.			
General	Top Tor (m MD)	TD (m MD)	Collapse depth (m MD)	Inclination @ collapse
	4402	6785	4765	85,8°
Top Perforations:	4570 - 6680 m, 12 x 1 m zones, 3 3/8" guns, 5 SPF, 180° phasing.			
Liner	OD (") / Grade	Weight (ppf)	Wall thickness (")	Slenderness ratio
	5 / Q-125	23,2	0,478	10,46
Well History	Perforated and fracture stimulated in 12 zones from 4570 to 6680 m MD. Production start-up in April 1999. Well ceased flowing due to chalk influx on 30th of May 1999. Tag at 4765 m MD, performed 4 attempts to mill without success on 19th of July 1999. Indication of liner collapse between zone 10 and 11. Acid pumped on several occasions; July 2000, March 2001, November 2001 and May 2003. Well defined as a terminal failure, experiences several influxes. Side-track candidate.			

Inclination	Porosity	Distance to perforation	Slenderness Ratio	Solids Production	Acid Stimulation
85,8°	**48%**	**35m**	**10,46**	**YES**	**NO**

Table 27 F-18 T6 impact assessment

2/8-G-22 (2006)	Deviated water injector in the Tor formation. Porosity 41%.			
General	Top Tor (m MD)	TD (m MD)	Collapse depth (m MD)	Inclination @ collapse
	3055	3085	3054	32,7°
Perforations:	3057-3063 m. 12 x 1 m zones, 3 3/8" guns, 5 SPF, 180° phasing.			
Liner	OD (") / Grade	Weight (ppf)	Wall thickness (")	Slenderness ratio
	5 / Q-125	23,2	0,478	10,46
Well History	Injection start was 20th of December 2007, and the well was acid stimulated on 28th of April 2008. Hold-up point, and possible collapse was discovered on February 19th, 2014.			

Inclination	Porosity	Distance to perforation	Slenderness Ratio	Solids Production	Acid Stimulation
32,7°	**41%**	**-3m**	**10,46**	**NO**	**NO**

Table 28 G-22 impact assessment

2/8-G-24 (2004)	Horizontal water injector in the Tor formation. Porosity 40%.			
General	Top Tor (m MD)	TD (m MD)	Collapse depth (m MD)	Inclination @ collapse
	3085	4134	4032	86,6°
Perforations:	3140 - 4050 m. 2 7/8" guns, 4 SPF, 180° phasing.			
Liner	OD (") / Grade	Weight (ppf)	Wall thickness (")	Slenderness ratio
	6 5/8 / Q-125	65,8	1,118	5,93
Well History	Injection start was 14th of May 2004, and the well was acid stimulated on September 4th, 2008. Hold-up point, and possible collapse was discovered on April 12th, 2015.			

Inclination	Porosity	Distance to perforation	Slenderness Ratio	Solids Production	Acid Stimulation
86,6°	**40%**	**0m**	**5,93**	**NO**	**NO**

Table 29 G-24 impact assessment

5.5.3 Analyses of the liner deformation parameters

This part presents an extraction of the 6 parameters for all the 27 wells in Section 0. Table 30 is sorted on well name and Table 31 on year drilled. The risk picture can be derived from the color coding.

Summary of liner deformation parameters							
Well	**Year**	**Inclin.**	**Porosity**	**Distance to perf.**	**Slend. Ratio**	**Solids Prod.**	**Acid Stim.**
A-7	1983	27°	30%	-2m	12,48	YES	NO
A-13 A	1987	28°	30%	-5m	13,81	YES	NO
A-16 C	1991	64°	45%	-1,5m	13,81	YES	YES
A-18 AT2	1986	60,1°	45%	-3m	13,81	YES	YES
A-20	1988	28,3°	37%	-2m	14,05	NO	NO
A-26	1992	69°	39%	0m	13,81	YES	YES
A-1 A	1993	3°	39%	4m	13,81	YES	NO
A-4 B	1994	87°	42%	3m	5,90	NO	NO
A-5 B	1997	75,3°	40%	-1m	5,90	YES	NO
A-6 A	1998	5,9°	42%	-1m	5,90	SEVERE	NO
A-10 B	1993	78°	40%	19m	17,16	YES	YES
A-14 B	1992	86,9°	43%	40m	13,81	YES	NO
A-24 A	1993	29°	40%	15m	17,15 13,81	NO	NO
A-26 A	1996	68°	41%	15m	5,93	YES	NO
A-27	1991	86,9°	42%	45m	13,81	YES	YES
A-28	1992	91,8°	37%	0m	13,81 17,16	YES	YES
S-3 T5	2004	90,7°	35%	1m	8,88	YES	NO
S-8	2006	88°	32%	0m	8,88	NO	NO
F-4 T5	1996	92,3°	42%	-1m	5,90	YES	NO
F-7 T3	1997	89,6°	44%	-10m	5,90	YES	NO
F-9 A	2001	77,8°	32%	-5m	13,81	YES	YES
F-10 T2	1999	92,1°	32%	-5m	13,81	NO	YES
F-11	1998	76,6°	45%	-46m	13,81	YES	YES
F-14	1998	3,6°	28%	8m	5,92	YES	NO
F-18 T6	1999	85,8°	48%	35m	10,46	YES	NO
G-22*	2006	32,7°	41%	-3m	10,46	NO	NO
G-24 T3*	2004	86,6°	40%	0m	5,93	NO	NO

Table 30 Liner deformation parameters summary – sorted on well name

* G-22 and G-24 T3 are injection wells

Well failure parameters summary							
Well	**Year**	**Inclin.**	**Porosity**	**Distance to perf.**	**Slend. Ratio**	**Solids Prod.**	**Acid Stim.**
A-7	1983	27°	30%	-2m	12,48	YES	NO
A-18 AT2	1986	60,1°	45%	-3m	13,81	YES	YES
A-13 A	1987	28°	30%	-5m	13,81	YES	NO
A-20	1988	28,3°	37%	-2m	14,05	NO	NO
A-16 C	1991	64°	45%	-1,5m	13,81	YES	YES
A-27	1991	86,9°	42%	45m	13,81	YES	YES
A-26	1992	69°	39%	0m	13,81	YES	YES
A-14 B	1992	86,9°	43%	40m	13,81	YES	
A-28	1992	91,8°	37%	0m	13,81 17,16	YES	YES
A-1 A	1993	3°	39%	4m	13,81	YES	NO
A-10 B	1993	78°	40%	19m	17,16	YES	
A-24 A	1993	29°	40%	15m	17,15 13,81	NO	
A-4 B	1994	87°	42%	3m	5,90	NO	NO
A-26 A	1996	68°	41%	15m	5,93	YES	
F-4 T5	1996	92,3°	42%	-1m	5,90	YES	
A-5 B	1997	75,3°	40%	-1m	5,90	YES	NO
F-7 T3	1997	89,6°	44%	-10m	5,90	YES	
A-6 A	1998	5,9°	42%	-1m	5,90	SEVERE	NO
F-11	1998	76,6°	45%	-46m	13,81	YES	YES
F-14	1998	3,6°	28%	8m	5,92	YES	
F-10 T2	1999	92,1°	32%	-5m	13,81	NO	YES
F-18 T6	1999	85,8°	48%	35m	10,46	YES	
F-9 A	2001	77,8°	32%	-5m	13,81	YES	YES
S-3 T5	2004	90,7°	35%	1m	8,88	YES	
G-24 T3*	2004	86,6°	40%	0m	5,93	NO	
S-8	2006	88°	32%	0m	8,88	NO	
G-22*	2006	32,7°	41%	-3m	10,46	NO	

Table 31 Liner deformation parameters summary – sorted on time

This summary table with colour codes is outlining especially three parameters; solids production, slenderness ratio and distance to perforations. Adding in well inclination and porosity, a pattern is starting to emerge. High-inclined wells, in high porosity zones, thin liners collapsing inside the perforated interval after producing chalk.

Suggesting the different deformation scenarios, these wells can be used as examples:

- A-1A: Vertical well with relative high porosity, which has collapsed within the perforation interval after producing solids. This well is most likely deformed because of buckling caused by loss of lateral constrain and thereby non-uniform loading.
- F-4 T5: Horizontal well in a high porosity zone, which has collapsed in the perforated area after producing solids. This is very similar to the vertical A-1A well, except for a different deformation mechanism. Horizontal well collapse from loss of lateral constrain and being exposed to non-uniform load is accommodated by liner ovalling.
- G-22: This deviated water injector has collapsed in the interface between the cap rock and reservoir. This is a classic example of liner deformation due to formation shear.
- F-18 T6: Horizontal production well with very high porosity and it has been acid stimulated and problems with chalk influx. However, this well has collapsed far away from any perforated interval. This is a clear indication of well deformation caused by a fault. The reason for fault shearing is hard to determine, it could be a pre-existing fault, or a production/compaction induced fault.

<u>Exceptions:</u>

- S-3: Completed with medium thick liner (SR=8,88). Produced for a long time, was not expected to produce solids due to the higher formation strength at the flanks. Water breakthrough weakened the chalk and chalk influx was observed, and the liner collapsed because of non-uniform load.
- A-24 A and A-28: Concentric liners, were first thought to have increased collapse resistance. However, complications regarding cement quality in the annulus between liners, severely impaired the design.

6. Conclusions and recommendations

6.1 Conclusions

- Because of indications of collapse in several heavy wall liners, the load case is probably more severe than first anticipated. It could be a dynamic load, releasing forces in seconds, deeming the original safety factor unreliable.
- 59% of all total wells on Valhall had instances of solids production. 80% of the collapsed wells have produced chalk. Collapse seems to be related to solids production.
- 22 of 27 wells, collapsed close (10 m) to or within the perforation interval. Chalk production lead to cavities around perforations. Loss of lateral constrain in addition to non-uniform load, resulted in liner collapse.
- 5 wells collapsing outside the perforated interval may be due to re-activation of faults or shear displacements along weak planes within the reservoir. This is a result of severe reservoir depletion and compaction.
- High-angle wells in high porosity zones seems to be more prone to collapse. Since horizontal wells have a greater risk of chalk production and compaction forces is larger in high porosity, gives weaker chalk.
- Focus on well management and understanding of chalk production mechanisms has been successful, as the ratio of solids producing, and failed wells has decreased drastically after the new millennium.
- The collapse of S-3 at the southern flank proved that going for a 26,7 ppf, 5” liner was too optimistic. Water breakthrough triggered chalk influx which ultimately led to well failure.

6.2 Recommendations

- Calliper logs should be run to verify collapse in heavy wall liners.
- As water breakthrough is imminent to happen on more wells, focus on water management should be assessed. A possibility could be to implement ICD/AICD in the lower completion to reduce the severity of the water front.

- If the collapses are verified, one solution is to try even thicker liner strings in addition to more careful well management to mitigate solids production.

7. References

Barkved, Olav, et al. 2003. *Valhall Field - Still on Plateau after 20 Years of Production.* s.l. : SPE 83957, 2003.

Bruno, Michael, Dusseault, Maurice and Barrera, John. 2001. *Casing Shear: Causes, Cases, Cures.* s.l. : SPE-72060, 2001.

Dawson, Rapier and Paslay, P. R. 1984. *Drillpipe Buckling in Inclined Holes.* s.l. : SPE-11167-PA, 1984.

Departement of Petroleum Engineering. 2017. *Grading, Tube Stress and Failure Analysis.* s.l. : University of Stavanger, 2017.

Guo, Y, Last, N and Blanford, M. 2018. *Simple Calculation of Compaction-Induced Casing Deformation Adjacent to Reservoir Boundaries.* s.l. : IADC/SPE-189694-MS, 2018.

Kallesten, Emanuela. 2015. *The North Sea Reservoir Chalk Characterization.* s.l. : University of Stavanger, 2015.

Kristiansen, Tron Golder and Pattillo, Phil. 2002. *Analysis of Horizontal Casing Integrity in the Valhall Field.* s.l. : SPE/ISRM 78204, 2002.

Kristiansen, Tron Golder. 2015. *An Evaluation of Non-Uniform Load and Shear Displacement Capacity of VWRD New Well Design* . s.l. : BP, 2015.

Kristiansen, Tron Golder and Meling, Sigve . 1996. *A Production Parameter Analysis Of Chalk Influxes in the Valhall Field.* s.l. : AMOCO, 1996.

Kristiansen, Tron Golder and Plischke, Bertold. 2010. *History Matched Full Field Geomechanics Model of the Valhall Field Including Water Weakening and Re-Pressurisation.* s.l. : SPE 131505, 2010.

Kristiansen, Tron Golder. 2008. *Evaluation of Valhall Casing design.* s.l. : SPE 123456, 2008.

—. 2018. *Personal conversations during spring 2018.* 2018.

—. 2014. *Valhall Well Life Prediction.* 2014.

Kristiansen, Tron Golder, Barkved, Ola and Pattillo, Phil. 2000. *Use of Passive Seismic Monitoring in Well and Casing Design in the Compacting and Subsiding Valhall Field, North Sea.* s.l. : SPE 65134, 2000.

Madland, Merete Vadla. 2005. *Water Weakening of Chalk: A Mechanistic Study.* s.l. : University of Stavanger, 2005.

Mantovano, Luciano and Grittini, Santiago. 2016. *Development of a Numerical Tool to Assess the Structural Resistance of Pre-perforated Liners.* s.l. : SPE-182505-MS, 2016.

Nester, J. H., Jenkins, D. R. and Simon, R. 1955. *REsistances to Failure of Oil-Well Casing Subjected to Non-Uniform Transverse Loading.* s.l. : API-55-374, 1955.

Norwegian Petroleum Directorate. 2018. Factpages - NPD. *Ekofisk.* [Online] 14 June 2018. [Cited: 14 June 2018.] http://factpages.npd.no/factpages/default.aspx?culture=en&nav1=field&nav2=PageView|All&nav3=43506.

—. 2018. Valhall. *Factpages - Norwegian Petroleum Directorate.* [Online] 12 June 2018. [Cited: 6 June 2018.] http://factpages.npd.no/factpages/Default.aspx?culture=nb-no&nav1=field&nav2=PageView|All&nav3=43548.

Offshore Technology. 2016. Valhall Oilfield - a timeline. [Online] Verdict Media Limited, 3 December 2016. [Cited: 6 June 2018.] https://www.offshore-technology.com/projects/valhall-oilfield-a-timeline.

Pasic, Borivoje, Gaurina-Medimurec, Nediljka and Matanovic, Davorin. 2007. *Wellbore Instability: Causes and Consequences.* s.l. : University of Zagreb, 2007.

Pattillo, Phil, Moschovidis, Z. A. and Manohar, Lal. 1995. *An Evoluation of Concentric Casing for Nonuniform Load Applications.* s.l. : SPE-29232-PA, 1995.

Settari, A. 2002. *Reservoir Compaction.* s.l. : SPE-76805-JPT, 2002.

Whaley, Jane. 2009. Geo Ex Pro. [Online] 2009. [Cited: 6 juni 2018.] https://www.geoexpro.com/articles/2009/05/the-valhall-story.

SPE-47274-MS - Reservoir Compaction and Seafloor Subsidence at Valhall, Kristiansen & Patillo, 1998

Analysis of Horizontal Casing Integrity in the Valhall Field, SPE-78204-MS, Kristiansen og Patillo, 1998